UNIVERSITA' degli STUDI di PADOVA

Facoltà di Ingegneria

Corso di Laurea Magistrale in Ingegneria Civile

Curriculum Geotecnico

Tesi di laurea

INCLINED PLANE TESTS: DETERMINATION OF FRICTION ON GEOSYNTHETIC INTERFACES

PROVE DI PIANO INCLINATO: DETERMINAZIONE DELL'ATTRITO NELLE INTERFACCE GEOSINTETICHE

Relatore: Prof. Paolo Carrubba

Prof J.-P. Gourc

Laureanda: Melissa Miuzzi

Matricola 1020009

Anno Accademico 2012/2013

INDEX

INTRODUCTION

Define a correct friction angle between two different materials is important issue in many geotechnical engineering applications. A right characterisation of mechanical properties could prevent slope failures in landfill liners, landslips, foundations collapse, and be useful for the correct design of walls, foundations, tie rod, covering ecc.

Nowadays in geotechnical, the use of polymeric materials, as the geosynthetics, is speedily increasing; in fact, they are employed in innumerable applications and fields. It is important to notice that most of times, geosynthetics are not individually employed but in combination each other. For this reasons, it is necessary to investigate the global interface behaviour.

The aim of this thesis is to examine the geosynthetic interface mechanical properties, to provide correct friction angles.

These geosynthetic lining systems are nowadays fully employed in landfill top covers.

An appropriate characterization of geosynthetic interface friction is important in landfill liners to prevent slope failures, damage of liners and of their impermeability with the consequently infiltration of leachate and waste in the ground. Be familiar with the interface friction should be helpful to design a modern landfill, facing the need of more steep slopes to face the growing need of new areas for the waste storage. Moreover, as base for a safe construction of the landfill itself.

The first part of this study concerns the determination of friction angles between different geosynthetics testing four different procedures: “Standard”, “Dsipalcement”, “Force” and “Residual Friction”. The second part is after dedicated to the analysis and investigation of the parameters that influences the friction interfacial behaviour.

Results and evaluation of friction parameters have been obtained through a test campaign using a modified Inclined Plane Device, during an internship in Grenoble (France) at the LTHE Laboratory of the University “Joseph Fourier”.

In this research, the interfaces tested are composed by a HDPE geomembrane and a geocomposite, analysed in all is parts: non-woven geotextile and geonet. At the end, three different interface are tested and examined: geomembrane-geotextile; geomembrane-geonet; geomembrane-geocomposite.

The first chapter reported the different types of geosynthetic families, their characteristics and properties, and the fields of applications.

In the second chapter there is a brief description of landfill parts, especially attention is given to the top cover where the interface tested are employed. After this, the different types of geosenthetics and interfaces used in ladfill top cover are described.

The third is reserved to the main important top cover problems: settlements and slope stability. For what concerns the second one, the parameters influencing slope stability and the stability of the geosynthetic lining systems are treaty. At the end, the different stability methods founded in literature are referred and illustrated.

Chapter 4 is dedicated to friction in generally and to interface friction in particularly.

The first part of Chapter 5 is dedicated to the illustration of Standard and Inclined Plane Procedures for the determination of geosynthetic interface friction. The second part reported the testing program, the procedures used and the experiment set up.

While in Chapter 6, experiment results are examined and discussed. There is an accurate analysis of the procedures tested, of the interfaces behaviour and of the parameter that could influence the interface friction.

The research conclusions are expressed, at the end, in Chapter 7.

1. GEOSYNTHETICS

Geosynthetic is “A generic term describing a product, at least one of whose components is made from a synthetic or natural polymer, in the form of a sheet, a strip or a three dimensional structure, used in contact with soil and/or other materials in geotechnical and civil engineering applications.” (EN ISO 10318:2000) They are plastic, organic or textile materials, commercialized in rolls that could be classified into categories based on the method of manufacture.

Geosynthetics have been used in civil engineering construction since the late 1970s, and their use is currently growing rapidly. Nowadays they are employed in most of environmental engineering solutions, as for examples in landfill. The reason of this wide use is essentially due to their lower cost their simpler installation with respect to the conventional materials and also to the numerous assortments of products.

1.1. GEOSYNTHETIC TYPES and CATEGORIES

In Figure 1. are reported the two main families of geosynthetics: permeable and impermeable; classified by the standard EN ISO 10318 (2000). There are also three main subcategories, divided by the method of manufacture: geotextiles, geocomposites and geomembranes. (Figure 1.1.)

According to the International Geosynthetic Society the reported herein the description of each category. (R. Bathurst (2007))

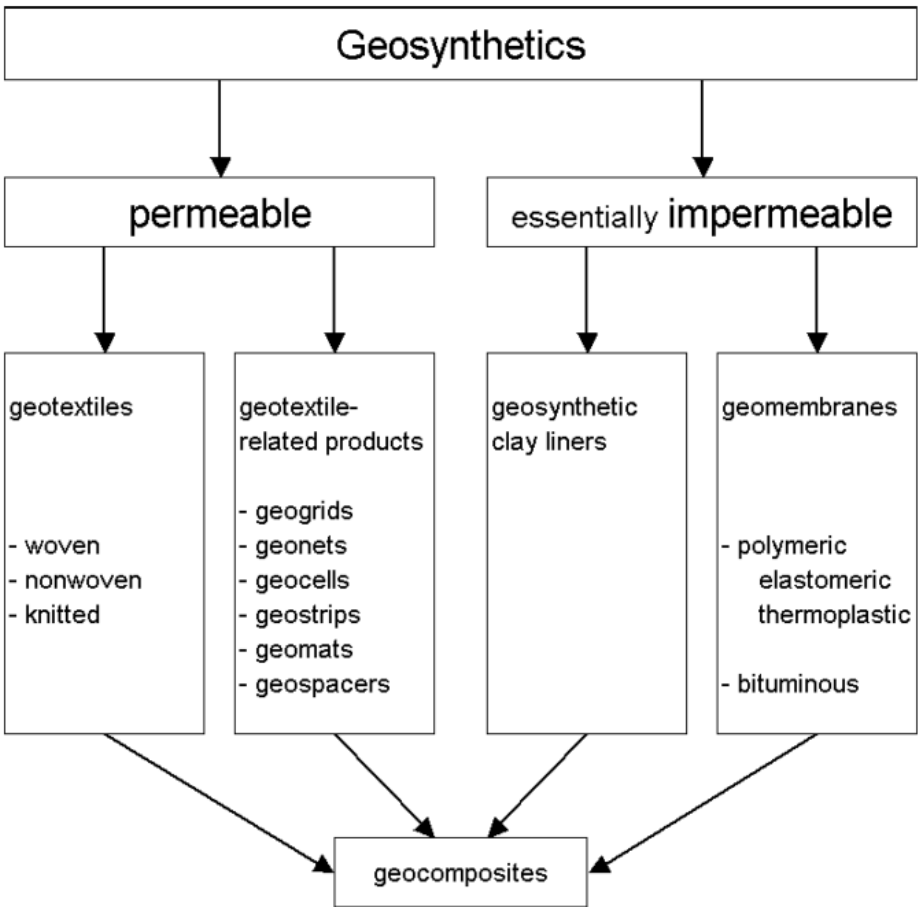

Figure 1.1. Geosynthetic summary categories (ISO EN 10318).

Geotextiles are permeable products, textiles in the traditional sense; however, the fabrics usually are made from petroleum products such as polyester, polyethylene and polypropylene. They are continuous sheets of woven, nonwoven, knitted or stitch-bonded fibers or yarns. (Figure 1.2.)

Woven geotextiles are made of two sets of parallel filaments or strands of yarn systematically interlaced to form a planar structure.

Knitted geotextiles are formed by interlocking a series of loops of one or more filaments of strands yarns to form a planar structure.

Non-woven geotextiles are formed from filaments, short fiber arranged in an oriented, or a random pattern in a planar structure.

Geotextiles are generally bonded by one of the following methods: chemical; thermal and mechanical bonding. The sheets of geotextile are flexible and permeable and generally have the appearance of a fabric. The main functions for this kind of geosynthetic are separation, filtration, drainage, reinforcement and erosion control.

Figure1.2. Woven and Non Woven Geotextile

Numerous related products compose the geotextile family: geogrides; geonets, geocells; geostrips; geomats; geospacers.

Geogrids are geosynthetic materials that have an open grid-like appearance. Their principal application is the soil reinforcement. (Figure 1.3.) Geogrids form a distinct category of geosynthetics designed for reinforcement and are available in a wide range of tensile strengths. These products are characterized by a relatively high tensile strength and a uniformly distributed array of large apertures throughout. The apertures allow soil particles on either side of the installed sheet to come into direct contact, thereby increasing the interaction between the geogrid and some soils. The apertures also ensure unrestricted vertical drainage of a reinforced free-draining soil.

Figure 1.3. Geogrid

Geonets are sort of open grid-like materials formed by two sets of course, parallel, extruded polymeric strands intersecting at a constant acute angle (Figure 1.4.). The most part of the available geonets are made of medium-density and high-density polyethylene. The main functions of this material are drainage, protection and reinforcement.

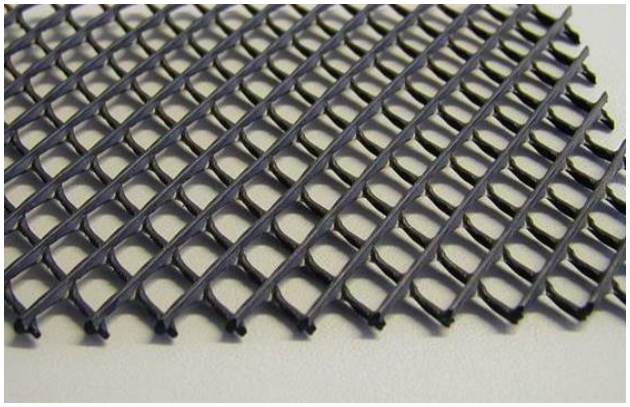

Figure 1.4. Geonet

Geocells are relatively thick, three-dimensional networks constructed from strips of polymeric sheet (Figure 1.5.). The strips are joined together to form interconnected cells that are filled with soil and sometimes concrete.

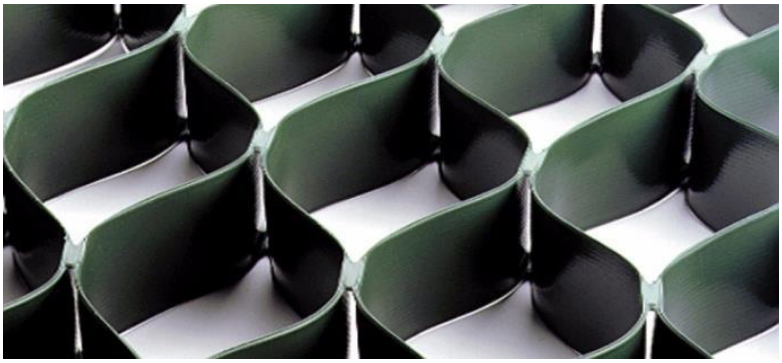

Figure 1.5. Geocells

Geopipes are perforated or solid-wall polymeric pipes used for drainage of liquids or gas; including leachate or gas collection in landfill applications (Figure 6a). In some cases the perforated pipe is wrapped with a geotextile filter.

Geofoam are blocks or slabs are created by expansion of polystyrene foam to form a low-density network of closed, gas-filled cells. (Figure 1.6.b) Geofoam is used for thermal insulation, as a lightweight fill or as a compressible vertical layer to reduce earth pressures against rigid walls.

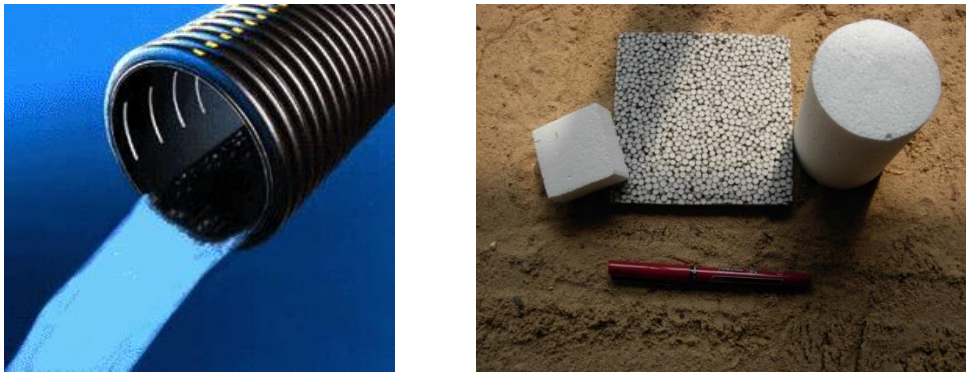

(a) (b)

Figure 1.6. Geopipes (a) and Geofoam (b)

On the other hand, geocomposites clay liners and geomembranes compose impermeable geosynthetics essentially.

Geocomposites, in generally, characteristics and functions will be better describes later, however they are made from a combination of two or more geosynthetics (Figure 1.7.). Layers examples include: geotextile-geonet; geotextile-geogrid; geonet-geomembrane; or a geosynthetic clay liner (GCL). Prefabricated geocomposite drains or a plastic drainage core surrounded by a geotextile filter forms prefabricated vertical drains (PVDs).

Figure 1.7. Geocomposite

Another kind of geocomposite is the geosynthetic clay liner (GCL). In this case a bentonite clay layer typically is incorporated between two geotextile layers (at the top and at the bottom), or bonded to a geomembrane and a single layer of geotextile. Geotextile-encased GCLs are often stitched or needle-punched through the bentonite core to increase internal shear resistance. When hydrated they are effective as a barrier for liquid or gas and are commonly used in landfill liner applications often in conjunction with a geomembrane.

Geomembranes (Figure 1.8.) are products used for fluid or gas containment and barrier. They are continuous flexible sheets made from one or more synthetic materials. The types of materials used for geomembrane are thermoplastic or thermoset polymers. The firsts are polymers that become pliable or moldable above specific temperature, and return to a solid state upon cooling. They also can be remolded because the intermolecular interaction spontaneously reform upon cooling. The thermosets instead are polymers with an irreversible deformation. The thermoplastic polymers include PVC, polyethylene and polyamide; the thermosets are made by ethylene vinyl acetate, polychloroprene and isoprene-isobutylene.

Figure 1.8. Geomembrane

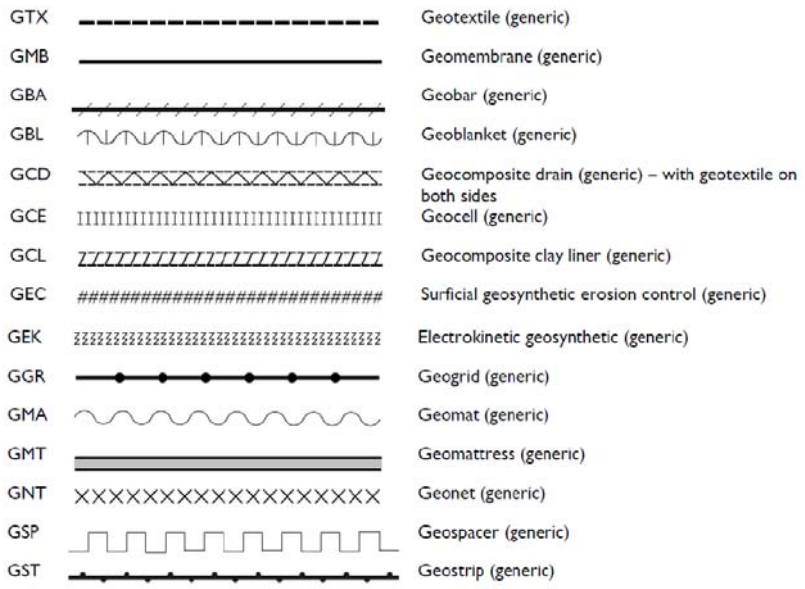

Figure 1.9. Abbreviation and symbology proposed by IGS:

1.2. GEOSYNTHETICS FUNCTIONS

Geosynthetics include a variety of synthetic polymer materials that specially are fabricated to be used in geotechnical, geoenvironmental, hydraulic and transportation engineering applications. It is convenient to identify the primary function of a geosynthetic as being one of separation, filtration, drainage, reinforcement, fluid/gas containment, or erosion control. In some cases, the geosynthetic may serve dual functions. (R. Bathurst, (2007))
The following table (Table 1.1) shows the functions of the principal Geosynthetics.

Table 1.1 Identification of the usual primary function for each type of geosynthetic (R. Koerner (1191))

Type of Geosynthetic (GS)	Primary Function				
	Separation	Reinforcement	Filtration	Drainage	Containment
Geotextile (GT)	✓	✓	✓	✓	
Geogrid (GG)		✓			
Geonet (GN)				✓	
Geomembrane (GM)					✓
Geosynthetic Clay Liner (GCL)					✓
Geopipe (GP)				✓	
Geofoam (GF)	✓				
Geocomposite (GC)	✓	✓	✓	✓	✓

Separation:

Geosynthetics used for separation has to avoid the co-penetration and mixing of different soil layer. For example, geotextiles are used to prevent road base materials from penetrating into soft underlying soft subgrade soils, thus maintaining design thickness and roadway integrity. The geosynthetics employed in these applications are essentially geotextiles and geocomposites. (Figure 1.10.)

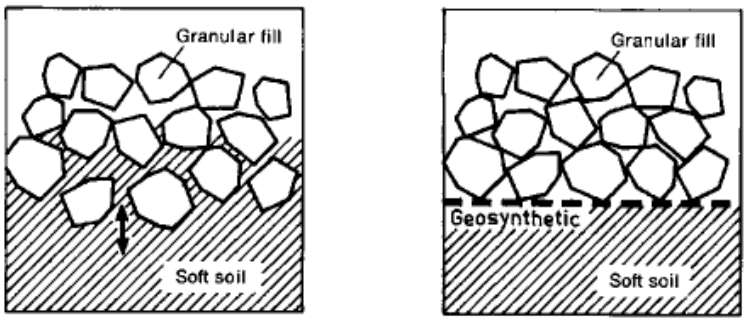

Figure 1.10. Geosynthetics used as separation

Filtration refers to the separation between two materials with different particle size distribution; the geosynthetic acts similar to a sand filter by allowing water to move through the soil while retaining all upstream soil particles. The aim is to prevent soil erosion and the removal of the fine fraction. For example, geotextiles are used to prevent soils from migrating into drainage aggregate or pipes while maintaining flow through the system. The geosynthetics used in these applications are essentially geotextiles and geocomposites. (Figure 1.11.)

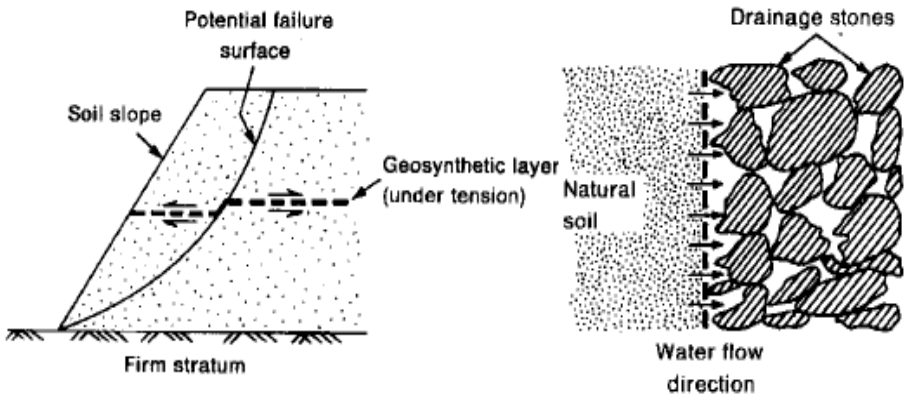

Figure 1.11. Geosynthetic used as reinforcement and filtration

Reinforcement:

Geosynthetic acts as a reinforcement element training traction actions, improving the global strength. For example, geotextiles and geogrids are used to add tensile strength to a soil mass in order to create vertical or near-vertical changes in grade (reinforced soil walls). Geosynthetics (usually geogrids) have also been used to bridge over voids that may develop below load bearing granular layers (roads and railways) or below cover systems in landfill applications. The geosynthetics employed in these applications are essentially geotextiles, geogrids and geonets.

Drainage:

Geosynthetic aim is to carry fluid flows through less permeable soils. For example, geotextiles are used to dissipate pore water pressures at the base of roadway embankments. For higher flows, geocomposite drains have been developed. These materials have been used as pavement edge drains, slope interceptor drains, and abutment and retaining wall drains. Prefabricated vertical drains (PVDs) have been used to accelerate consolidation of soft cohesive foundation soils below embankments and preload fills. (Figure 1.12.)

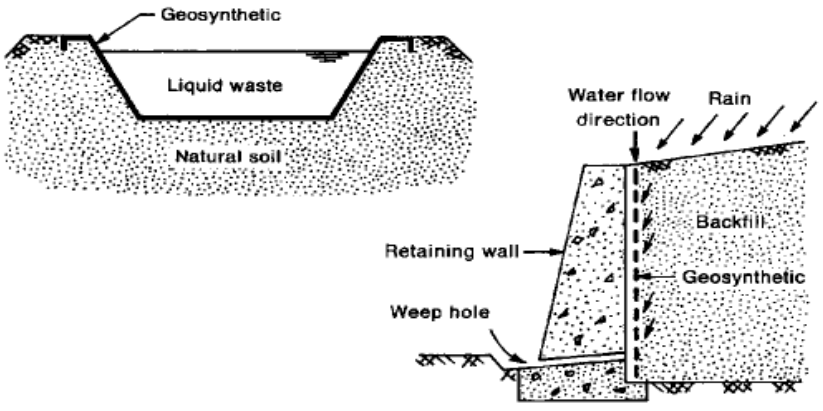

Figure 1.12. Geosynthetic used as dranaige

Erosion control:

Geosynthetic acts to reduce soil erosion caused by rainfall impact and surface water runoff on slopes for example. Geotextile silt fences are used to remove suspended particles from sediment-laden runoff water. Some erosion control mats are manufactured using biodegradable wood fibres.

Fluid/Gas (barrier) containment:

Total separation of the volume considered, realization of an impermeable barrier to fluids or gases. For example, geomembranes, thin film geotextile composites, geosynthetic clay liners (GCLs) and field-coated geotextiles are used as fluid barriers to impede flow of liquid or gas. This function is also used in asphalt pavement overlays, encapsulation of swelling soils and waste containment.

1.3. GEOSYNTHETICS PROPERTIES

The most part of geosynthetic are polymer materials, and that is the first parameter that influences their behavior. Main polymers used for geosynthetic materials are specified in Table 1.2

Table 1.2. Polymer materials used in Geosynthetics:

Geosynthetic materials	Polymer materials
GEOMEMBRANES	Polyethylene (HDPE and LLDPE) Plasticized PVC Polyropylene
GEONETS	HDPE
GEOGRIDS	HDPE Polyesters Polypropylene
GEOPIPES	HDPE PVC
GEOTEXTILES	Polypropylene polyester

The material influences the Geosynthetic mechanical behavior, the shear resistance, the hydraulic behavior, the UV, chemical and biological resistance.

In Table 1.3 are listed some of the principal characteristics of the polymers used in geosynthetic production.

Table 1.3. Typse of commonly used polymers materials and their principal characteristics

POLYMER MATERIALS	Density (Kg/m^3)	Fusion Temperature (°C)	UV resistance Critic wave length
Polypropylene(HDPE)	950	130	330-360
PVC	1250	235	320
Polyester (PET)	1380	260	325
Polypropylene (PP)	910	165	<300,340-400
Polyamide (PA)	1140	250	335-360

In civil engineering, geosynthetic materials are designed to fulfill their function over a given period. It depends on their formulation as well as on the environmental conditions they will experience between their manufacture to their actual service life.

According to Kay et al. (2004) the degradation mechanism can be divided into two categories: physical and chemical degradation.

Physical aging is related to degradations, which do not involve a modification in the molecular structure of polymer chains. Chemical aging can be defined as a mechanism involving a modification in the molecular structure of polymer chains.

For geosynthetic materials the numbers of relevant properties that have to be determined are much larger than for soil. These properties can broadly be grouped under six types as listed in Table 1.4. Table 1.4 also lists the parameters that should be evaluated for each of these six types:

Table 1.4. Properties and parameters of geosynthetic

Type of property	Parameters
Physical	Thickness, specific gravity, mass per unit area, porosity, apparent opening size.
Chemical	Polymer type, filler material, carbon black percentage, plasticizer and additive details, manufacturing process for fiber and geosynthetics.
Mechanical	Tensile strength, compressibility, elongation, tear/impact/puncture resistance, burst strength, seam strength, fatigue resistance, interface friction with soil, anchorage in soil
Hydraulic	Permittivity (cross-plane permeability), trasmissivity (in-plane permeability), clogging potential.
Endurance	Installation damage potential – tear/impact/puncture resistance, abrasion resistance, creep.
Degradation	Resistance to ultra-violet radiation, temperature, oxidation, ecc.

Molecular weight can affect physical and mechanical properties, heat resistance and durability of geosynthetics. The molecular level of the crystalline system of the polymer also influences the physical and mechanical properties of the polymers. The chemical composition of polymer chains will determine the families of physical and chemical degradation mechanisms likely to take place into the material. In addition, temperature as a first order influence on it. (Figure 1.13.) (Vashi, M. Desai, A. Desai).

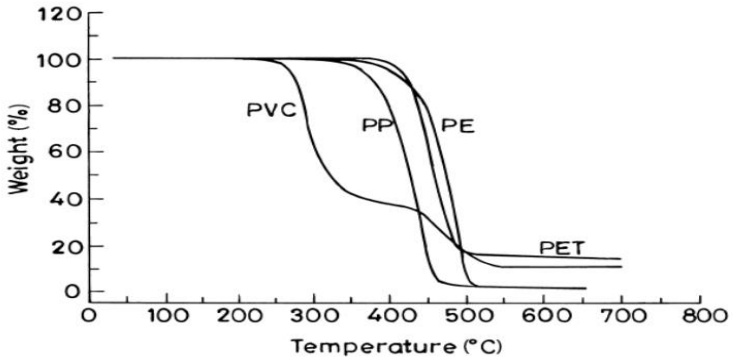

Figure 1.13. Effect on temperature on some geosynthetic polymers
(Thomas & Verschoor, 1998)

The most part of polymers are very sensitive to the ultra violet light: the polymer bonds breakdown and consequently a loss in resistance properties occurs. If geosynthetics are exposed it is recommended that they should contain a well-dispersed UV inhibitor that protects the polymer chains. Carbon black is the most cost-effective agent for these purposes. It is normal to mix the particles with a carrier to make a dispersion that is easier to handle. Some geosynthetics are used in aggressive environments such as in the containment of landfills and contaminated land. As the rate of chemical attack relates directly to the surface area available, it is important for engineers to request proof of stability with the specific chemicals present. This information, generated by the polymer manufacturers, should be available from the geosynthetic manufacturer. In some cases, it may be necessary to carry out a specific immersion test at elevated temperatures using the actual mix of chemicals.

From the engineering point of view, the durability of geosynthetics is studied as construction survivability and longevity. Construction survivability addresses the Geosynthetics survival during installation.

Geosynthetics in fact, may suffer mechanical damage (e.g. abrasion, cuts or holes) during installation due to placement and compaction of the overlying fill.

The rigorous of installation can often be more demanding than the ultimate in-service requirements. Laboratory tests have been developed to closely simulate in-service conditions. In some cases, the installation stresses might be more severe than the actual design stresses for which the geosynthetic is intended. The susceptibility of some geosynthetics to mechanical damage during installation can increase under frost conditions. The severity of the damage increases with the coarseness and angularity of the fill in contact with the geosynthetic and with the applied effective) effort, and it generally decreases with the increasing thickness of the geosynthetic. This damage may reduce the mechanical strength of the geosynthetic and, when holes are present, it will also affect the hydraulic properties.

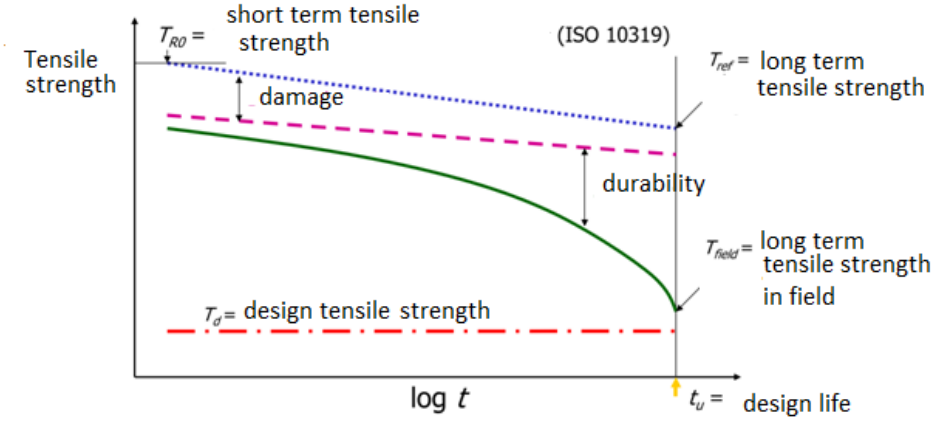

Figure 1.14. Tensile strength of Geosynthetics and durability
(S. Cola, corso di “Miglioramento dei terreni ed opera in terra” UNIPD);

The tensile strength is the geosynthetic maximum resistance to deformation mobilized when it is subjected to tension by an external force. The tensile strength can be determined by axial and multi-axial tests. (Figure 1.14.)

Index tests enable a direct comparison to be made between different geotextiles. They are also used for quality control during manufacturing. Tensile strength, pore size, water flow, CBR puncture resistance and cone drop perforation are the most common properties to be listed in a specification. Mass per unit area is also frequently specified though this is not necessary, as it is not a performance characteristic.

2. LANDFILLS

In this research, the interface friction between different geosynthetic layers is investigated and the landfill geosynthetic layers are chosen and described as applicative example. It is herein proposed a brief description of a landifill.

According to the Concise Oxford Dictionary, a landfill is described as follows:
LANDIFILL: n,

1. Waste material etc. used to landscape or reclaim areas of ground;
2. The process of disposing rubbish in this way;
3. An area filled in by this way.

The third definition is operable one used for the purposes of this thesis.
A landfill is a site for the disposal of waste materials by burial and it is the oldest form of waste treatment. Historically landfills have been the most common methods of organized waste disposal. Some landfills are also used for waste management purpose, such as the temporary storage, consolidation and transfer, or processing of waste material.
The waste management in Europe is governed by the European Standard 99/31/CE of 26 April 1999, in which there are three different models of landfill:

- For inert waste;
- For not dangerous waste;
- For dangerous waste.

The Directive's overall aim is "to prevent or reduce as far as possible negative effects on the environment, in particular the pollution of surface water, groundwater, soil and air, and

on the global environment, including the greenhouse effect, as well as any resulting risk to human health, from the landfilling of waste, during the whole life-cycle of the landfill". This legislation also has important implications for waste handling and waste disposal.

2.1. LANDFILL ANATHOMY

All the next descriptions are given by the USA Waste Management disposal for landfills constructions.

The landfill can be divided in five main parts, down to top: composite liner system, leachate and gas collection system, working landfill, composite lateral system, composite cap system and protective cover (Figure 2.1. and 2.2.).

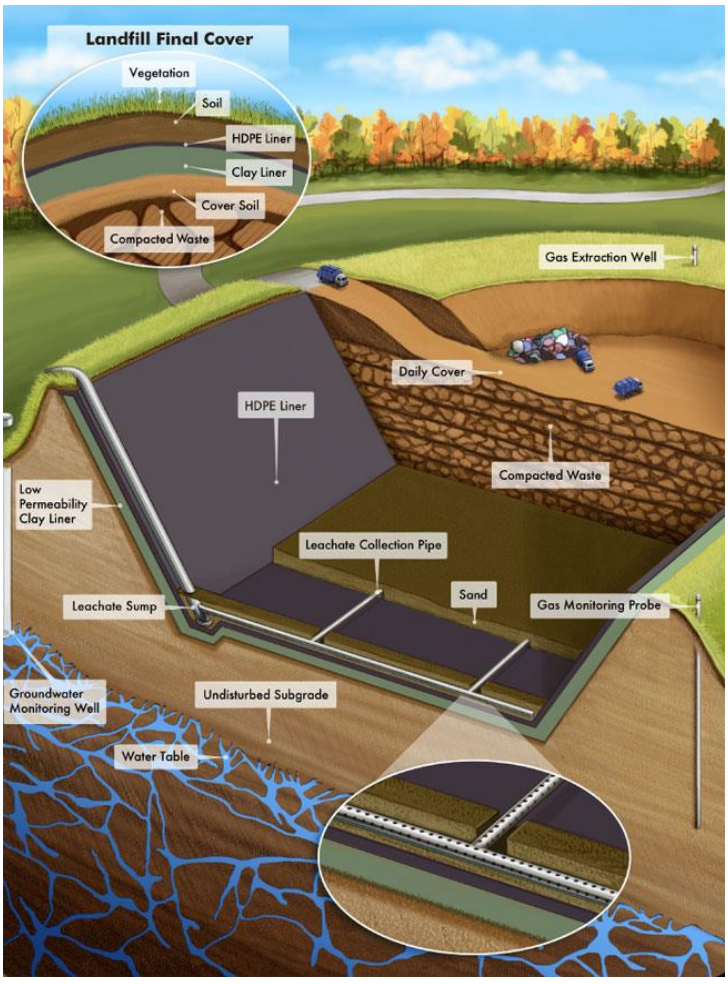

Figure 2.1. Landfill structure (www.greengroupholding.com)

Down to top, the first part is the component liner system. Its principal aims are collecting leachete, isolating the waste, preventing infiltrations, giving mechanical support.
This pack is composed by three main parts: a prepared subgrade; a compacted clay and a geomembrane.

The prepared subgrade is the native soil beneath the landfill prepared as needed prior to beginning landfill construction. The compacted clay layer is located directly below the geomembrane and they work as an additional barrier to prevent leachate leaving from the landfill and entering the environment. These materials prevent also the escape of gas. The layer permeability is around 10^{-9} (m/s).

The following part is the leachate and gas collection system. Leachate is a liquid that has filtered through the landfill. It consists primarily of precipitation with a small amount coming from the natural decomposition of the waste. The collection system collects the leachate to be removed from the landfill and properly treated or disposed of. The leachate collection system has the following components: leachate and gas collection pipe system; filter geotextile; leachate collection layer.
Perforated pipes, surrounded by a bed of gravel, compose the first one, transport collected leachate to specially designed low points called sumps. Pumps, located within the sumps, automatically remove the leachate from the landfill and transport it to the leachate management facilities for treatment or another proper method of disposal.
The geotextile filter is a geotextile fabric, similar in appearance to felt, may be located on top of the leachate collection pipe system to provide separation of solid particles from liquid. This prevents clogging of the pipe system.

The last layer is the sand or gravel or a thick plastic mesh called a geonet collects leachate and allows it to drain by gravity to the leachate collection pipe system.

The working landfill is composed by the waste and a daily cover of soil in order to reduce odors, keeps litter from scattering and helps deter scavengers.

Afterwards the next part is the composite cap and lateral system, composed by a compacted clay layer, a geomembrane and a drainage layer. The latter includes sand or gravel or a thick plastic mesh called a geonet drains that excesses precipitation from the protective cover soil to enhance stability and help prevent infiltration of water through the landfill cap system. A geotextile fabric, similar in appearance to felt, may be located on top of the drainage layer to provide separation of solid particles from liquid. This prevents clogging of the drainage layer.

At the end, in the upper part of the landfill the protective cover soil is applied to support and maintain the growth of vegetation by retaining moisture and providing nutrients, and the cover vegetation at the end

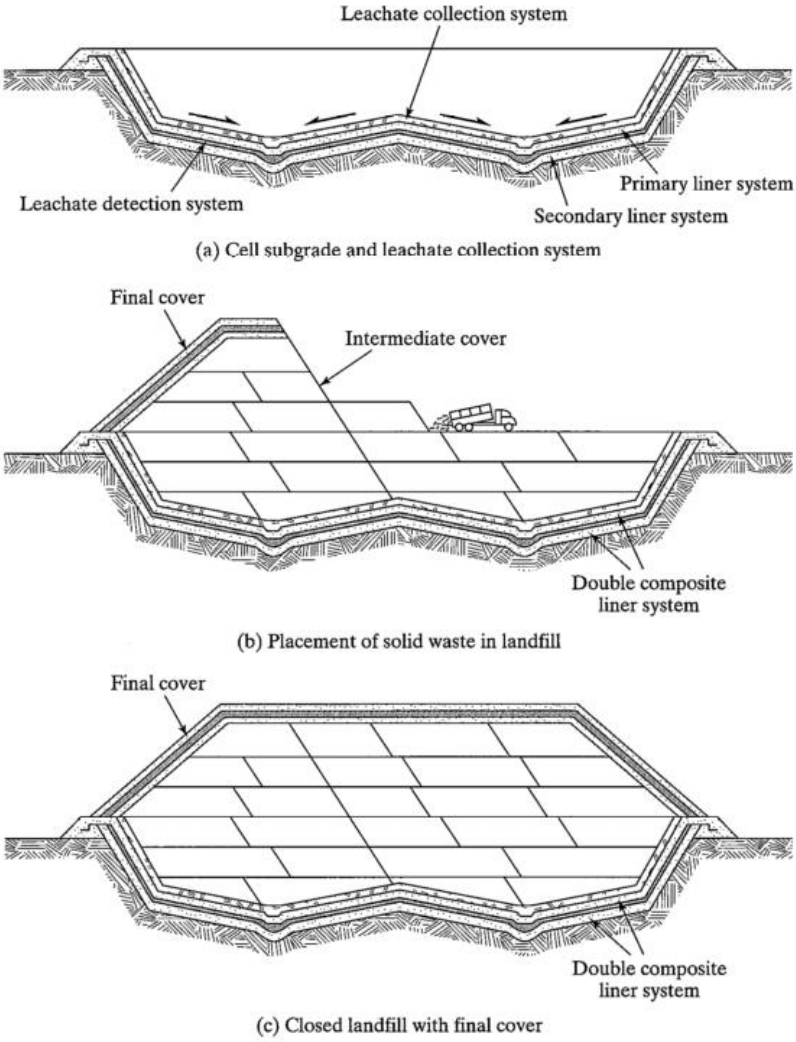

Figure 2.2. Development and completion of a solid waste landfill
(P. Simonini, corso di "Geotecnica nella difesa del suolo", UNIPD)

2.3. LANDFILL TOP COVER

Particularly attention has to be given to the landfill top cover. In fact here the geosynthetic layers are employed and exposed to settlements and instability, which can originate the material damage.

The purpose of the top cover in a landfill is to contain the waste and to provide a physical separation between the waste and the environment for the public health protection. Most landfill covers are designed with the primary goal to reduce or prevent infiltration or perception into the landfill, in order to minimize leachate generation. In addition, the cover also has to control the release of gases produced in the landfill so the gas can be ventilated, collected and utilized.

The landfill cover should minimize erosion and support vegetation and it is finally landscaped in order to fit into the surrounding area or meet specific plans for the final use of the landfill.

The top cover schematized in Figure 2.3., may be placed immediately after the landfill section has been filled or several years later depending on the settlement patterns. Significant differential settlements may disturb the functioning of the top cover.

The specific design of the cover system depends on the type of waste landfilled.

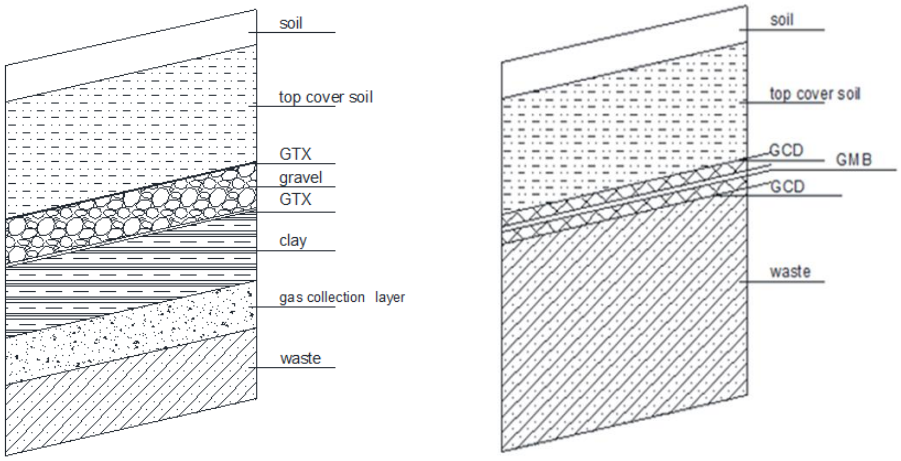

Figure 2.3. Landfill top cover without geosynthetics and with geosynthetics

2.4. GEOSYNTHETICS IN LANDFILL

Geosynthetics, as defined by the International Geosynthetic Society are: “planar, polymeric (synthetic or natural) material used in contact with soil/rock and/or any other geotechnical material in civil engineering application”. They are extensively used in the design of both base and cover liner systems of landfill facilities.

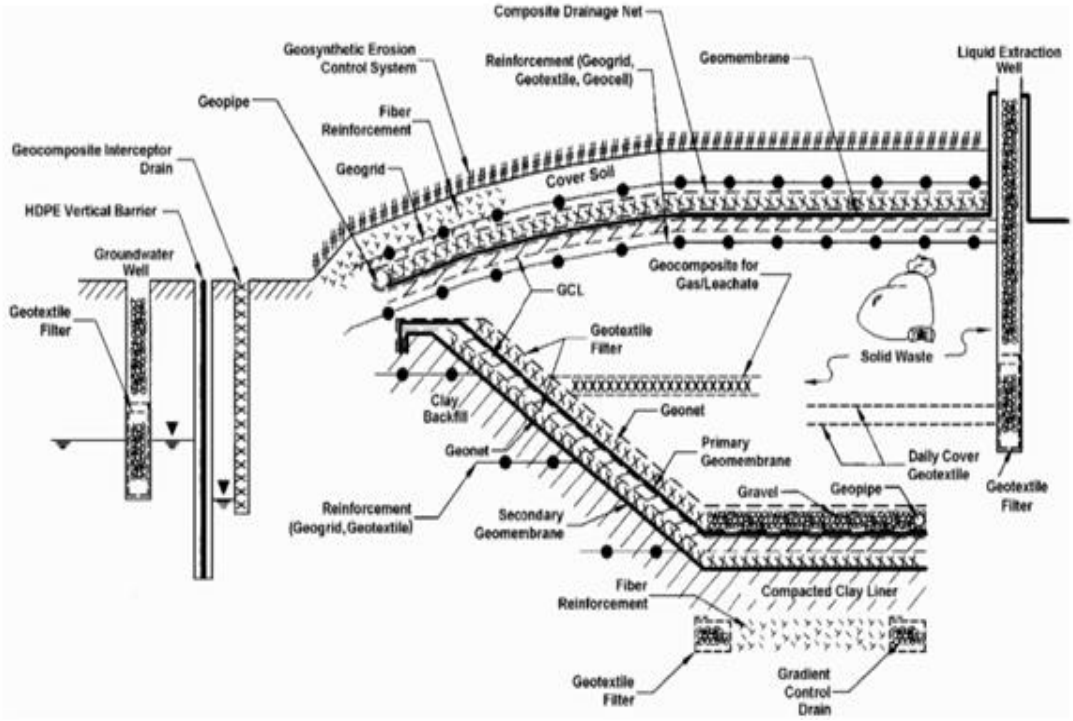

Figure 2.4. Multiple uses of geosynthetics in landfill design.
(M. Bouazza and J. Zornberg (2002))

Geosynthetics employed in landfill could be principal divided in two main groups: impermeable and for drainage. The principals used are: geomembranes; geocomposite and geogrids. (M. Bouazza and J. Zornberg) (Figure 2.4.)

The design concept for landfills presumes accurate knowledge on the distribution of groundwater flow paths and barriers, their hydraulic properties, the structure and deformation behaviour of the subsoil and the potential for improving the sealing effect of the subsoil. Besides the mechanical and biological effects the chemical loads, including highly concentrated or undiluted fluid matters, diluted fluid matters, leachate, landfill gas and gas condensate are of major importance for the selection of resistant construction materials used in landfills.
Generally, landfill capping sealing systems are designed with components made of mineral or composite liners in conjunction with components for degasification, drainage and vegetation. (M. Sadlier)

2.4.1 IMPERMEABLE GEOSYNTHETICS

Geomembranes are relatively impermeable sheet of polymeric materials and can be used as a barrier to liquids, gases and/or vapors already described in chapter 1. They are characterized by a low permeability to gas and liquids, good/excellent flexibility. In landfills the most used are GMB in PE/HDPE because they provide a good chemist resistance and durability. This kind of GMB is difficult to joint and also to lay out, in fact, sometimes GMB in PVC could be used instead of the ones in PE/HDPE, because they are more flexible and easy to joint. Instead of a GMB as impermeable layer could be used a geosynthetic clay liners (GCLs), which is composite materials consisting of bentonite and geosynthetics that can be used as an infiltration/hydraulic barrier too.

2.4.2 DRAINAGE GEOCOMPOSITES

In the landfill top cover it is necessary to give particularly attention to the drainage geocomposites (GCD); tridimensional products obtained by the combination of two or more geosynthetics. The prevalent function is the drainage of liquids and leachate in the waste body.

Geocomposite drains consist in two or more geosynthetics, can be used for separation, filtration or drainage. The components are often: geotextile and geonet**.** The first one used for separation of different soil layers, with different particles size or as protection for the GMB. The first function of geonets in landfill is improving the drainage of water or leachate as for the geopipes.

In this thesis, particularly attention is given to the GCD because its use is growing in geotechnical applications.

In a GCD two principal parts can be distinguished:

- Internal drainage component;
- External seeping/isolating part.

The most important property of GCD is the drainage capacity in the planar plane under given loading and hydraulic conditions.

In landfill top cover the GCD should also have a high resistance to chemical and bacterial attacks. Often geocomposites are used on inclined surface and covered with soil, for these reasons they should be strongly resistant, during the installation and the exercise period.

2.5 TOP COVER DESIGN WITH GEOSYNTHETICS

Five main layers compose landfill top cover: erosion; protection; drainage; barrier and gas collection layer. (Floss, R.; Fillibeck, J. (1998)) (Figure 2.5.-2.7.)

The first one thickness is from 0.15-0.60 [m]. It allows the vegetation growth and that gives to the landfill a pleasant aspect. It also minimizes wind and water erosion and protects the lower layers by the temperature excursions. It is composed by natural soil and geosynthetics.

The protection layer is a real separation between the waste and the natural soil, it is necessary to prevent the interaction of trees and animals with the waste. This layer is also a protection for lower layers by drying and freezing.

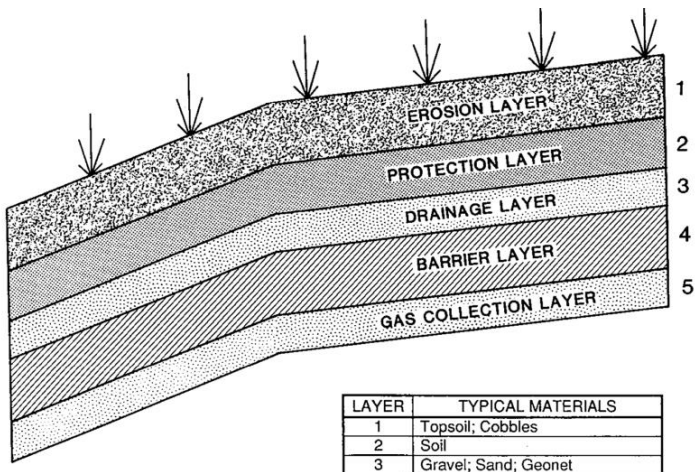

LAYER	TYPICAL MATERIALS
1	Topsoil; Cobbles
2	Soil
3	Gravel; Sand; Geonet
4	Compacted clay; Geomembrane; Geosynthetic clay iner
5	Gravel; Sand; Geonet; Geotextile

Figure 2.5. Top cover system of a landfill
(P. Simonini, corso di “Geotecnica nella difesa del suolo”, UNIPD)

The drainage layer principal aim is to drain the excessive of precipitations, collected with a specific system. It is made by sand, gravel or geonets in collaboration with geotextiles and geocomposite. The hydraulic conductivity has to be more than 10^{-2} [cm/s] with a minimum inclination of 2%. (Figure 2.6.)

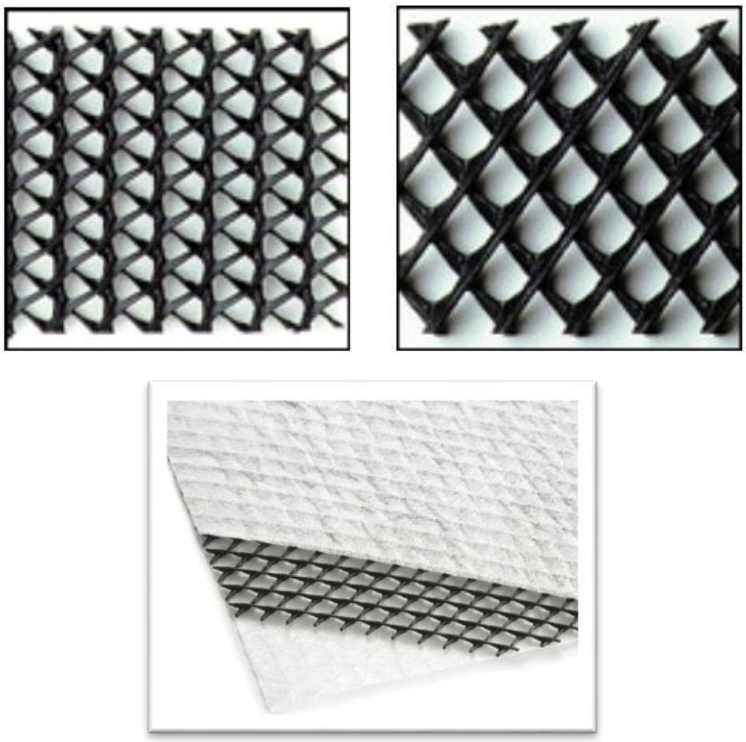

Figure 2.6. Geonets and Geocomposite used in the drainage layer

The principal aim of the barrier layer is to reduce the water infiltration in the waste body and control the gas. The materials used are clay, geomembranes and geocomposite (bentonite). It is often employed a clay layer (0.3-0.6 m) with a low hydraulic conductivity but there are some disadvantages:

- Difficult compact action;
- Danger of freezing and drying with resulting cracking;
- Damage due to different settlements;
- Difficult reparability process.

Conversely, using geomembranes with a better resistance to humidity and temperature, it is possible to have the following problems:

- Damaging problems;
- Ageing of the geomembrane;
- Low friction angle between geombrane and soil.

The last layer is necessary to collect the gas.

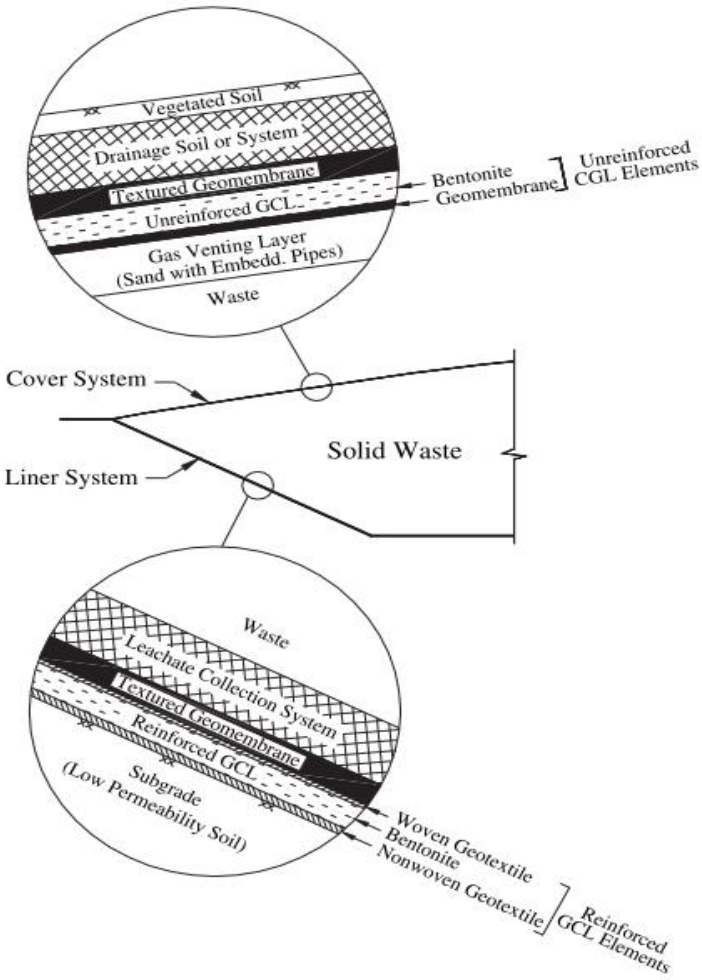

Figure 2.7. Examples of GLS (Eid, Hisham T.2011)

The following design principles have to be considered for a landfill top cover design according with the standard (EN 13257/65, GLR (1993): Geotechnics of landfill design and remedial work – Technical recommendations. Ed: Ger- man Geotechnical Society. Ernst und Sohn, Berlin):

- For sealing systems on slopes, the inner and outer stability must be proven. The inner stability is substantially determined by the shear behaviour of the single layers of the system. The outer stability can be improved by the absorption of tensile forces from the single layers. The interlocking between the single layers is decisive for the transmission of forces between the layers and therefore for the absorption of tensile forces.
- Load dependent deformations, affecting the function of the sealing system, have to be avoided.

- Resistance to sliding shall be ensured for all interfaces and boundary surfaces, for all loading conditions due to the intrinsic weight of the waste and also external loads. These calculations should consider the construction, operational and post-closure phases of the landfill.
- In addition shear resistance should be confirmed for each interface between the individual sealing components that the maximum transferable shear strength is capable of taking the tension from downslope stresses with the required factor of safety, (Giroud, et al., 1995). The sealing elements should be designed to transfer shear stresses only. The development of unacceptable tensile stresses can be eliminated by geosynthetic reinforcing.

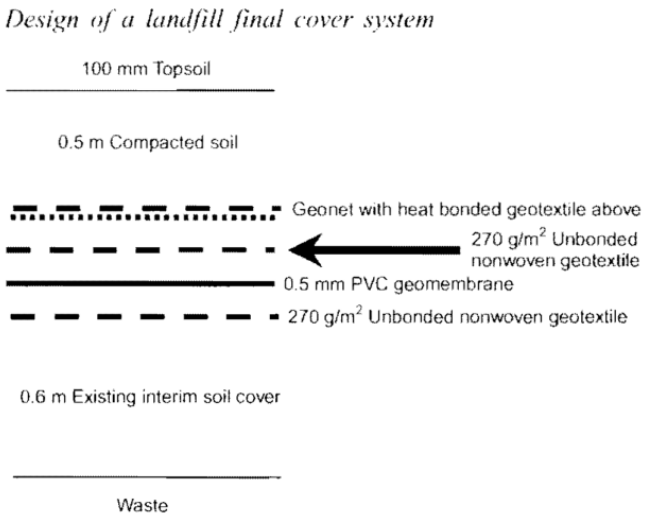

Figure 2.8. Example of a Landfill top cover system
(Stark, T.D. & Newman, E,J. (2010))

Figure 2.8. shows a design for a landfill top cover following Stark and Hillman (2010) indication. The system included two unbounded nonwoven geotextiles, a 0.5-mm (20 mil) thick polyvinyl chloride (PVC) geomembrane, and a single- sided drainage composite. The single-sided drainage composite was a geonet with a nonwoven geotextile heat bonded to the top side of the geonet. A double-sided drainage composite is a geonet with two nonwoven geotextiles heat-bonded to the top and bottom sides of the geonet. In this case, a single-sided drainage composite was used with an unbounded geotextile below the geonet and not a double-sided drainage composite. The unbounded geotextiles above and below the PVC geomembrane were designed to provide a cushion between the geomembrane and the overlying geonet and the underlying interim soil cover. respectively.

Fortunately, the unbounded nonwoven geotextile underlying the geonet was removed from the design in the first addendum to the contract bid package. (Stark, T.D. & Newman, E,J. (2010))

To design and use geosynthetics in landfill structure, the following consideration should be regarded (GLR (1993): Geotechnics of landfill design and remedial work – Technical recommendations. Ed: Ger- man Geotechnical Society. Ernst und Sohn, Berlin)

:

- The design can be based either on an analytical (reinforcement, drainage) or a semiempirical (filtration, protection) approach. There is a need to guarantee the long-term performance of geosynthetics. The properties of geosynthetics may be affected by induced mechanical stresses, radiation, temperature, chemicals and micro-organisms.
- Geomembranes are used as structural components, either in composite base liner or capping systems, in connection with their function as fluid (liquids or gases) barrier. The integrity of geomembranes is related to requirements, which can be specified by design calculations or empirical rules. The geomembrane has to be protected against load dependent damages by a protection layer.
- Geosynthetic clay liners (GCL) are alternative sealing elements in particular for capping sealing systems.
- In all cases where geotextiles are used as drainage layers, adequate transmissivity must be guaranteed under the imposed load at every stage of the landfill operation and after closure. A high factor of safety on the transmissivity should be incorporated into the design required as long term performance.
- In landfill sealing systems geotextile filters can be dimensioned using known rules. For a depth filtration the pore structure of the geotextile should be chosen to be as open as possible. The requirements must be set up for the specific filtration length and the thickness of the geotextile.

The function and effective operation of geotextile filters can be complicated by the nature of the material to be filtered, the liquids and the gases. For geotextile filter layers in landfill capping systems in particular, a safe filtration effect even in deformed condition must be proven.

3. TOP COVER PROBLEMS

In the landfill top cover different critic surfaces could be defined, especially at the interfaces between different materials, for examples geosynthetic-geosynthetic or soil-geosynthetic. The preservation and stability of the different interfaces are two of main issues in the landfill top cover design. Top cover problems can be divided in two categories: settlements and instability.

3.1. SETTLEMENTS

The main mechanisms involved in the landifill settlements can be describes as: physical compression due to mechanical distortion, bending, crushing and re-orientation; raveling due to migration of small particles into voids among large particles; viscous behavior and consolidation involving both solid skeleton and single particles; physical and chemical changes such as corrosion and oxidation and biodegradation of organic components.

As proposed in literature, three settlements stages could be discerned dependent by the time (Skempton, A.W., (1951))

- Step 1: “**instantaneous settlement”,** takes place instantaneously during the filling by waste and is analogous to the elastic compression of soil.
- Step 2: **“primary settlement”**, corresponds to a stress dependent mechanical compaction due to dissipation of pore water and gas from the avoid spaces. This

component of settlements occurs rather quickly after the waste disposal is completed.

- Step 3: **"secondary settlement"**, is a non-stress dependent long-term creeping biological degradation phenomenon. The secondary settlement is rate limited but can takes place over many years and maybe be episodic.

The facility must be designed to account for the stresses and strains that result from settlement occurring in the foundation and waste mass. Settlement is considered completed when at least 100% of primary settlement is occurred and the secondary settlement is expected using a time-frame of 100 years. (Sowers, G. F., (1973), Wall, D. K. and Zeiss, C., (1995))
Settlement analyses also include any differential settlement across a facility to ensure that engineered components will not be damaged, liquid drainage paths will be maintained, and the facility will satisfy design requirements, not only at the time of construction but also after differential settlement is complete.

Since the solid waste is an highly heterogeneous material and can settle either due to biodegradation of waste, or by its own weight or by overlying pressure applied above the barrier, development of differential settlement within the landfill area is common. The excessive differential settlements can result in the development of tension cracks in the soil barrier or tearing of geomembrane or displacement of bentonite from GCL, near the zone of sharp curvatures there by resulting in loss of integrity of the whole cover system (Jessberger, H.L., Stone, K.J.L., (1991); Fox, P.J., DeBattista, D.J., Mast, D.G., (2000); Keck, K.N., Seitz, R.R., (2002); Sharma, H.D., De, A., (2007)).
Once the geomembrane is not in contact with soil barrier, compatibility between it and the soil barrier will be lost, the soil barrier behaves like an independent barrier and hence effectiveness of the composite liner system is compromised. If this situation occurs in a differentially settled zone, the separated soil barrier tends to experience cracking and may lose its integrity as shown in Figure 3.1.

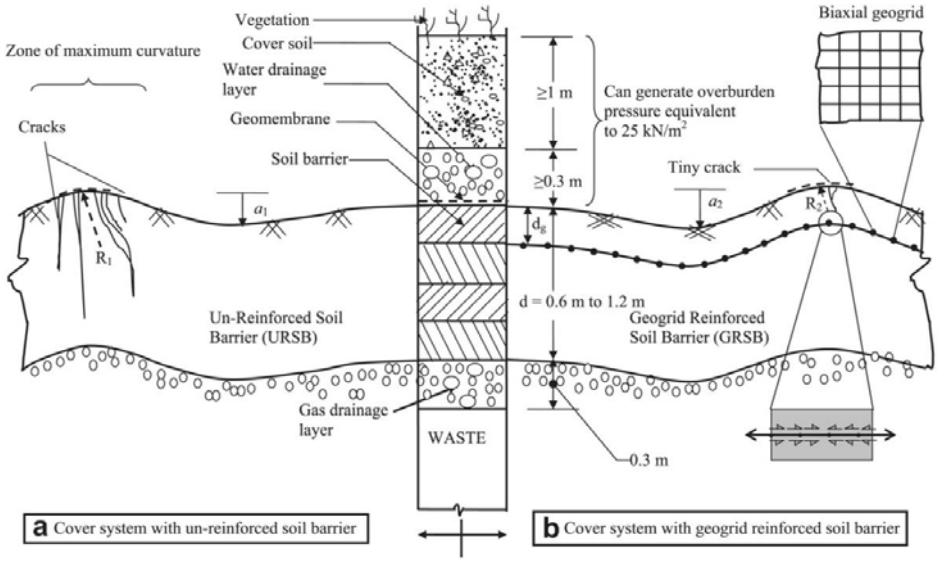

Figure 3.1. Schematic representation of flexural distresses in cover system subjected to differential settlements (Rajesh, S; Viswanadhanìm, B.V.S, (2010))

3.2. SLOPE STABILITY

Disposal of municipal solid waste in engineered landfills has become a common practice. The typical geometry of an engineered landfill consists of having very high and steep slopes, to contain great amount of waste in less space. This geometry helps slope failures (Figure. 3.2.). Therefore the major problem for landfill slopes is their stability.

To design landfill geometry, it is necessary to consider the height and the slope angle. The slope inclination and the kind of ground upon which the landfill is placed are also important. Increasing height, steeper cover angles and slopes must be compensated for to insure stability.

Furthermore landfill must be designed and constructed to prevent contamination of the surrounding environment. For this reason, composite liner systems are usually used.

In order to guarantee the stability of these systems, the slope inclination, the weight of the soil layers and the shear strength between geosynthetic-geosynthetic and geosynthetic-soil interfaces must be taken into the account.

Figure 3.2. Typical landfill geometry with steep slopes.

A liner system, GLS (geosynthetic lining system), generally consists of one or more soil and/or geosynthetic materials such as geomembranes, geotextiles and geonet in contact, as already explained. One of the main problems is the sliding of one layer to another. In fact, each liner system component can slide, depending on the force applied to it. (Figure. 3.3.). Generally an interface can slide if the shear resistance is less than the shear forces induced by the material above it. Landfill top cover system faces similar concerns; some or all of the cover may slide off the waste, because the stresses applied are low, in order to 5-10 [KPa].

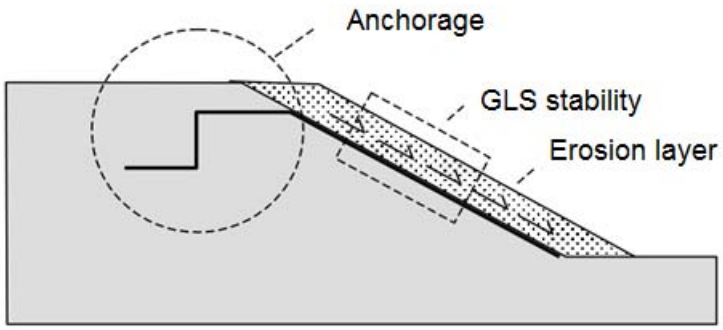

Figure 3.3. Main issues related to the stability of Geosynthetic Lining Systems on landfill slopes

3.2.1 PARAMETERS INFLUENCING SLOPE STABILITY

As slope incline and length increases, the shear forces caused by gravity increase. The shear forces must be resisted by the shear strength of the weakest soil-geosynthetic or a geosynthetic-geosynthetic interface in the cover system. If the shear forces are greater than the friction of the weakest interface, sliding will occur and lead to geosynthetic tears or slope failure. To design a landfill for slope stability it is important to analyze the elements that influence stability.

First of all the geometry and the anchorage are two of the most important parameters in slope stability analyses. After that, the foundation soils must be capable of supporting the landfill weight. In fact, failures occur when foundation soil beneath or adjacent to the landfill yield collapses because of the applied load. The applied load corresponds to the material weight above the foundation soil.

Obviously also the landfill liner system construction is important to slope stability. The constituent materials shear strength and the interface friction between the layers determine how susceptible the slope is to lateral movement along a geosynthetic interface in response to forces generated by the waste weight.

The geosynthetic complex is a preferential slip surface for layers that covers and protects it. The stresses applied to the GLS interface are therefore relatively weak. In these conditions, the characterization of these interfaces and in particular the measurement of the friction angles is necessary to provide slope stability. This procedure will be better explained in the next chapters. (Chapter 5 and 6).

Another parameter that may be considered is the influence of the water. Water can affect significantly the stability of the soil veneer. The presence of liquids, as water and lecheate, increases the weight of soil above the geosynthetics and reduces the effective stresses and shear resistance. Water flow significantly reduces the factor of safety for slip surface located above geomembranes whereas it reduces only slightly the factor of safety for slip surface. (J.P. Giroud, R.C. Bachus and R. Bonaparte (1995))

3.3. STABILITY OF GEOSYNTHETIC LINING SYSTEMS (GLS) ON SLOPE

The design of veneer slopes poses significant challenges to designers. A review of analyses for veneers reinforced using geosynthetics and reinforcement inclusions is presented in this section.
To verify slope stability, geotechnical engineering proposed numerous analytic methods. At the beginning were be used a conventional limit equilibrium method such as Bishop (1955) and Janbu (1973) or approximate methods such as the charts proposed by Taylor (1973). The use of geosynthetics often introduce potentially weak planes into the system and require special consideration.

Giroud and Ah-Line proposed one of the first discussion about cover soil stability above geosynthetic materials in 1984. They gave an equation for a very general case taking into account the reinforcing effect of the toe of the slope, the interface shear strength along the slip surface, the tension in the geosynthetic and even the stability of the anchorage of the geosynthetic on the top of the slope. This method can be used instead of the thickness of the soil is uniform or not.

Each methods is referred to a factor of safety generally defined by equation 3.1:

$$FS = \frac{Available\ interface\ shear\ strength}{Required\ strength\ for\ equilibrium} \tag{3.1}$$

3.2.1. INFINITE SLOPE APPROACH

Contemporaneously Martin & Koerner discussed this issue in 1985 (Figure 3.4.), using infinite slope approach they presented the factor of safety (Equation 3.2) against the failure of a uniform cover soil as:

$$FS = \frac{N\ \tan\delta}{W\ \sin\beta} = \frac{W\ \cos\beta\tan\delta}{W\sin\delta} = \frac{\tan\delta}{\tan\beta} \tag{3.2}$$

Where:

W is the top cover weight; N the normal load; β the slope inclination angle and δ the interface friction angle between the geosynthetic and the cover soil.

After that Giroud and Beech, 1989, published a detailed analysis of the three mechanisms involved in stability of layered system on slope:

- The interface friction angle along the slip surface;
- The toe reinforcing effect that results from the internal friction angle of the soil components of the layered system, located above the slip surface, and the tension provided by tall geosynthetic located above the slip surface.

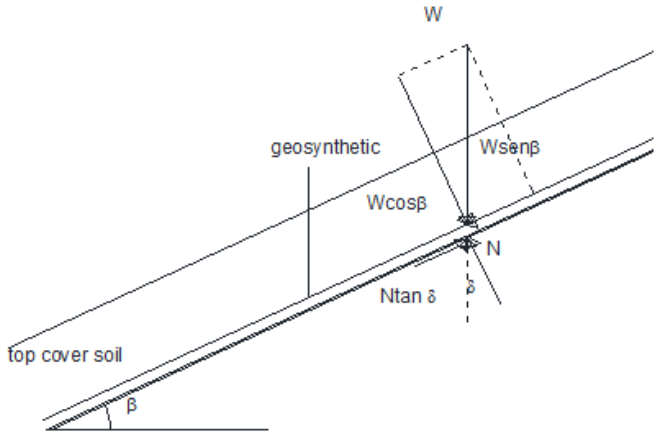

Figure 3.4. Infinite slope approach (Koener (1985))

3.2.2. FURTHER APPROACHES

Koener and Hwu (1991) (Figure 3.5.) further proposed a model to assess the tension in geosynthetic due to unbalance interface shear forces. By assuming uniform mobilisation of the interface shear strengths along the GMB, they developed an expression for the tensile force per unit width of slope as follows (Equation 3.3):

$$T = [(\alpha_u - \alpha_l) + \gamma h \cos\beta (\tan\delta_u - \tan\delta_l)]L \quad (3.3)$$

Where γ is the unit weight, h thickness of cover soil, L slope length, β slope angle, δ_u and δ_l the interface angle of the upper and lower interface and α_u and α_l the apparent cohesion of the upper and the lower interface.

Balancing the vertical force we obtain an equation of the following type: $ax^2 + bx + c$; in function of the safety factor (Equation 3.4):

$$aFS^2 + bFS + c = 0 \tag{3.4}$$

Using the traditional solution of a second grade equation 3.5:

$$FS = \frac{-b \pm \sqrt{b^2 - 4ac}}{2a} \tag{3.5}$$

With:

$$a = (W_a - N_a \cos\beta)\cos\beta \tag{3.6}$$

$$b = -\left[(W_a - N_a \cos\beta\,)\sin\beta \tan\varphi + (N_a \tan\delta + C_a)\sin\beta\cos\beta + \sin\beta(C + W_p + \tan\varphi)\right] \tag{3.7}$$

$$c = (N_a \tan\delta + C_a)\sin 2\beta \tan\varphi \tag{3.8}$$

Where:

W_a and W_p are respectively the active and passive wedge weight; N_a is the normal load of the active wedge; C_a adhesion between soil and geosynthetic; C adhesion force along the passive wedge; β the slope inclination angle and δ the interface friction angle between the geosynthetic and the cover soil.

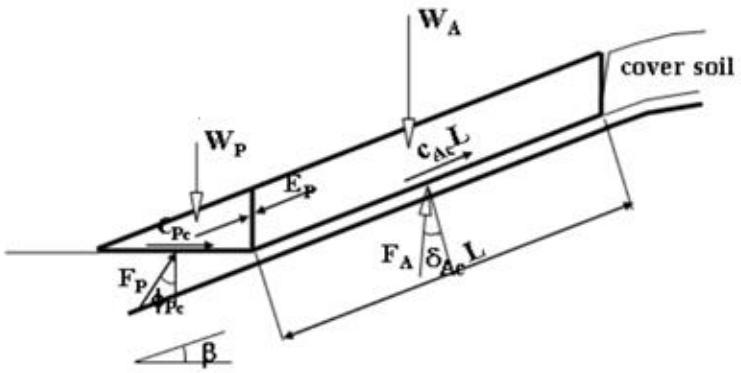

Figure 3.5. Typical stability design method for GSL (Koener et al. 1991)

At last, Giroud proposed the most completed method in 1995.
This method needs only three elements to be considered in the analysis of the stability of a geosynthetic-soil layered system on slope:

- The slip surface;
- The soil located above the slip surface;
- Geosynthetics, if only, located above the slip surface.

The main benefit of this method is that the factor of safety is generally expressed as follows in Equation 3.9:

$$FS = \frac{F_{R,slope}}{F_{D,slope}} \tag{3.9}$$

Where $F_{R,slope}$ is the projection on the slope of the resisting forces and $F_{D,slope}$ the projection on the slope of the driving forces. Figure 3.6. describes the two different geometrically definitions of the safety factor: the first one with FS >1, in favor of safety, and au contrary the second one with FS < 1.

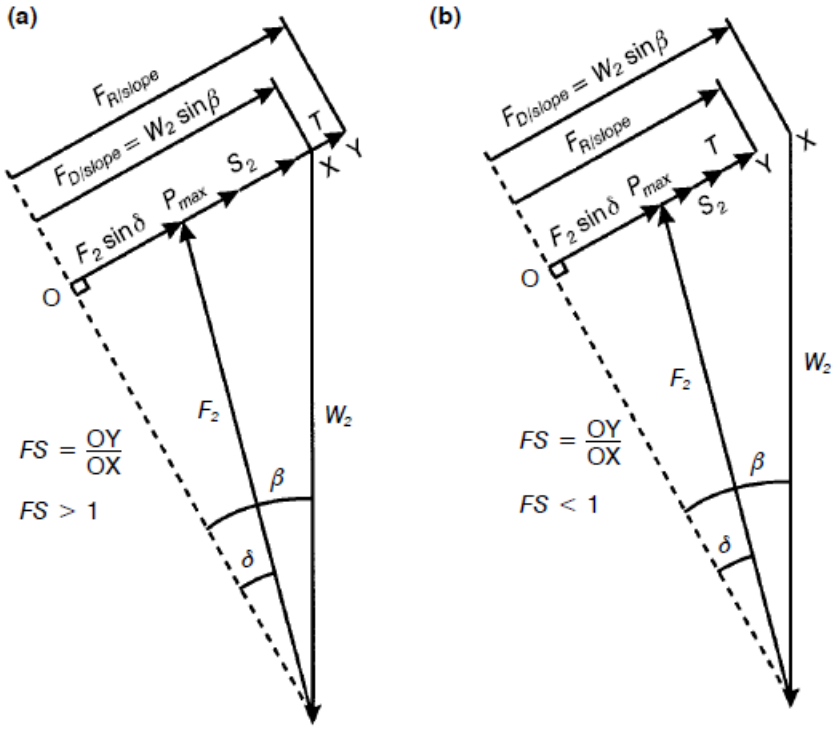

Figure 3.6. Illustration of the safety factor (a) FS>1; (b) FS <1 (Giroud et al. 1995)

The safety factor equation consists in the sum of five terms (Equation 3.10 and Table 3.1): the interface friction angle, interface adhesion along the slip surface, the internal friction angle of the soil component of the layered system located above the slip surface, the cohesion of soil component of the layered system located above the slip surface and the tensile strength of the geosynthetic located above the slip surface. (Figure 3.6.)

At the end Giroud safety factor can be express as follows:

$$FS = \frac{\tan\theta}{\tan\beta} + \frac{a}{\gamma t \sin\beta} + \frac{t}{h}\frac{\sin\emptyset}{\sin(2\beta)\cos(\beta+\emptyset)} + \frac{c}{\gamma h}\frac{\cos\emptyset}{\sin\beta\cos(\beta+\emptyset)} + \frac{T}{\gamma h t} \quad (3.10)$$

Where: t is the soil layer thickness; γ is the unit weight of the soil; ϕ is the internal friction of the soil; c the cohesion of the soil; a the interface adhesion along the slip surface; T the tension in the geosynthetics above the slip surface; h height of the slope; β slope angle and δ the interface friction angle along the slip surface.

Table 3.1. Effect of different terms in the factor of safety estimated using Giroud et al (1995a) methodology (adopted from Giroud et al 1995a)

Slope	Infinite slope		Additional terms for finite slope		
Mechanism	Interface shear		Toe buttressing		Geosynthetic
Parameter	Interface friction	Interface adhesion	Soil internal friction	Soil cohesion	Geosynthetic tension
Symbol	δ	a	ϕ	c	T_a
Factor of safety	$\frac{\tan\delta}{\tan\beta}$	$+\frac{a}{\gamma\ T\sin\beta}$	$+\frac{T}{H_T}\frac{\tan\phi/(2\sin\beta\cos^2\beta)}{1-\tan\beta\tan\phi}$	$+\frac{c}{\gamma\ H_T}\frac{1/(\sin\beta\cos\beta)}{1-\tan\beta\tan\phi}$	$+\frac{T_a}{\gamma\ H_T\ T}$
$\phi\nearrow$	$\leftrightarrow$	$\leftrightarrow$	$\nearrow$	$\nearrow$	$\leftrightarrow$
$\beta\nearrow$	$\searrow$	$\searrow$	$\searrow$	$\searrow$	$\leftrightarrow$
$h\nearrow$	$\leftrightarrow$	$\leftrightarrow$	$\searrow$	$\searrow$	$\searrow$
$\gamma\nearrow$	$\leftrightarrow$	$\searrow$	$\leftrightarrow$	$\searrow$	$\searrow$
$t\nearrow$	$\leftrightarrow$	$\searrow$	$\nearrow$	$\leftrightarrow$	$\searrow$

Notes:
H_T: *total height of the slope*; T_a: *allowable tensile strength of geosynthetic reinforcement*; *Influence of FS*: $\nearrow$ *increasing*; $\searrow$ *decreasing*; $\leftrightarrow$ *no influence*; ? *either increasing or decreasing*.

3.2.3. INFLUENCE of the CHATERISTICS of the LAYERED SYSTEMS on SLOPE STABILITY

The layered system is characterized by the following parameters (Giroud et al. (1995)):

- Geometry: (Figure 3.7., 3.8.)
  - slope angle β;
  - slope height h;
  - Thickness of the soil layer above the slip surface t.

- Properties of the soil layer:
  - Unit weight γ;
  - Internal friction angle Φ;
  - Cohesion c.

- Geosynthetic(s):
  - T, which is the sum of the tension developed in the geosynthetics located above the slip surfaces at the strain considered in the stability analysis.

- Interface properties: (Figure 3.8.)
  - **Interface friction δ;**
  - Interface adhesion a.

In this research, particularly attention should be given to the definition of the parameter **δ,** the interface friction angle between the different geosynthetics.

Figures 31 shows a comparison between the slope stability safety factor obtained by Koener and Giroud methods, referring to characteristics of the layered system.

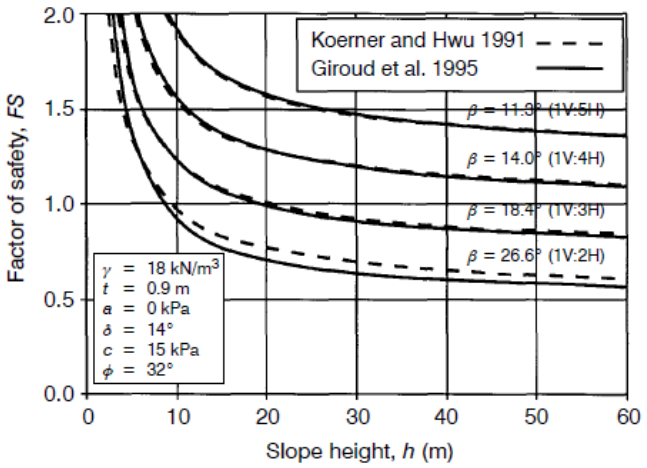

Figure 3.7. Influence of the slope height and angle on the safety factor, and comparison between Koener&Huw and Giroud safety factor. (Giroud et al. (1995))

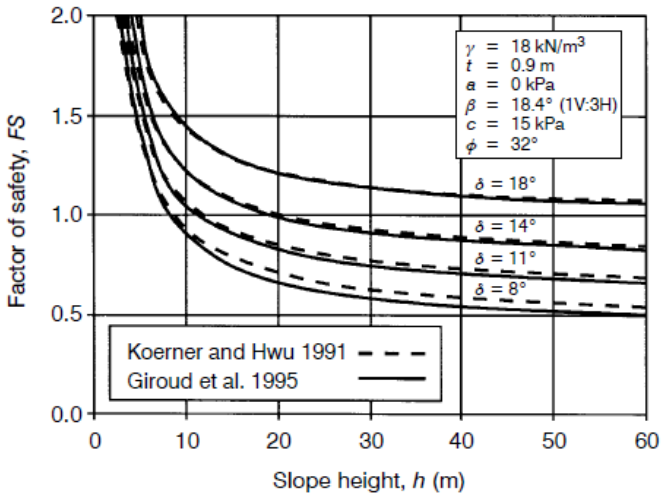

Figure 3.8. Influence of the slope height and the interface friction angle, and comparison between Koener&Huw and Giroud safety factor. (Giroud et al. (1995))

As already explained the design methods of layered systems on landfill slopes, consider the failure calculation or are based on the limit equilibrium analysis (Giroud and Beech 1989; Koener and Hwu 1991; Giroud 1995). Their principal limitation is that they do not

consider the compatibility between forces and displacements, notably at the interface. (Giroud et al.,1989). For this reason, design methods of landfill slopes require the proper assessment of the friction angles between different geosynthetics (Briançon et al.,2002). In fact, preferential failures planes are generally located at the interface of these materials.

A waste containment facility side slope liner system must not only provide a sound hydraulic/gas barrier but must also be structurally stable during all phases of a project.
Thereby to design properly the liner and the cover system in a landfill, it is necessary to investigate the friction between the geosynthetic materials. Moreover, a careful estimation of applied stresses is needed, in case of liner and cover systems, as base for a safe construction of the landfill.
Several laboratory-testing techniques have been introduced during the years to study the friction angles in geosynthetic interfaces. The most common is the “direct shear box”, but concerning the specific case of landfill covers, the “inclined plane apparatus” seems the more appropriated to investigate interface friction at low vertical stress (Briançon et al., 2002)
A more deepened description of test methods, analysis and results for the determination of the interface friction angle will be given in the following chapters. (Chapters 5 and 6).

4. FRICTION

As referred in the Oxford Concise dictionary the friction is:

- the resistance that one surface or object encounters when moving over another: a lubrication system which reduces friction;
- the action of one surface or object rubbing against another: the friction of braking;
- Conflict or animosity caused by a clash of wills, temperaments, or opinions: a considerable amount of friction between father and son.

The origin is dated somewhere about the 16th century (denoting chafing or rubbing of the body or limbs, formerly much used in medical treatment).

The important definition for us is the first one, where friction is interpreted in a physic and mechanic way. The friction is always opposite to the motion or attempted motion of one surface across another one. The friction force depends on the amount of contact force pushing two surfaces together. (Galligan, J.M., McCullough, P.(2001))

4.1. FRICTION GENERATILIES

When an object attempts to slide across another, the contact force is called "Normal Force" (Figure 4.1.) and its direction is always perpendicular to the plane, instead of the friction force that is the parallel component of the normal force amplified with a coefficient, identified with μ.

$$F = \mu N \tag{4.1}$$

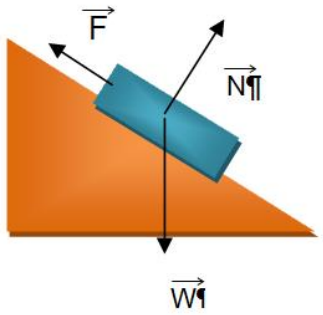

Figure 4.1. Free body diagram

Friction can be divided in static friction and dynamic (or kinetic) friction; distinction made for the first time by Johann Andreas Van Segner (1704-1777). The friction coefficient is a number, which represents the friction between two surfaces, and it depends on the surfaces chosen and also on the kinematic conditions.

The static friction is always present when two object are in contact. It is motionless, and it increases with the increase of tangential displacement up to the value necessary to initiate the slide (Figure 4.2.). The dynamic friction is related to the motion. The slide can be divided in micro and macro sliding. The micro sliding occurs when the bodies are at rest, it is a sort of preliminary displacement. When the micro sliding becomes macro sliding the static friction becomes dynamic friction, and it the maximum value of the static force is reached.

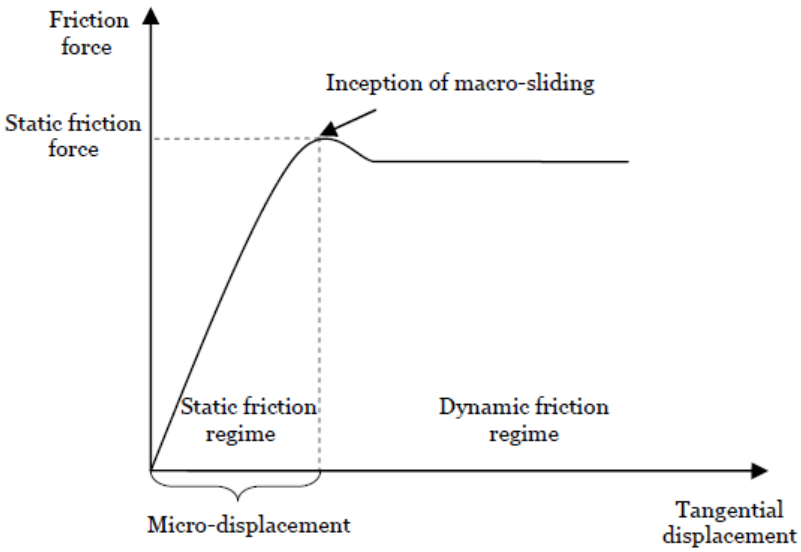

Figure 4.2. Friction force in different kinematic conditions.

(E. Deladi)

Friction has been explored since ancient times. The first recorded studies on friction are dated in fifteenth century and belong to Leonardo da Vinci. Afterwards Guillaume Amontons (1663-1705), elaborating Da Vinci’s studies, introduced the well-known laws of friction:

1. The force of friction is directly proportional to the applied load
2. The force of friction is independent of the apparent area of contact.

Almost one century after, Coulomb introduced the third friction law:

3. Kinetic friction is independent of the sliding velocity.

However, these laws are not universally valid for all material couples. In fact, for examples the coefficient of friction between polymers sliding against themselves or against metal or ceramics decreases by increasing the normal stress. At higher velocity the polymers becomes stiffer, then the contact area decreases determining a reduction of the coefficient of dynamic friction, and this contrasts the third law. As shown in Figure 4.3. the dynamic friction coefficient is related to the velocity in polymers. (E. Deladi. (2006))
Therefore, the friction laws cannot be valid for polymers and other couples of material with particular viscoelastic proprieties.

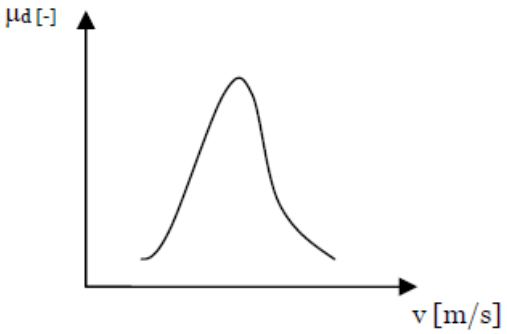

Figure 4.3. Dependence of coefficient of dynamic friction on velocity (polymeric friction) (E. Deladi)

For certain applications it is more useful to define the friction in terms of the maximum angle before which one of the items will begin sliding. This is called the angle of friction or friction angle:

$$\tan\theta = \mu_s \tag{4.2}$$

Where θ is the angle from the vertical.

4.1.1. STATIC FRICTION

The static friction is always present when two objects are in contact. At the beginning, there is a micro-sliding regime at the interface between them and the static friction force reaches the maximum when the motion starts.
Different parameters can be indicated responsible for the static friction, in fact, the static coefficient is not a constant value but it depends on the material in contact.
According to Nolle and Richardson studies also the pressure influence the static friction. At low pressure, the coefficient of friction is constant and it starts to change when a higher pressure is applied.
The roughness is a several parameter that is important in the analysis of static friction, as the presence of asperities on the surface that slack the motion. Roughness depends on the plastic index of the material that depends on material proprieties. Smooth surface has a low plasticity index and the contact between the surfaces is almost elastic for polymeric materials. (Broniec, Z., Lenkiewicz, W., (1982); Roberts, A.D., Thomas, A.G.)
Another parameter that could influence the material proprieties is the temperature. The effect of the temperature on the static friction was investigate by Gallian and McCullough (2001).

4.1.2. DYNAMIC OR KINETIC FRICTION

When the static friction force between two objects reaches its maximum, the macro-sliding regime starts and the friction became kinematic. It is directly involved in the object motion, in the materials used, and in the atomic interaction forces between them.
In contrast with the Coulomb's law μ_k, the kinetic coefficient could be also related to the movement velocity, especially when the surface is a polymeric material. (Johnson, K.L.)

4.1.3. FRICTION AND ADHESION

The earliest work dealing with the relationship between the proprieties of interface layer and the resulting frictional behaviour is from Tabor (1950). After that Bowden and Tabor (1964) considered the more complex description of the friction phenomena in polymeric materials. The increased complexity is due to three main factors: area of contact, geometry of the surfaces and load. The friction also depends by speed and temperature in a manner that reflects the viscoelastic proprieties of the polymers.

They explained that the kinetic friction force is composed by two components: adhesion and deformation. Depending on the materials in contact, these two factors can be caused by different mechanisms. Adhesion is not the only resistance encountered during the motion of one body over another. If one of the surfaces in contact is harder and rougher than the other one, the hard one will plough through the soft surface giving rise to the deformation term of friction.

The deformation component is caused by the delayed recovery viscoelastic behaviour of materials.

Generally is considered that a thin elastic layer of thickness joins two bodies.

Hereafter Ganghofler and Schultz (1997) investigated the relationship between adhesion and friction with a three-model body. They considered the presence of a third layer separating the two sliding bodies submitted to continuous damage (Figure 4.4.). Both the solids are considered linearly elastic, and the third is assume to behave as an isotropic plastic material.

Adhesion is sometimes considered as a damageable interface as shown in Rous studies.

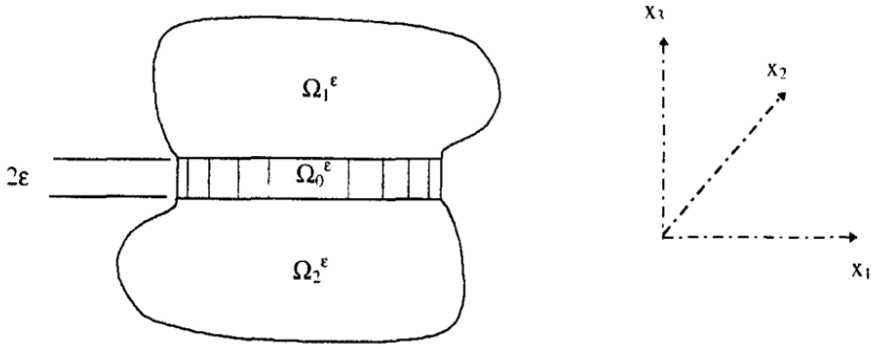

Figure 4.4. Contact between two solids involving a third intermediate layer.
(Ganghifler and Schultz, 1997)

4.2. INTERFACE FRICTION

In geotechnical engineering is often really important to define the friction parameters (soil internal angle and interface friction angle) taken into account in the design project. As already explained in Chapter 3, the interface between the different materials layers composing a multi-layered lining system often represent potential slip surfaces that need to be considered in slope stability analyses. Sometimes the shear strength is not sufficient to guaranties the stability, then is necessary to define a correct friction angle between the different interfaces.

The most common devices used to test the interface shear strength are:

1. Large scale direct shear box;
2. The conventional shear box;
3. The torsional or ring shear device;
4. The inclined plane device;
5. The cylindrical shear device.

Table 4.1 summarises the advantages and disadvantages of these devices. The range of interface strengths between geosynthetics and mineral liners or geosynthetics collected from available literature are given in Table 4.2. The range takes into the account the variability of the geosynthetics material testing conditions, testing protocols and testing equipment.

One of the major concerns with the use of geosynthetics in side slopes in their behaviour when subjected to shear forces. Their stability is controlled by the shear strength mobilized at the interface between various soil and geosynthetics and sometimes within the geosynthetics themselves (Bouazza, Zorneberg, Adam 2002)

Inclined plane test will be better described in the Chapert 5.

Table 4.1: summary of advantages and disvantages associated with test devices for measuring interface shear strength (from Gilbert et al. 1995; Shallenberg & Filtz 1996; Lalaratokason et al. 1991; Jones and Dixon 2000; Gourc et al 2001; Marr 2001; McCartney et al. 2002)

TEST DEVICE	ADVANTAGES	DISVANTAGES
Large scale direct shear box	Industry standard Large scale Large displacement Minimal boundary effects Expedient specimen preparation	Machine friction Load eccentric Limited continuous displacement Limited normal stress Expesive
Large displacement shear box	Large area of interface Capable of detecting and effects Determination of residual strength with a linear displacement device	Influence of end effects Availability
Conventional direct shear box	Experience with soil Inexpensive Large normal stress Expedient specimens preparation	Small geosynthetic experience base Machine friction Load eccentricity Small scale Limited displacement Boundary effects
Ring shear device	Unlimited continuous displacement	Machine friction Mechanism of friction not comparable to that exhibited in the field Small scale Expensive No lateral restrain for migration of plastic soil
Tilt table	Minimal machine effects Minimal boundary effects Ability to monitor tensile forces Low normal stresses Inexpensive	Limited continuous displacement Limited normal stresses No post peak behaviour
Cylindrical shear	Unlimited continuous displacement Better controlling confined during shearing Large sample size with less ledge effects Area of shear plane remains constant Constant direction of shear displacement	Availability Experience with dry materials only No restrain for migration of plastic soils

Table 4.2 Ranges for strength parameters of different interfaces in landfill liner systems (from Manassero et al 1997)

GEOSYNTHETIC - SOIL INTERFACE

Geomembrane (HDPE) - Sand	$\phi = 15°$ to $28°$
Geomembrane (HDPE) - Clay	$\phi = 5°$ to $29°$
Geotextile – Sand	$\phi = 22°$ to $44°$
Geosynthetic clay liner - Sand	$\phi = 20°$ to $25°$
Geosynthetic clay liner - Clay	$\phi = 14°$ to $16°$
Textured HDPE – Compacted clay	$\phi = 7°$ to $35°$ $c' = 20$ to 30 kPa
Textured HDPE - Pea gravel	$\phi = 20°$ to $25°$
Textured HDPE – Sand	$\phi = 30°$ to $45°$
Geotextile – Clay	$\phi = 15°$ to $33°$

GEOSYNTHETIC - GEOSYNTHETIC INTERFACE

Geonet – Geomembrane (HDPE)	$\phi = 6°$ to $10°$
Geomembrane (HDPE) – Geotextile	$\phi = 8°$ to $18°$
Geotextile – Geonet	$\phi = 10°$ to $27°$
Geosynthetic clay liner - Textured HDPE	$\phi = 15°$ to $25°$
Geosynthetic clay liner - Geomembrane (HDPE)	$\phi = 8°$ to $16°$
Geosynthetic clay liner - Geosynthetic clay liner	$\phi = 8°$ to $25°$ $c' = 8$ to 30 kPa
Textured HDPE – Geonet	$\phi = 10°$ to $25°$
Textured HDPE – Geotextile	$\phi = 14°$ to $52°$

This thesis focuses on the definition and analyses of the interface friction angle between different geosynthetics. The proper assessment of the interface friction allows understanding:

Therefore the interface friction is a fundamental issue to understand:

- Strength and functionality of geosynthetic materials;
- Stability problems in landfill top covers and lateral barriers.

Several studies have demonstrated that inclined plane and tilting table tests more appropriate then the direct shear box test for the characterization of the geosynthetics friction under normal stresses lower than 10 [KPa] (Carbone et al 2013, Briançon et al., 2011; Girard et al., 1990; Palmeira et al., 2002; Palmeira, 2009; Reyes-Ramirez and Gourc, 2003; Wu et al., 2008). Whereas the direct shear box test is more suited for higher normal stresses.

4.2.1. PARAMETERS INFLUENCING GEOSYNTHETIC INTERFACE FRICTION

Quite a lot of parameters are involved in the interface friction such as: material roughness, the contact area, temperature and humidity, velocity and kinematic conditions, time of reponse.
The material roughness has a first order effect on the strength and shear mechanisms. Testing geomembrane with different roughness, as smooth and textured, Frost (2001) found higher residual friction angles in textured GMB, even if these angles are primarily controlled by the macroscale surface roughness. Therefore, especially in test employing textured geomembrane in contact with geotextile, the main mechanism is due to the pulling out and tearing of geotextile fibers. As shown in Hebeler (2005) studies a better compliance and interaction between the geosynthetics is proposed, thanks to the surface roughness and clearly to the hook and loop interaction.

Other parameters, influencing the friction analysis, are: different normal loads, samples orientation and damage, thickness and mass per unit area of the material.

Summarizing the parameter that must be considered in the interface friction analysis, are:

- Material roughness;

- Extension of the surface contact area;
- Temperature and humidity;
- Velocity and kinematic conditions;
- Different normal loads;
- Samples orientation and damage;
- Samples thickness and mass per unit area
- Time of reponse (the length of time that the surfaces remained in contact).

Some of these parameters are fully treated in Chapter 6.

5. INCLINED PLANE TEST

5.1. INTRODUCTION

The inclined plane test is commonly performed to measure the interface shear strength between different materials as soil and geosynthetics. The mechanisms of interaction between these materials can be very complex, depending on their type and properties.

In landfill top covers is often used a geosynthetic lining systems (GLS). A liner system generally consists of one or more soil and/or geosynthetic materials such as geomembranes, geotextiles and geonet in contact. In these systems, the correct assessment of interfacial proprieties between the different geosynthetic surfaces is an important issue to prevent possible stability problems.

The mechanical characterization of the interfacial properties in landfill covers is an important issue concerning the stability of lining systems (Girard et al. 1990).

Studying the system stability generally requires calculating the friction angles of the different materials. This could carried out using a direct shear box or an inclined plane device. The classical or ring shear boxes require the application of high normal stress >50 [kPa] and the tests must be carried out on geosynthetic samples of small dimensions. This is not the case of GLS that is subjected, in landfill top cover systems, to low normal stress lower than 10 [kPa]. For these reasons, as demonstrated by several studies, (Izgin & Wasti 1998, Lalarakotoson et al. 1999, Wasti & Özdüzgün 2001, Palmeira et al. 2002, Palmeira 2009, Reyes Ramirez & Gourc 2003, Wu et al. 2008, Briançon et al. 2011); the inclined plane is nowadays recognized as one of the most suitable methods to analyse friction angle at the soil/geosynthetic interface under low normal stress.

The test procedure is based on the European Standard EN ISO 12957-2 (2005); which, as referred in: Gourc & Reyes Ramirez 2004, Pitanga et al. 2009, Briançon et al. 2011 researches, it is not an accurate method. For this reasons Gourc and Reyes Ramirez (2004) and Briançon et al. (2011) proposed two alternative test procedures in order to improve the evaluation of the interface friction angles.

The aim of this thesis and experimentation program is to provide a more precise friction characterization of the parameters that influence the geosynthetic interface friction angles using an inclined plane device in static conditions, involving different procedures and different materials.

The followings tables proposed a literally review of articles about Inclined Plane Test on geosynthetic interfaces. For each papers is reported the author, the Standard considered, the kind of test, the device employed, the test conditions, the materials tested, the stress applied and the angles calculated.

TEST AUTHOR	STANDARDS	TEST TYPE	BOX DIMENSIONS	TEST CONDITIONS	STRESS	MATERIAL TESTED	ANGLES DEFINED
BRIANCON ET AL. 2002	French STD AFNOR NF P 84-522 European STD prEN ISO 12957-2	**IPT** Large dimensions plane	LOWER BOX: L=2.0m; W=1.2m; H=0.3m UPPER BOX: L=1.0m; W=1.0m; H=0.5m	Plane speed: 0.5-3.2°/min Measurement of: -displacement of the upper box; -displ of the upper box and tension in GST; -force required to hold back the upper box	5 ±0.1[KPa]	Sand 3 smooth GMB 1 textured GMB 4 nonwoven GTX	$\tan\delta = \frac{W_s \sin\beta_r + f_r(\beta_r)}{W_s \cos\beta_r}$ $\tan\delta = \frac{W_s \sin\beta + f_r(\beta_r) - \Delta T_{gtx} - \Delta T_{gmb}}{W_s \cos\beta}$ $\tan\delta = \frac{W_s \sin\beta_r + f_r(\beta) - F_B}{W_s \cos\beta}$
PALMEIRA 2003		**IPT**	LOWER BOX: L=1.92m; W=0.47m; H=0.2m UPPER BOX: L=1.92m; W=0.47m; H=0.2m		2-7 ±0.1[KPa]	Sand 3 smooth GMB 7 types GEOGRIDS 1 nonwoven GTX	
PITANGA-GOURC 2009	European STD prEN ISO 12957-2	**IPT** (no large displacement)	LOWER BOX: L=0.8m; W=1.30m; UPPER BOX: L=1.0m; W=0.70m; H=0.18m	Plane speed: 3.°/min Measurement of: -displacement of the upper box every 0.05s; 3 different phase during the test: 1) Static phase; 2) Transitory phase; 3) Non stabilized sldiing phase	5 ±0.1[KPa]	1 smooth GMB 1 reinforced GEOMAT 3 GTX	$\tan\emptyset_0 = \frac{(m_b + m_s) g \sin\beta_0 - T}{m_s g \cos\beta_0}$ $\tan\emptyset_{50} = \frac{(m_b + m_s) g \sin\beta_{50} - T}{m_s g \cos\beta_{50}}$ $\tan\emptyset_{lim} = \frac{(m_b + m_s) g \sin\beta - T - (m_b + m_s)\gamma_c}{m_s g \cos\beta_{lim}}$

Notes

m_s and m_b soil mass and mass of the upper box; W_s weight of the soil in the upper box; T and ΔT: tangential force due to the guidance system and geosynthetic tensile strenght; β inclined plane inclination; δ and $\emptyset$ firction angles; λ parametre representing the friction plotted along the entire friction test in force procedure γ: upper box acceleration; $F(\beta)$ and $f(\beta)$ force required to hold back the upper box full or empty; g gravity acceleration

TEST AUTHOR	STANDARDS	TEST TYPE	BOX DIMENSIONS	TEST CONDITIONS	STRESS	MATERIAL TESTED	ANGLES DEFINED
REYES RAMIREZ GOURC 2003	European STD prEN ISO 12957-2	**SB IPT**	LOWER BOX: L=0.8m; W=1.30m; UPPER BOX: L=0.8m; W=0.18m;	Plane speed: 3°/min 2 different kinds of sliding: Sudden and gradual Replicable tests	<10 KPa]	Lower GST: Geospacer Upper GST HDPE GMB PP GMBSAND	Direct shear test angle $\delta_{50} = \delta_{standard}$ δ_{lim}
GOURC REYES RAMIREZ 2004	European STD prEN ISO 12957-2	**IPT**	LOWER BOX: L=0.8m; W=1.30m; UPPER BOX: L=0.8m; W=0.18m;	Plane speed: 3.0±0.5°/min 3 different phase during the test: 1) Static phase; 2) Transitory phase; 3) stabilized sldiing phase 4) 2 different kinds of sliding: Sudden and gradual	5 ±0.1[KPa]	sand Smooth GMB (HDPE) GEOSPACER GTX	$\tan \emptyset_0^{stand} = \tan \beta_0$ $\tan \emptyset_{50} = \frac{(m_b + m_s) g \sin \beta_{50} - T}{m_s g \cos \beta_{50}}$ $\tan \emptyset_{\lim(dyn)} = \tan \beta_{dyn} - \frac{1}{\cos \beta_{dyn}} \frac{\gamma_c}{g}$
BRIANCON ET AL. 2011	European STD prEN ISO 12957-2	**IPT** Large dimensions plane	LOWER BOX: L=2m; W=1.2m; UPPER BOX: L=1.0m; W=1m;	Plane speed: 0.5-3.2°/min 3 different phase during the test: 1) Static phase; 2) Transitory phase; 3) Non stabilized sldiing phase 2 different kinds of sliding: Sudden and gradual	5 ±0.1[KPa]	smooth GMB (HDPE; PVC; PP; EPDM) GCD	$\tan \delta = \frac{W_s \sin \beta \quad + f_r(\beta \quad) - F(\beta)}{W_s \cos \beta_r}$ $\tan \delta = \frac{W_s(\sin \beta \quad - \frac{\gamma}{g}) + f_r(\beta) - F(\beta)}{W_s \cos \beta}$

Notes:

m_s *and* m_b *soil mass and mass of the upper box;* W_s *weight of the soil in the upper box;* T *and* ΔT*: tangential force due to the guidance system and geosynthetic tensile strenght;* β *inclined plane inclination;* δ *and* $\emptyset$ *firction angles;* λ *parametre representing the friction plotted along the entire friction test in force procedure* γ*: upper box acceleration;* $F(\beta)$ *and* $f(\beta)$ *force required to hold back the upper box full or empty;* g *gravity acceleratio*

TEST AUTHOR	STANDARDS	TEST TYPE	BOX DIMENSIONS	TEST CONDITIONS	STRESS	MATERIAL TESTED	ANGLES DEFINED
PITANGA ET AL. 2011	European STD prEN ISO 12957-2	**IPT** Large dimensions plane	LOWER BOX: L=1.3m; W=0.8m; UPPER BOX: L=0.3m; W=0.8m;	Plane speed: 3.0±0.5°/min 3 different phase during the test: 1) Static phase; 2) Transitory phase; 3) stabilized sldiing phase 4) 2 different kinds of sliding: Sudden and gradual	5 ±0.1[KPa]	Smooth & textured GMB (HDPE) GCL GNT GTX	Phase 1: $\tan \emptyset_{50/std} = \tan \beta_{50}$ Phase 2 $\tan \emptyset_{lim} = \tan \beta_{lim} - \frac{1}{\cos \beta_{lim}} \frac{\gamma_c}{g}$ Phase 3 $\tan \emptyset_{\lim(dyn)} = \tan \beta_{dyn} - \frac{1}{\cos \beta_{dyn}} \frac{\gamma_c}{g}$
STOLTZ ET AL. 2012	European STD prEN ISO 12957-2	**IPT**	L=1.0m; W=1.0m;	Plane speed: 2°/min Using a spring system to obtain an almost static displacement Residual friction angle	4 ±0.1[KPa]	Textured GMB GTX	$\tan \emptyset_{stan} = \tan \beta_{50}$ $\tan \delta = \frac{W_s(\sin \beta \quad - \frac{\gamma}{g}) + f_r(\beta) - F(\beta)}{W_s \cos \beta}$ RESIDUAL FRICTION ANGLE
CARBONE ET AL. 2013	European STD prEN ISO 12957-2	**IPT** Large dimensions plane	LOWER BOX: L=1.3m; W=0.8m; UPPER BOX: L=0.3m; W=0.8m;	Plane speed: 3.0±0.5°/min 3 different phase during the test: 5) Static phase; 6) Transitory phase; 7) stabilized sldiing phase 8) 2 different kinds of sliding: Sudden and gradual Replicable tests	5 ±0.1[KPa]	Smooth GMB GTX GNT GCD	Standard angle $\tan \lambda_{50} = \tan \emptyset_{stand} = \tan \beta_{50}$ Phase 1: $\tan \lambda_0 = \tan \emptyset_0 = \tan \beta_0$ Phase 2 $\tan \lambda_s = \tan \emptyset_s = \tan \delta - \frac{1}{\cos \beta_s} \frac{\gamma}{g}$ Phase 3 $\tan \lambda_{lim} = \tan \emptyset_{lim} = \tan \beta_{lim} - \frac{F(\beta)}{W \cos \beta_{lim}}$

Notes:

m_s *and* m_b *soil mass and mass of the upper box;* W_s *weight of the soil in the upper box;* T *and* ΔT*: tangential force due to the guidance system and geosynthetic tensile strenght;* β *inclined plane inclination;* δ *and* $\emptyset$ *firction angles;* λ *parametre representing the friction plotted along the entire friction test in force procedure* γ*: upper box acceleration;* $F(\beta)$ *and* $f(\beta)$ *force required to hold back the upper box full or empty;* g *gravity acceleration.*

5.2. THE INCLINED PLANE TESTS

5.2.1. INCLINED PLANE DEVICE

According with the European Standard EN ISO 129 57-2 (2005) the apparatus is composed by two boxes, one for the upper and one for the lower layer. The minimum dimensions of the boxes are l_u=0.3 [m] in length along the displacement direction, and b_u=0.3 [m] in width for the upper box; while l_l=0.4 [m], b_l=0.325 [m] for the lower box.
In the case of geosynthetic–geosynthetic contact, the upper geosynthetic is fixed firmly to the upper box while the lower is fixed to the inclined support. The lower geosynthetic could be fastened by: sewing, gluing, using a rough support to increase the adherence between the geosynthetic and the plane, or anchoring the layer outside the contact area.

In literature, there are many examples of inclined planes. Reyes-Ramirez and Gourc, (2003), proposed a "modified inclined plane device" since it permits to testing geosynthetic interfaces under condition of large displacement. This modification concerns in the lesser longitudinal dimension (length L=0.18 m) of the upper box, and consequently of the geosynthetic sample, that slides over the lower geosynthetic fixed to the plane as already explained (width l_s=0.80 m, length L_s=1.30 m).
Besides the characteristic configuration of the conventional inclined plane equipment used for the interface geosynthetic/geosynthetic (rigid support, motorized system of inclination β, inclination β, and displacement δ sensors), the modified equipment has the following elements:

- A mobile metallic plate that receives the upper geosynthetic sample, which is glued on a wooden plate of surface S.
- A wooden plate with a length in the direction of the sliding, L, of 0.18 m and width, l, of 0.70 m.
- Metal plates with dimensions that are equal to those of the wooden plate (surface S=0.18*0.70 m), height=0.02 m, weight W=216 N and that serve as overload.

It also possible to replace the upper box with another one that can be filled by soil to test a soil-geosynthetic interface.

During the test the normal stress (<10 kPa) must be applied to obtain a regular distribution on the entire surface of the specimen and the plane tilts slowly and at a constant rate, i.e. $d\beta/dt=3.0\pm0.5°/min$ where β is the plane angle related to the longitudinal position.

This campaign program was carried out using the "Modified Inclined Plane Device" (Figure 5.1.), in order to test not only the European Standard but also the others procedures proposed in literature.

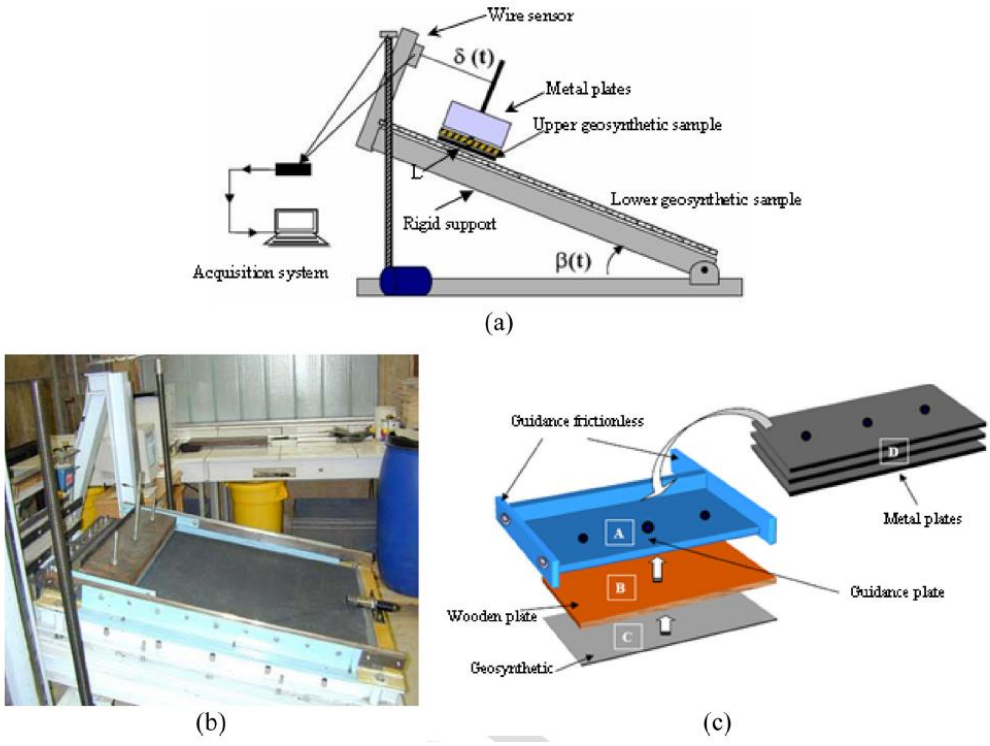

Figure 5.1. Modified IP device. (Reyes Ramirez and Gourc (2003))

Briançon (2002) used another apparatus in his researches (Figure 5.2.). This time the two boxes can be filled with soil and their dimensions (l=2.0; w=1.2 and h=0.3 [m] for the lower box; l=1.0; w=1.0 and h=0.5 [m] for the upper box) permits to conduct the tests on geosynthetics samples of large dimensions.

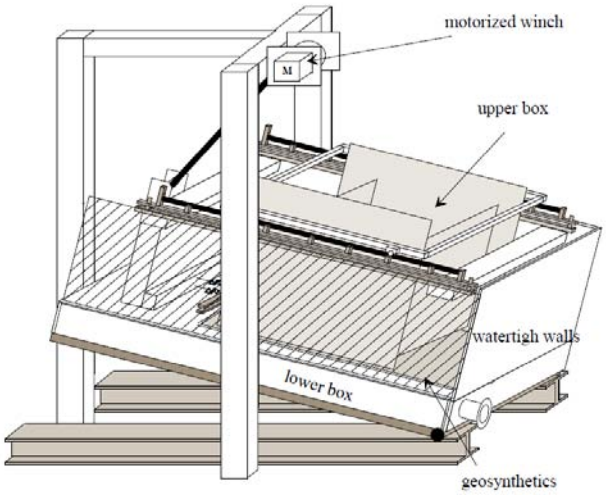

Figure 5.2. Briançon inclined Plane apparatus. (Briançon (2002))

5.2.2. STANDARD PROCEDURE EN ISO 129 57-2 (2005)

According to the European Standard, the interface friction angle is the plane inclination angle β corresponding to a conventional displacement of the upper box u=50 [mm]. Considering a static equilibrium along the plane direction, it is possible to evaluate the relative friction angle ϕ_{stan}, as follows:

$$W \cos \beta_{50} - N \tan \emptyset_{stan} = 0 \tag{5.1}$$

$$W \cos \beta_{50} = N \tag{5.2}$$

Where: N is the reactive force balancing the normal component of the weight, W, of the upper box.

Through the combination of equation 5.1 and 5.2, the value of the interface friction angle proposed by the European Standard is obtain in the following equation:

$$\tan \emptyset_{stan} = \tan \beta_{50} \tag{5.3}$$

5.2.3. DISPLACEMENT PROCEDURE

In 2004, Gourc & Reyes Ramirez introduced a more careful study of the dynamic phase that takes account during the sliding of a geosynthetic interfaced in an inclined plane test. As they demonstrated during the sliding, the uniformly accelerated movement takes place. The test was performed using a "modified inclined plane device" (Figure 5.1.a). The apparatus presents a sufficient length in the slope direction to measure the acceleration of the upper box during the motion. Therefore ϕ_{stan} calculated following Equation (5.3), obtained from a static approach, and was no more representative of the procedure ruled out.

With this modified setup, they proposed a new interpretation, here called "Displacement Procedure" where the sliding behaviour could be divided into three characteristic phases (Figure 5.3.), as follows:

- Phase 1 (Static Phase): The upper box is practically immobile (the displacement of the upper box equals zero) over the inclined until reaching an angle $\beta_0 = \phi_0$,
- Phase 2 (Transitory Phase): With increasing inclination beyond β_0, the upper box moves gradually downward, and the acceleration γ of the upper box is not constant,
- Phase 3 (Stabilized - Sliding Phase): At $\beta = \beta_s$, the upper box undergoes stabilized sliding with constant acceleration γ_c, and the speed progressively increases.

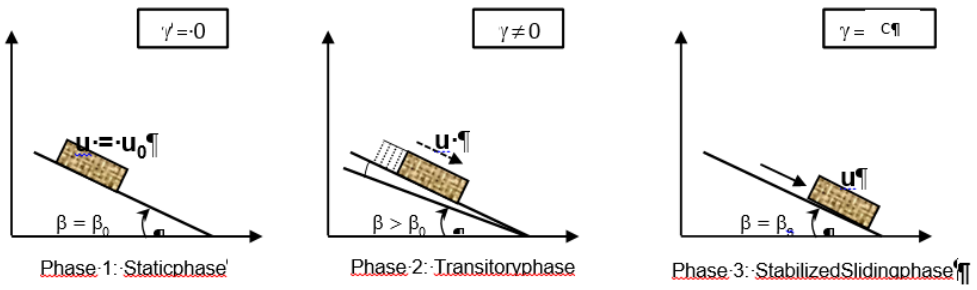

Figure 5.3. Different phases of the "Displacement Procedure" Test. (Carbone (2013))

In the Phase 1, at the beginning of the sliding (u~1÷2mm) the following equation is valid:

$$\tan \emptyset_0 = \tan \beta_0 \qquad (5.4)$$

Where, β_0 is defined as the plane inclination angle before the initialization of the sliding corresponding to the static interface friction angle, ϕ_0.

Phase 2 may be of two types, as already demonstrated by Pitanga et al. 2009:

a) Sudden sliding: abrupt displacement of the upper box with $\beta_0 \sim \beta_s$, (Figure 5.4.)

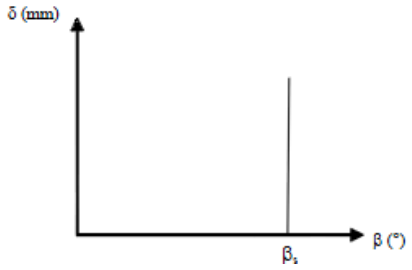

Figure 5.4. Type (a): sudden sliding

b) Gradual sliding: displacement u increases with inclination β, progressively or as a stick-slip mode (Figure 5.5.)

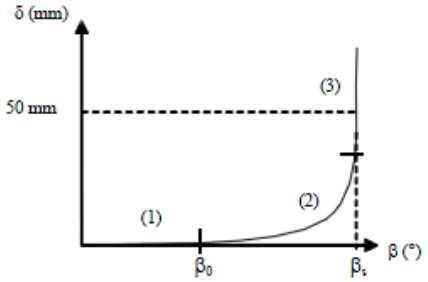

Figure 5.5. Type (b): Gradual sliding

As demonstrated by Gourc et al. (2004) the Phase 3 starts when the acceleration reaches a constant value γ_c; under this condition, the relations (Equations 5.1 and 5.2) should be replaced by equations 5.5 and 5.6:

$$W \cos \beta_s - N \tan \emptyset_s = W \frac{\gamma_c}{g} \quad (5.5)$$

$$W \cos \beta_s = N \quad (5.6)$$

Where a constant acceleration $\gamma = \gamma_c$ of the upper box.

The value of the kinematic friction angle, ϕ_s, in place of ϕ_{stan}, is obtained by combining Equations 5.5 and 5.6 to give:

$$\tan \emptyset_s = \tan \beta_s - \frac{1}{\cos \beta_s} \frac{\gamma_c}{g} \quad (5.7)$$

Where β_s is the plane inclination angle corresponding to the constant acceleration γ_c of the upper geosynthetic during the stabilized-sliding phase.

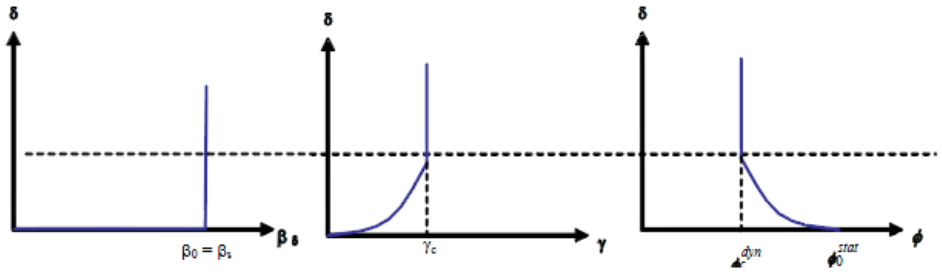

Figure 5.6. Evolution of the displacement δ, the acceleration γ and the interface friction angle ϕ with the plane inclination β, in case of sudden sliding (Gourc, JP Reyes-Ramirez, R Villard, P (2004)).

5.2.4. FORCE PROCEDURE

Briançon et al. in 2011 proposed a new procedure called "Force Procedure" because the evaluation of the upper box acceleration during the motion in the "Displacement Procedure" could be very complex for some interfaces. The difference lies in the acceleration evaluation, in fact the methods is based on determining the interface friction angle through the inclined plane apparatus by measuring the force required to restrain the upper box after reaching a limiting value of the sliding displacement u_{lim}, corresponding to an inclination $\beta = \beta_{lim}$.
In his research, Briançon utilised an inclined plane device where the upper box is connected with a loose cable (Figure 5.7.) to a force sensor fixed to the device frame.

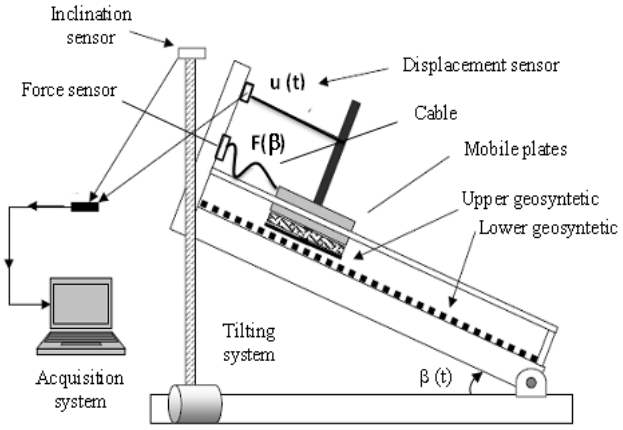

Figure 5.7. IP apparatus geosynthetic–geosynthetic configuration. (Briançon, L Girard, H Poulain, D (2002))

When the maximum displacement u_{lim} is reached, the cable is stretched and the force F(β) required to hold back the upper box is measured (Briançon et al. 2011). The test consists of three steps (Figure 5.8.), (Carbone et al. (2013)):

- Step 1: corresponds to the static state of the upper box with respect to the lower plane during the tilting process ($\beta < \beta_0$),
- Step 2: corresponds to the transitory state where the upper box slides, gradually or suddenly, it is in the dynamic state until the cable is stretched for a displacement u_{lim}($\beta_0 \leq \beta \leq \beta_{lim}$), and
- Step 3: the upper box reaches the end of the slide ($u = u_{lim}$) and it could be considered in a static state because the only possible movement is due to the elongation of the cable that could be neglected. Here, the variation of F is monitored during the test, in particular it increases with the continuous tilting process of the plane ($\beta > \beta_{lim}$).

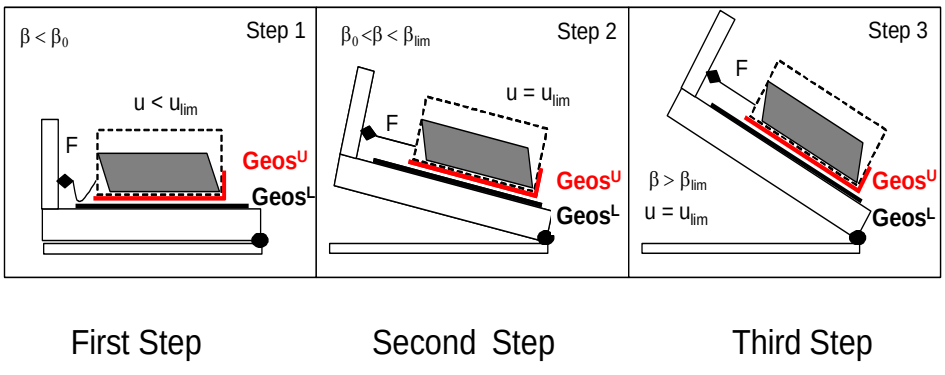

Figure 5.8. Schematization of the different steps during the "Force Procedure" test. . (Carbone et al (2013))

During the Step 1 F(β) = 0 and the equilibrium is expressed by the equation 5.8:

$$\tan \emptyset_0 = \tan \beta_0 \tag{5.8}$$

During Step 2, the equilibrium should take into account the acceleration during the sliding and it is not consider in this method.
During the Step 3 F(β) > 0 and the equilibrium takes into account the force at the cable:

$$W \cos \beta \quad - N \tan \emptyset \quad - F(\beta) \tag{5.9}$$

$$W \cos \beta \quad = N \tag{5.10}$$

$$\tan \emptyset \quad = \tan \beta \quad - \frac{F(\beta)}{W \cos \beta} \tag{5.11}$$

Where W is the total weight of the upper box and F(β) is the force required to hold back the upper box.
Thus, for convenience the whole test may be represented in terms of the parameter λ, the parameter representing the friction plotted along the entire friction test in the Force Procedure, as follows:

$$\tan \lambda = \tan \beta \quad - \frac{F(\beta)}{W \cos \beta} \tag{5.12}$$

In particular, tanλ could be characterized during the entire test as follows:
During Step 1:

$$\tan \lambda_0 = \tan \phi_0 = \tan \beta_0 \tag{5.13}$$

During Step 2:

$$\tan \lambda \quad = \tan \emptyset \quad - \frac{1}{\cos \beta} \frac{\gamma_c}{g} \tag{5.14}$$

During Step 3:

$$\tan \lambda_{lim} = \tan \phi_{lim=} \tan \beta \quad - \frac{F(\beta)}{W \cos \beta} \tag{5.15}$$

If the acceleration γ is not monitored during the Step 2, it is possible to calculate the interface friction angles corresponding to the Step 1 and Step 3. In particular, as found by Briançon et al. (2011), ϕ_{lim},is considered the key parameter of this method because it is not sensitive to the test conditions. (Carbone et al. (2013))

5.2.5. RESIDUAL FRICTION PROCEDURE

In 2012 Stoltz proposed a light modification to the "Force Procedure". It is a testing method to determine the residual friction properties at geosynthetic interfaces using an inclined plane device. (Stoltz (2012)). The procedure is ruled out following the same principle proposed by Briançon, the force required to old back the upper box. The main difference lies in the connection between the box and the device frame. In fact, Stolz utilised a spring (Equation 5.16) to allow a very slow displacement of the upper box, obtaining an almost static displacement whatever the plane inclination is.

$$F = ku \tag{5.16}$$

Where k is the spring constant and u the displacement.
As well this time the test could be divided in three steps (Figure 5.9.)

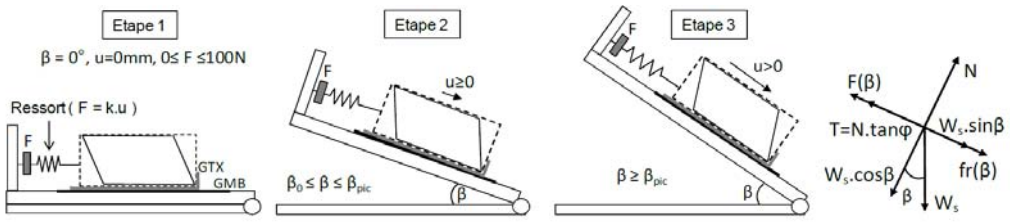

Figure 5.9. Schematization of the different steps during the "Residual friction test" and force balance to calculate the interface friction angle φ. (Stoltz (2012))

In the step 1 the spring is necessary to retain the upper box and, for this reason, it is pretended with a force F< 100 N.
The step 2 accords with the box initial sliding, (u≥ 0.0 mm), and it corresponds to the plane inclinationβ_0.
At the end of step 2 the angle β_{pic} is reached, and when $\beta > \beta_{pic}$ step 3 starts.
With the force balance, the friction angle could be expressed by the following equation:

$$\tan\phi = \frac{T}{W_s \cos\beta} = \frac{W_s \sin\beta + f_r(\beta) - F(\beta)}{W_s \cos\beta} \quad (5.17)$$

This equation is correct considering the upper box acceleration negligible during the test.
Considering the acceleration:

$$\tan\phi = \frac{T}{W_s \cos\beta} = \frac{W_s (\sin\beta - \frac{\gamma}{g}) + f_r(\beta) - F(\beta)}{W_s \cos\beta} \quad (5.18)$$

Where T is the friction force, W_s the box weight and F the force measured by the force sensor.

5.3. TESTING PROGRAM

5.3.1. MATERIAL TESTED

In the top cover of landfill the use of a geocomposite drain (GCD) with a geomembrane (GMB) is a common situation. For this reason, the assessment of the behaviour of this interface is very important. The GCD is composed by a geonet in the middle and two layers of geotextile on both sides and the during the test series all the materials that constitute the GCD are tested separately in direct contact with the geomembrane. Thus, the lower layer used is always a smooth geomembrane while, as upper layer three different type of geosynthetics (geotextile, geonet and geocomposite drain) are used.
For every interface tested, virgin sample are used in the machine direction.

The GCD used in this case is a thermobonding rhomboidal shape HDPE geonet with two non-woven geotextiles on both sides. The geomembrane is a smooth high density polyethylene geomembrane representing, in all tests conducted, the lower layer, while the other geosyntetics are glued to the upper box, in the way herein described. (Figure 5.10.a.and 5.10b)

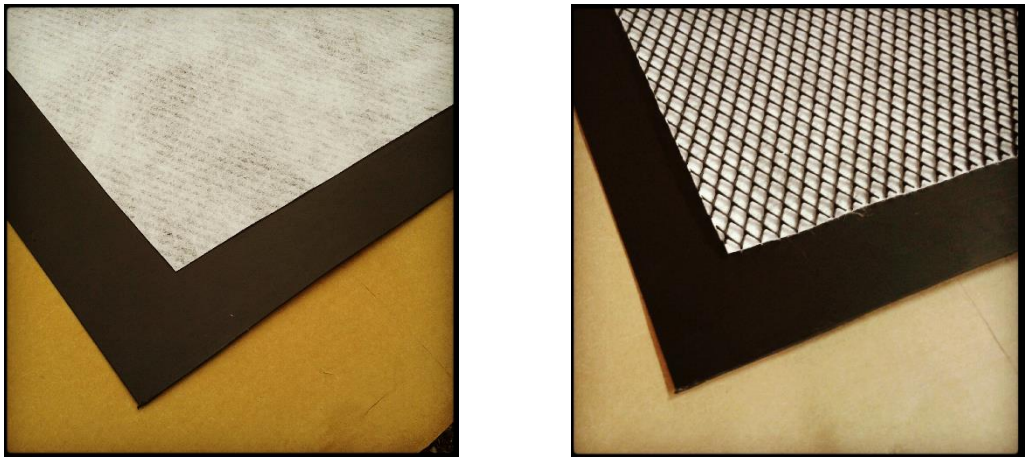

Figure 5.10.a. Geosynthetics and interfaces tested: 1) GTX-smooth GMB HDPE; 2) GNT-smooth GMB

Figure 5.10.b. Geosynthetics and interfaces tested: GMB HDPE; 3) GCD- smooth GMB HDPE.

After this first part, some tests are carried out on a textured geomembrane, as lower layer. (Figure 5.11.)

Figure 5.11. Geosynthetics tested: textured GMB HDPE.

Materials characteristics are reported in Table 9

Table 9. Characteristics of tested geosynthetics.

Type of geosynthetic	Material	Thickness	Mass per unit Area
Geotextile (GTX)	Thermally bonded Nonwoven	1	130
Geonet (GNT)	Thermononding rhomboidal shape High Density Polyethylene	3.5	520
Geocomposite Drain (GCD)	External filler + Drainage core	5.5	780
Geomembrane (GMB)	High Density Polyethylene	2	/

During the test program some different interfaces where tested, to asset a correct friction angle:

- Geotextile (GTX^U) – smooth geomembrane (GMB^L);
- Geonet (GNT^U) – smooth geomembrane (GMB^L);
- Geocomposite (GCD^U) – smooth geomembrane (GMB^L);
- Geotextile (GTX^U) - textured geomembrane (GMB_T^L);
- Geonet (GNT^U) - textured geomembrane (GMB_T^L).

5.3.2. PROCEDURES UTILISED

The testing program consists, for the major part, on the frictional analysis of a geosynthetic interfaces typically present in landfill liners. In fact, it was been investigated the behaviour of the composite drain-geomembrane interface since its use is very widespread in the composite system.

For the Inclined Plane test program, the Standard Procedure; the Displacement Procedure; the Force Procedure are carried out in order to compare the results.
Furthermore, some modification to the usual procedures are rulled out during the test campaign following the researches of the Phd student Laura Carbone.
Two types of tests are carried out to assess the different interface friction angles and to understand how different kinematic condition can influence them.
The first kind of tests is performed with a slow plane's rate inclination $\delta\beta/\delta t$=0.01 [°/min], with β the plane angle related to the longitudinal position, acquisition time of 50 [ms]. Although, in the second type the plane inclination is fixed and the upper box is not connected to the force captor.
The applied load is always 5 KPa and each test is performed at three different temperature: 10°; 20°; 30° to understand the temperature influence on the interface friction. Moreover, the sample are both virgin and already tested to investigate the damaging process on the geosynthetic materials.
At the end it is considered furthermore the procedure introduced by Stoltz, which involved the use of a spring.
The parameters measured in the tests are: plane inclination angle, displacement, acceleration of the upper box, force required to hold back the upper box and time.

Friction angles determined:

- ϕ_0= critical angle where the upper box moves gradually downward;

$$\tan \phi_0 = \tan \beta_0 \tag{5.19}$$

- ϕ_{stand}= angle defined by the Standard Procedure EN ISO 12957-2 (2005);

$$\tan \phi_{stand} = \tan \beta_{50} \tag{5.20}$$

- ϕ_s= interface friction angle calculated taking into account the acceleration of the upper box during the slide according to the Displacement Procedure

$$\tan\ \phi_s = \tan\beta_s - \frac{1}{\cos\beta_s} * \frac{\gamma_s}{g} \quad (5.21)$$

γ_c is the upper box's constant acceleration during the slide.

- λ_{lim}= the parameter representing the friction plotted along the entire friction test in the Force Procedure.

$$\tan\lambda_{lim} = \tan\phi_{lim=}\tan\beta \quad -\frac{F(\beta)}{W\cos\beta} \quad (5.22)$$

5.3.3. EXPERIMENT SETUP

The device utilised during the campaign program is reported in Figure 5.1, Figure 5.12. and it is the same used by Gourc et al (2003-2004) and Carbone (2012-2013).
It consist in a "Modified Inclined Plane Device" described in paragraph 5.2.1. with a cable needed to connect the Force Captor to the upper box.
To measure all the parameters needed to assess a correct value of the interface friction angle some sensors were connected to the Inclined Plane: inclinometer; accelerometer, force captor; laser; extensometer (Figure 5.13.).
In all tests the lower layer is represented by a geomembrane sample, fixed to the plane with a series of bolts, as shown in Figure 5.13. Meanwhile GCD or its parts, glued to a wooden plate, represent the upper layer.

During the experiment the parameters recorded and needed to elaborate the friction angles values, from the different procedures, are:

- Time (milliseconds);
- Plane angle inclination (°);
- Upper box acceleration (g);
- Upper box displacement (mm);
- Force (Kg).

Figure 5.12. IP device utilized in the campaign program.

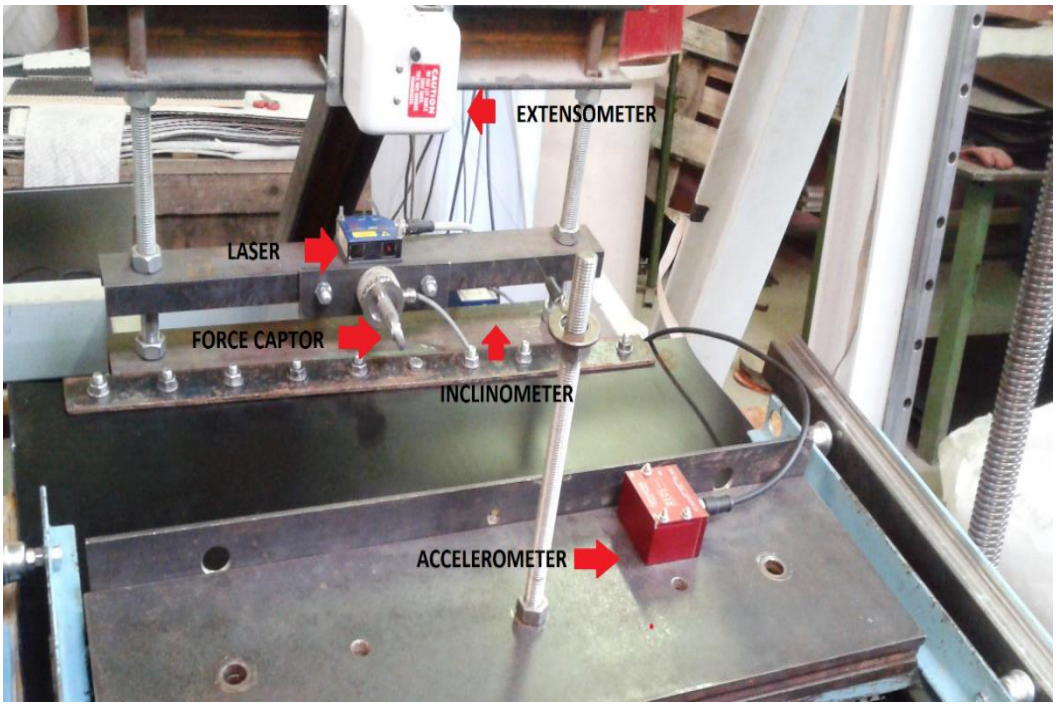

Figure 5.13. Sensors utilized in the campaign program.

6. RESULTS and DISCUSSION

6.1. INTRODUCTION

Quite a lot of parameters are involved in the interface friction such as material roughness, contact area materials, temperature and humidity, velocity and kinematic conditions, samples damage, time of response.
In this thesis closer attention is pointed, not only to the differences between the procedures utilised, but also on some of these parameters. In particularly on temperature, velocity and kinematic conditions and samples damage. For these reasons, the tests are performed for each interface at three different temperatures: 10°; 20°; 30°; and both on virgin and already tested samples.

Test at 30° were executed by the researcher Laura Carbone and are here reported only to analyse the temperature influence, and to check the different angles obtained ruling out the diverse procedures.

6.2. RESULTS and DISCUSSION

6.2.1. IP TESTS ON GEOSYNTHETIC INTERFACES AT T=20°

At 20° the Standard, Displacement and Force Procedure were performed. The following tables reported the friction angle values for each interface tested with an applied load of 5 kPa constant in all tests.

On the tests, the samples utilised are 3 for each type of interface, and the GTX, GNT and GCD tested are virgin sample, instead of the GMB which are already tested samples.

- **GTX^U – GMB^L**

Table 6.1 Angle of fist displacement values. GTX-GMB interface

Angle of first displacement ϕ_0 (°)			
# test number	Sample 4	Sample 5	Sample 6
1	12.9	14.8	14.2
2			
3			
4	10.8	13.4	12.0
5	13.8		
6	12.3		
7	14.5		
Average angle value	**ϕ_0**	**13.2°**	

Table 6.1. shows the angle of first displacement tests results. Many parameters influence ϕ_0, in fact, the angles range is between 10.8° and 14.8°, which is quite a wide range of values in the same interface. The average value is 13.2° for GTX^U – GMB^L. Figure 6.1. shows the upper box displacement against the plane inclination.

Table 6.2 Standard Procedure angle values. GTX-GMB interface

Angle of the Standard Procedure ϕ_{stand} (°)			
# test number	Sample 4	Sample 5	Sample 6
1	13.3	14.9	15.2
2			
3			
4	12.4	14.3	14.2
5	14.0		
6	13.7		
7	14.6		
Average angle value	**ϕ_{stand}**	**14.1°**	

Table 6.2 reported the Standard Procedure results. The angle ϕ_{stand} corresponds to the plane inclination when the upper box displacement is 50 mm, according to the European Standard EN ISO 129 57-2 (2005). The average value is 14.1°. This value is higher than ϕ_0 and it is higher than the one provide by the Force Procedure as will be explained in the following Tables. As reported in Carbone 2012 the Standard Procedure overestimates the interface friction angle, especially in the case of gradual sliding and it is not rigorous because a static approach is proposed for dynamic conditions.

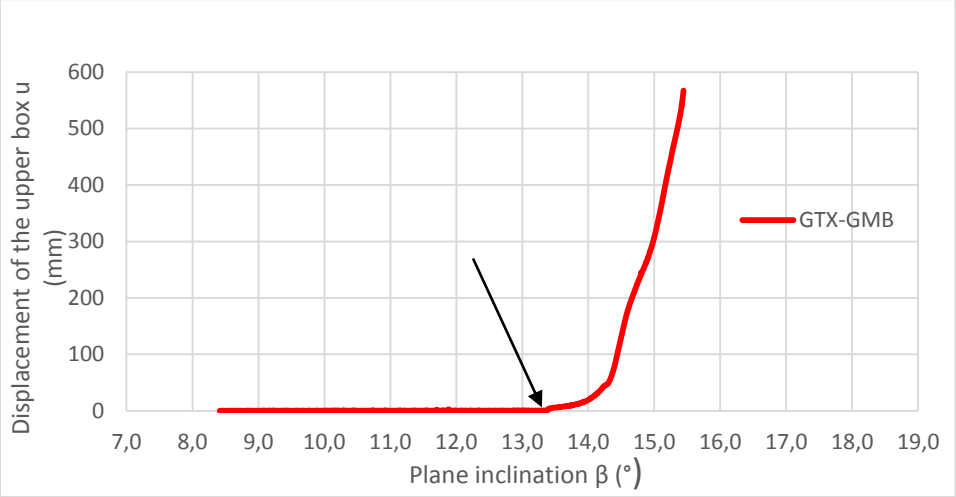

Figure 6.1. IP test according to the Displacement Procedure; Displacement of the upper box against the plane inclination, interface GTX-GMB.

For this type of interface, the movement is gradual sliding characterised by a very low velocity. In fact, in the tests performed with a plane rate of 3±0.5°/min it is quite impossible to evaluate the upper box velocity that is close to zero, and consequently also the acceleration. The problem with the Displacement procedure is always related to the definition of the kinematic parameters.

To define easily the dynamic parameters, some over test are performed. The plane inclination β is keep fixed at two different angles 20° and 25° and the upper box is free to slide until the plane end. In this way, it is possible to evaluate the kinematic characteristics during the sliding process: upper box velocity and acceleration. Into the sliding phase the uniform accelerated motion take place. The results of these tests are shown in Table 6.3

Table 6.3 Displacement Procedure angle values, performed at different fixed plane inclination, average velocity values and acceleration values. GTX-GMB interface

Angle of the Displacement Procedure $\phi_{dyn,a}$ (°)

		Sample 4			Sample 5			Sample 6		
# test number	β_{fixed} (°)	$\phi_{dyn,a}$	Vaverage (cm/s)	γ (m/s²)	$\phi_{dyn,a}$	Vaverage (cm/s)	γ (m/s²)	$\phi_{dyn,a}$	Vaverage (cm/s)	γ (m/s²)
1										
2	**20**	**17.6**	50.2	0.24				**17.3**	35.7	0.46
3	**20**	**17.4**	54.3	0.30	**17.8**	27.6	0.25	**16.9**	49.8	0.41
4										
5	**25**				**16.8**	110.8	1.4	**18**	105.7	1.32
6										
7										
8	**25**	**16.7**	110.5	1.54						

Average angle value $\phi_{dyn,a}$ **17.3 °**

The average value $\phi_{dyn,a}$ is 17.3°, which is more higher than the values prematurely founded. It could be interesting to notice how the different inclination of the plane have no influence on the friction angle. Effectively, while the upper box acceleration and velocity increase, this is not happening for the angle values.

These tests, with a fixed plane inclination, are performed to define the kinematic parameters when it is difficult to implementing them. They are evaluated during the linear phase of sliding, clearly visible in Figure 6.2. and 6.3.

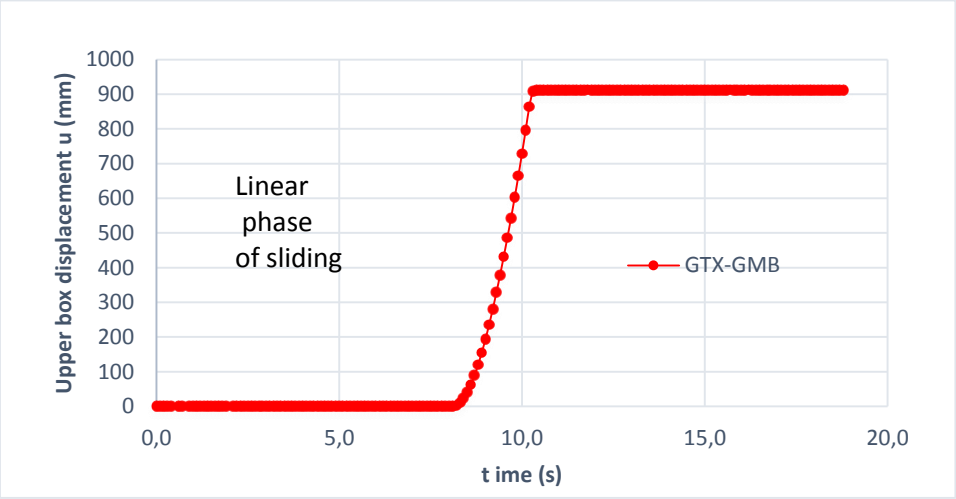

Figure 6.2. IP test Displacement Procedure with plane fixed inclination; Displacement of the upper box against the plane inclination, interface GTX-GMB.

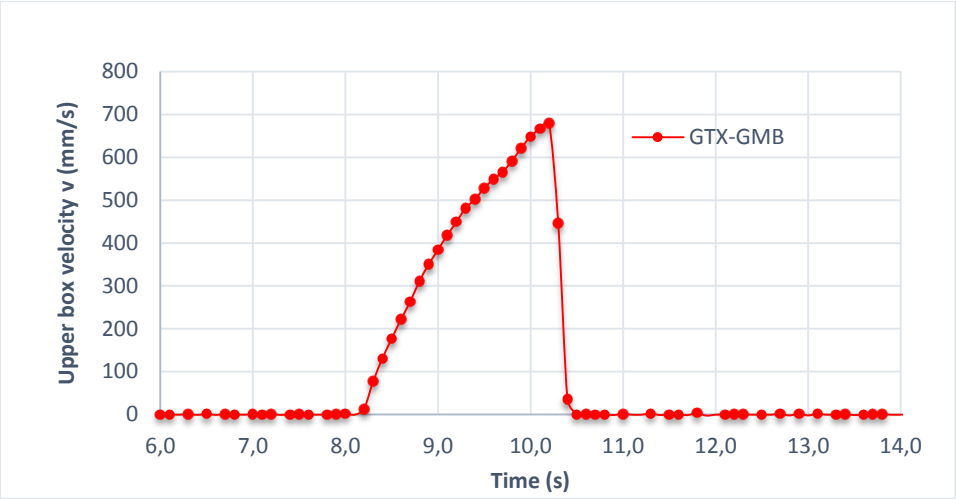

Figure 6.3.Velocity of the upper box against time, interface GTX-GMB.

As reported in Carbone et al. 2013 (the interfaces tested are the same), this interface is characterized by a gradual sliding of the upper box at very low velocity. This kind of behaviour indicates that the resisting friction force gradually decreases respect the value at rest during the slide. Consequently the angle $\phi_{dyn,a}$ is lower than the standard value $\phi_{0,}$ as already explained.

The last procedure tested is the Force Procedure, results are shown in Table 6.4

Table 6.4 Force Procedure angle values. GTX-GMB interface

Angle of the Force Procedure ϕ_{lim} (°)			
# test number	Sample 4	Sample 5	Sample 6
5			
6		**11.8**	**11.6**
9	**10.5**		
Average angle value	**ϕ_{lim}**	**11.3°**	

The average value ϕ_{lim} is 11.3° and it represents the lower value founded for this interface using the different procedures. Generally, the parameter ϕ_{lim} seems not affected from the limit displacement u_{lim} and by the plane inclination rate. It seems that it could be considered as an intrinsic parameter common to different types of sliding. The Force Procedure is a repeatable procedure (Briançon et al. (2011), Carbone (2012)).

It is easier to implement than the Displacement, because it is not related to the dynamic phase of sliding.

The friction angle is expressed by equation 5.15 (Chapter 5.2.4 Force Procedure)

$$\tan \lambda_{lim} = \tan \phi_{lim=} \tan \beta \quad - \frac{F(\beta)}{W \cos \beta} \tag{5.15}$$

In Figure 6.4. the force required to hold back is plotted versus the plane inclination for the entire test. The procedure starts when is reached u_{lim}, (step 3) that corresponds to the end of the Displacement Procedure and the complete stretch of the cable, that connects the upper box to the force captor.

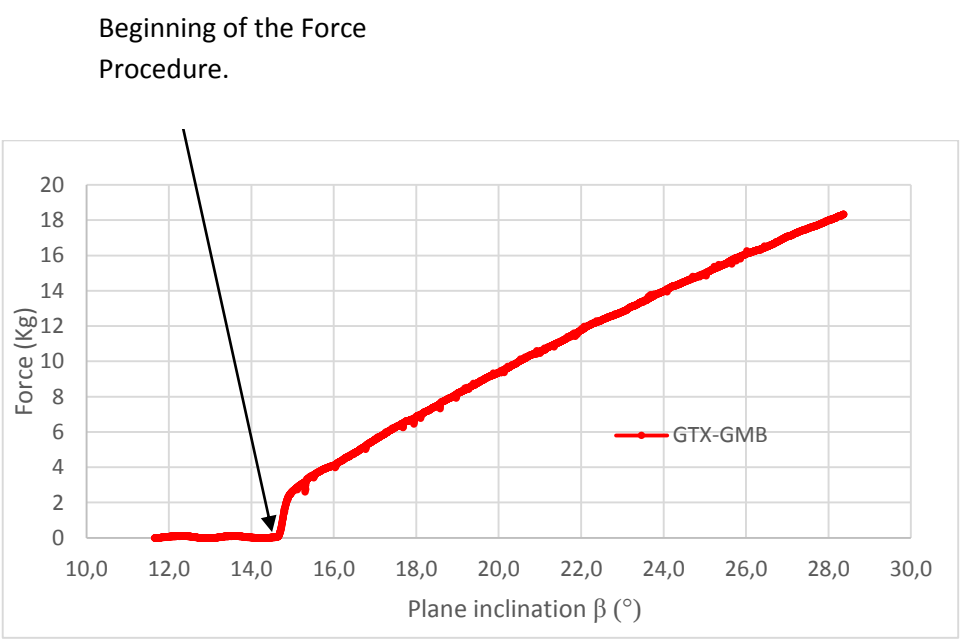

Figure 6.4. IP test according to the Force Procedure, force required to hold back the upper box against plane inclination, interface GTX-GMB.

At the beginning the parameter $\lambda_{lim} = \phi_{lim}$ augments as the force required to hold back the upper box. Secondarily, after reaching a peak, it starts to decrease and to stabilized while the plane inclination continues to increase until β_{lim}, the end of the procedure. (Figure 6.5.)

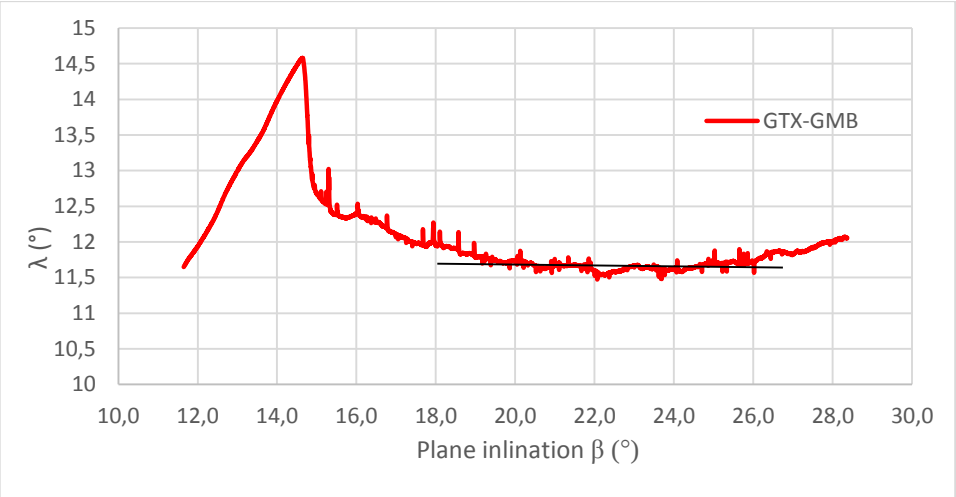

Figure 6.5. IP test according to the Force Procedure, parameter $\lambda_{lim} = \phi_{lim}$ against plane inclination, interface GTX-GMB.

The average value of the parameter $\lambda_{lim} = \phi_{lim}$ is represented by the asymptotic value, the black line in Figure 6.5.

- **GNT^U – GMB^L**

Table 6.5 Angle of fist displacement values. GNT-GMB interface

Angle of first displacement ϕ_0 (°)

# test number	Sample 4	Sample 5	Sample 6
1	11.2	12.6	13.3
2			13.3
3			
4	16.1	14.3	15.7
5			
Average angle value	**ϕ_0**	**13.8°**	

In Table 6.5 Are reported the angle of first displacement results. Ad explained for the previous interface many parameters could influence ϕ_0. The range is between 11.2° and 16.1°, that is almost of 5°. The average value is 13.8° for GNT^U – GMB^L. Figure 6.6. shows the upper box displacement against the plane inclination.

Table 6.6 Standard Procedure angle values. GNT-GMB interface

Angle of the Standard Procedure ϕ_{stand} (°)			
# test number	Sample 4	Sample 5	Sample 6
1	12.5	14.6	15.1
2			15.1
3			
4	16.2	16.1	15.8
5			
Average angle value	**ϕ_{stand}**	**15.5°**	

Table 6.6. reported the Standard Procedure results. The average value is 15.5°. This value, as already underlined for the GTX-GMB, is higher than the angle of first displacement.

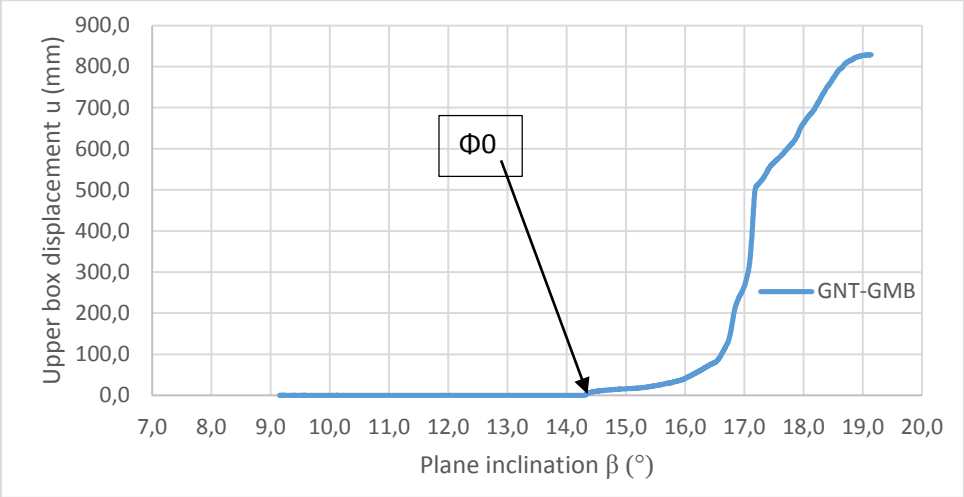

Figure 6.6. IP test according to the Displacement Procedure; Displacement of the upper box against the plane inclination, interface GNT-GMB.

The movement of this interface is not a gradual sliding characterised by a very low velocity. In fact, GNT-GMB is characterised by an abrupt initial displace of 5 mm approximately, with a stick slip behaviour. The gap between ϕ_0 and ϕ_{stan} is here about 2°. After this phase, the upper box goes slowly downward. This behaviour is the same founded by Carbone in her researches (2013). Even if it has an initial

displacement and after a slower phase this interface could be characterised by gradual sliding.

Regarding the way of sliding for this interface is not simple to define the dynamic parameters. For these reasons also for the GNT-GMB interface, tests at different fixed plane inclinations are performed. This time the fixed angle are 19° and 23°. The results of these tests are shown in Table 6.7.

Table 6.7 Displacement Procedure angle values, performed at different fixed plane inclination, average velocity values and acceleration values. GNT-GMB interface

Angle of the Displacement Procedure $\phi_{dyn,a}$ (°)

		Sample 4			Sample 5			Sample 6		
# test number	β_{fixed} (°)	$\phi_{dyn,a}$	$v_{average}$ (cm/s)	γ (m/s²)	$\phi_{dyn,a}$	$v_{average}$ (cm/s)	γ (m/s²)	$\phi_{dyn,a}$	$v_{average}$ (cm/s)	γ (m/s²)
1										
2										
3	**19**	**16.5**	36.17	0.28	**17.4**	40.47	0.13	**17.0**	68.87	0.36
4										
5	**23**	**15.3**	68.29	1.16	**15.4**	79.27	1.08	**14.0**	83.11	1.34
Average angle value		$\phi_{dyn,a}$	**15.9 °**							

The average value $\phi_{dyn,a}$ is 15.9°, really close to ϕ_{stand} provided by the Standard Procedure. On the contrary, of GTX-GMB interface, the values range is wider. This could be referred to the type of sliding of the GNT-GMB interface.

Figure 6.7. and 6.8. show the upper box displacement and velocity during the entire test. The linear phase is clearly visible, during which is possible to define the upper box acceleration necessary to calculate the Displacement Procedure angle using Equation 5.7 (Chapter 5.2.3)

$$\tan \emptyset_{dyn,a} = \tan \emptyset_s = \tan \beta_s - \frac{1}{\cos \beta_s} \frac{\gamma_c}{g} \qquad (5.7)$$

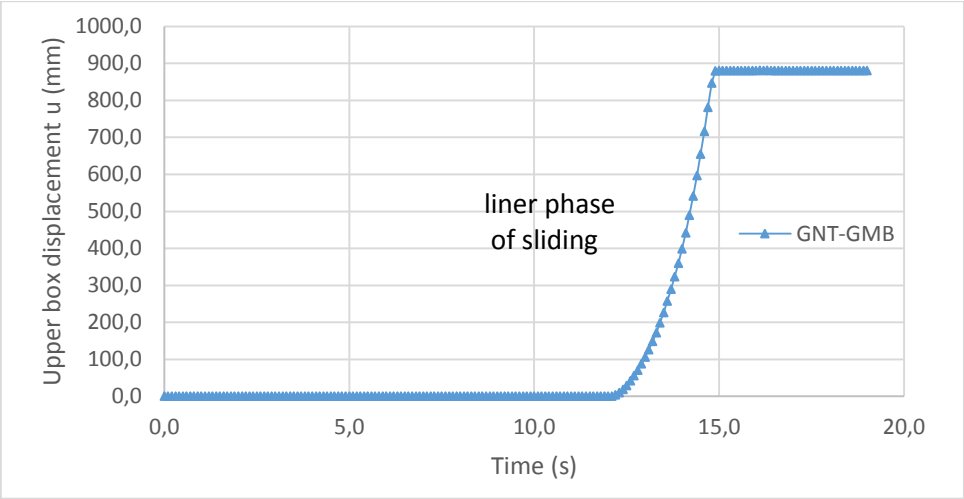

Figure 6.7.IP test Displacement Procedure with plane fixed inclination; Displacement of the upper box against the plane inclination, interface GNT-GMB.

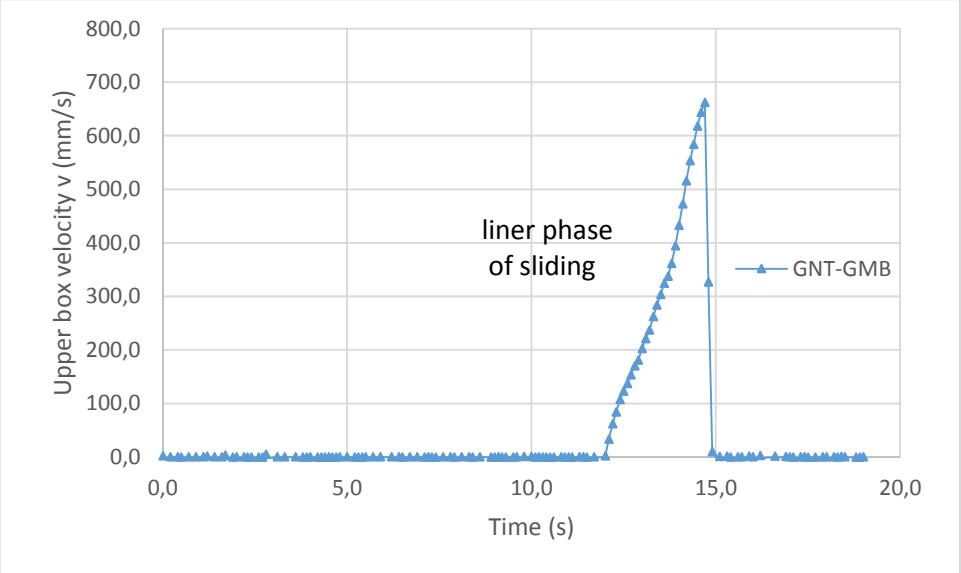

Figure 6.8.Velocity of the upper box against time, interface GNT-GMB.

The last procedure tested is the Force Procedure, results are shown in Table 6.8.

Table 6.8. Force Procedure angle values. GNT-GMB interface

Angle of the Force Procedure ϕ_{lim} (°)			
# test number	Sample 4	Sample 5	Sample 6
5			
6	**14.6**	**15.4**	**13.9**
Average angle value	ϕ_{lim}	**14.6°**	

The average value ϕ_{lim} is 14.3° and with this interface, it is not the lower value founded using the different procedures as for the GTX-GMB. The lower value is represented by the angle of first displacement, because the sliding starts earlier.

In Figure 6.9. the force required to hold back is plotted versus the plane inclination for the entire test. The procedure starts when is reached u_{lim}, (step 3) that corresponds to the end of the Displacement Procedure and to the complete stretch of the cable, that connects the upper box to the force captor.

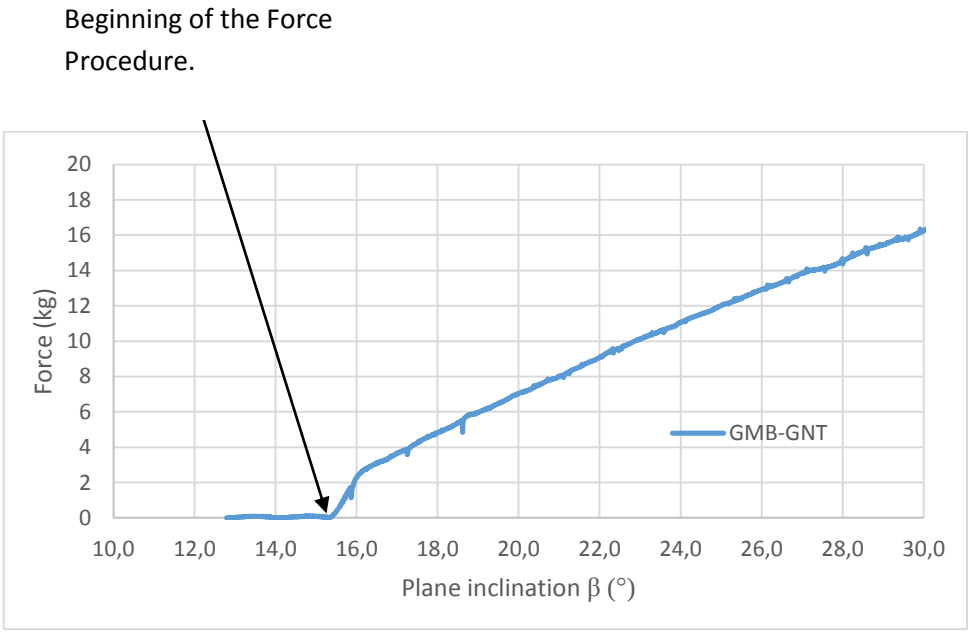

Figure 6.9. IP test according to the Force Procedure, force required to hold back the upper box against plane inclination, interface GTX-GMB.

At the beginning the parameter $\lambda_{lim} = \phi_{lim}$ augments as the force required to hold back the upper box, secondarily, after reaching a peak, it starts to decrease and to

stabilized while the plane inclination continues to increase until β_{lim}, the end of the procedure. (Figure 6.10.)

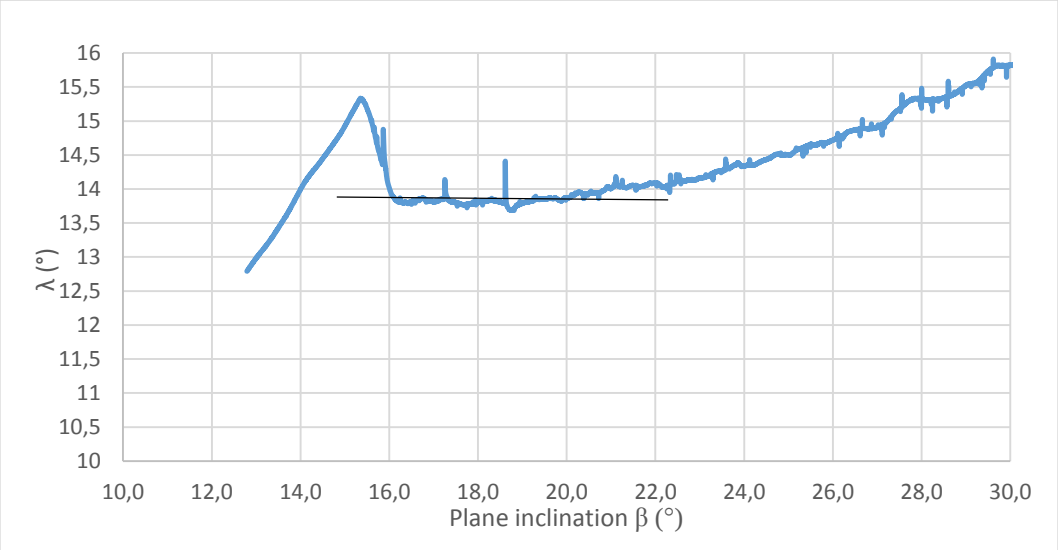

Figure 6.10. IP test according to the Force Procedure, parameter $\lambda_{lim} = \phi_{lim}$ against plane inclination, interface GTX-GMB.

The average value of the parameter $\lambda_{lim} = \phi_{lim}$ is represented by the asymptotic value, the black line in Figure 6.10.

- **GCD^U – GMB^L**

Table 6.9 Angle of fist displacement values. GCD-GMB interface

Angle of first displacement ϕ_0 (°)			
# test number	Sample 4	Sample 5	Sample 6
1	13.6	13.5	12.9
2			
3			
4	15.1	12.3	15.4
5			
Average angle value	ϕ_0	**13.8°**	

Table 6.9 shows the angle of first displacement tests results. The average value is 13.8° for GCD^U – GMB^L. Meanwhile Figure 6.11. shows the upper box

displacement against the plane inclination. With this interface the GTX is directly in contact with the geomembrane.

Table 6.10 Standard Procedure angle values. GCD-GMB interface

Angle of the Standard Procedure ϕ_{stand} (°)			
# test number	Sample 4	Sample 5	Sample 6
1	13.7	13.6	14.1
2			
3			
4	15.2	13.5	15.5
5			
Average angle value	**ϕ_{stand}**	**14.2°**	

Table 6.10 reported the Standard Procedure results. The angle ϕ_{stand} corresponds to the plane inclination when the upper box displacement is 50 mm, according to the European Standard EN ISO 129 57-2 (2005). The average value is 14.2°. This value is higher than ϕ_0 and it is higher than the one provide by the Force Procedure as will be explained in the following Tables.

The first part of the GCD-GMB interface sliding behaviour seems to be close to the GTX-GMB interface behaviour. The influence of the geonet core has to be investigated.

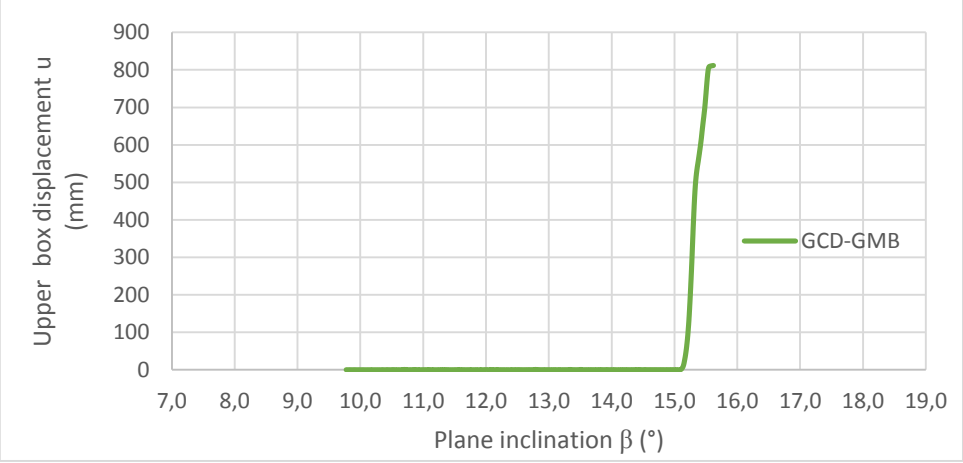

Figure 6.11. IP test according to the Displacement Procedure; Displacement of the upper box against the plane inclination, interface GTX-GMB.

For this interface, as for the GTX-GMB, the movement is gradual sliding characterised by a very low velocity. The problem with the Displacement procedure is always related to the definition of the kinematic parameters.

For this reason, some over tests are performed in dynamic conditions. The plane inclination β fixed at two different angles 20° and 25° and the upper box free to slide to until the end of the plane. In this way it is easier to evaluate the kinematic characteristics of the sliding process; upper box velocity and acceleration. Into the sliding phase the uniform accelerated motion take place. The results of these tests are shown in Table 6.11.

Table 6.11 Displacement Procedure angle values, performed at different fixed plane inclination, average velocity values and acceleration values. GCD-GMB interface

Angle of the Displacement Procedure $\phi_{dyn,a}$ (°)

		Sample 4			Sample 5			Sample 6		
# test number	β_{fixed} (°)	$\phi_{dyn,a}$	$v_{average}$ (cm/s)	γ (m/s^2)	$\phi_{dyn,a}$	$v_{average}$ (cm/s)	γ (m/s^2)	$\phi_{dyn,a}$	$v_{average}$ (cm/s)	γ (m/s^2)
1										
2										
3	**20**	**16.8**	52.89	0.42	**16.3**	50.18	0.349	**15.6**	56.47	0.639
4										
5	**25**	**16.2**	76.09	1.405	**17.2**	85.62	1.126	**15.9**	110.2	1.574
6										
7										
8										

Average angle value $\phi_{dyn,a}$ **16.3 °**

The average value $\phi_{dyn,a}$ is 16.3. The Displacement Procedure angle is also this time the highest. The procedure is ruled out at the same fixed inclination chosen for the GTX-GMB, 20° and 25° degrees. In Figure 6.12. and 6.13. are plotted respectively the upper box displacement during the dynamic tests and the upper box velocity.

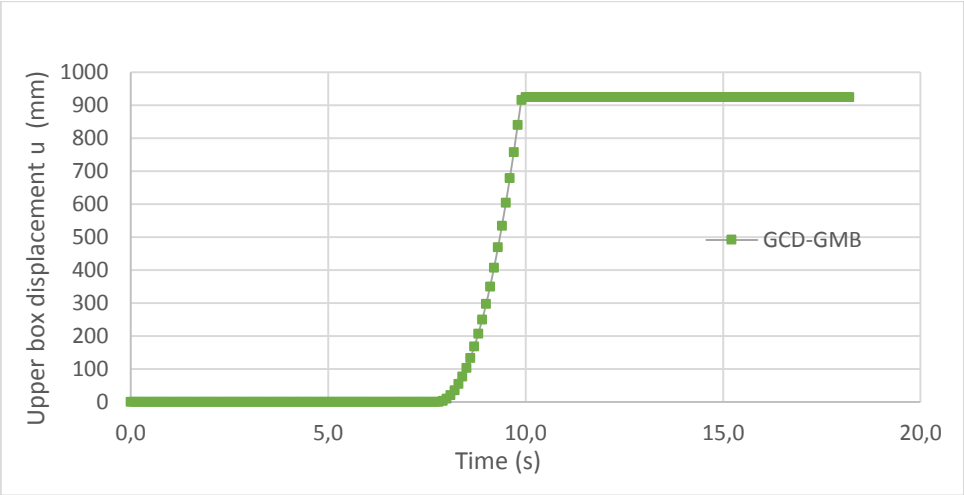

Figure 6.12. IP test Displacement Procedure with plane fixed inclination; Displacement of the upper box against the plane inclination, interface GCD-GMB.

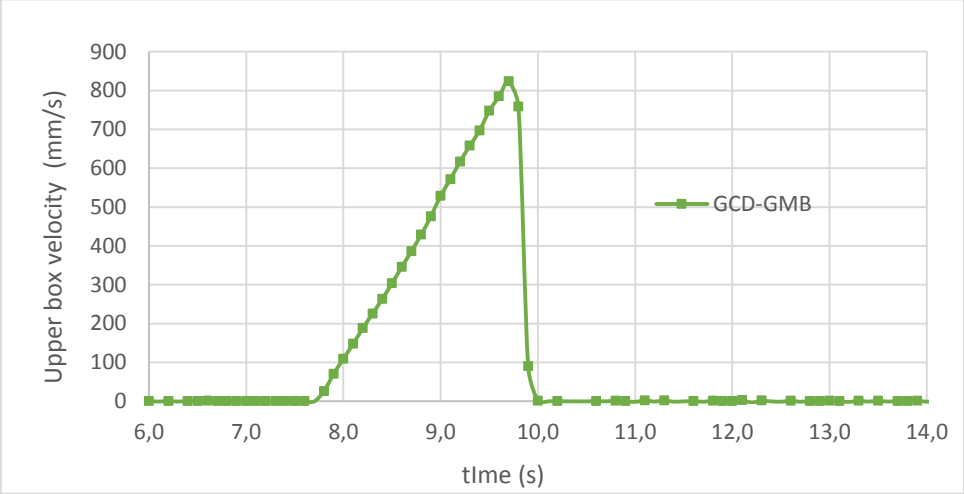

Figure 6.13. Velocity of the upper box against time, interface GCD-GMB.

The behaviour of GCD-GMB interface is quite similar to GTX-GMB, in fact the upper box undergoes a gradual sliding until the end of the plane.

The last procedure tested is the Force Procedure, results are shown in Table 6.12.

Table 6.12. Force Procedure angle values. GCD-GMB interface

Angle of the Force Procedure ϕ_{lim} (°)			
# test number	Sample 4	Sample 5	Sample 6
5			
6	**11.9**	**9.1**	**12.5**
Average angle value	ϕ_{lim}	**12.2°**	

The average value ϕ_{lim} is 12.2° (not considering 9.1°) and it represents the lower value founded for this interface using the different procedures. Generally, the parameter ϕ_{lim} seems not affected from the limit displacement u_{lim} and by the plane inclination rate as already explained.

In Figure 6.14. the force required to hold back is plotted versus the plane inclination for the entire test.

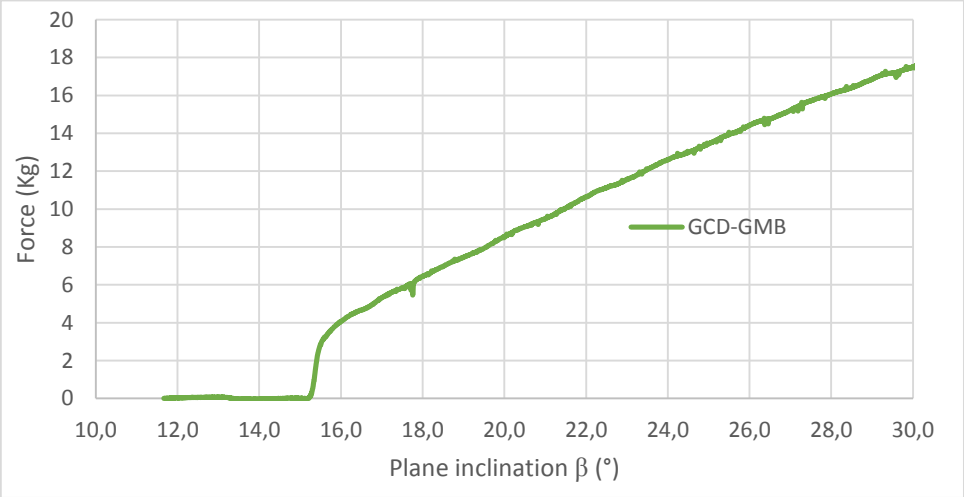

Figure 6.14. IP test according to the Force Procedure, force required to hold back the upper box against plane inclination, interface GCD-GMB.

At the beginning the parameter $\lambda_{lim} = \phi_{lim}$ augments as the force required to hold back the upper box, secondarily, after reaching a peak, it starts to decrease and to stabilized while the plane inclination continues to increase until β_{lim}, the end of the procedure. (Figure 6.15.)

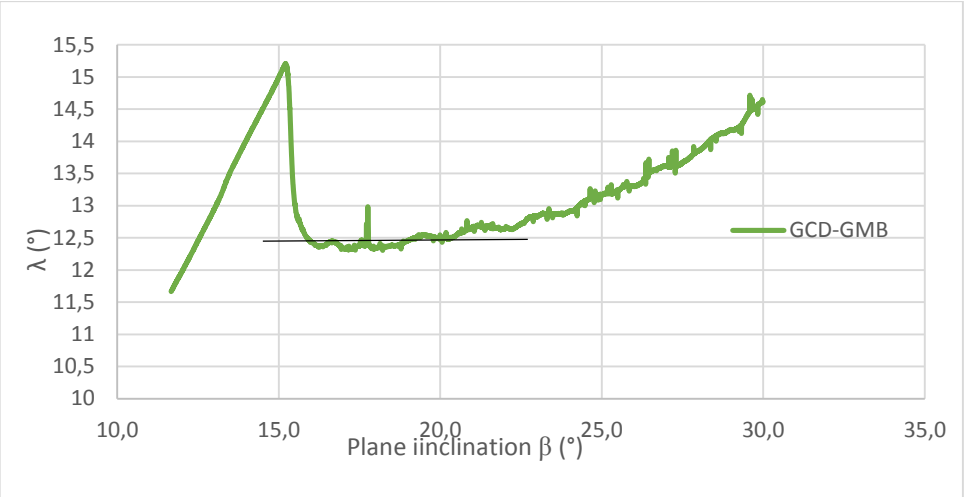

Figure 6.15 IP test according to the Force Procedure, parameter $\lambda_{lim} = \phi_{lim}$ against plane inclination, interface GCD-GMB.

The average value of the parameter $\lambda_{lim} = \phi_{lim}$ is represented by the asymptotic value, the black line in Figure 6.15.

Summarising, the friction angles from the different procedures for each interface are:

Table 6.12 Summary of friction interface tests at 20°

Interface	ϕ_0 (°)	ϕ_{stand} (°)	$\phi_{dyn,a}$ (°)	ϕ_{lim} (°)
GTX-GMB	13.2	14.1	17.3	11.3
GNT-GMB	13.8	15.5	15.9	14.6
GCD-GMB	13.8	14.2	16.3	12.2

In Table 6.12 are reported the average values for each procedure and for each interface tested, which are also plotted in Figure 6.16.

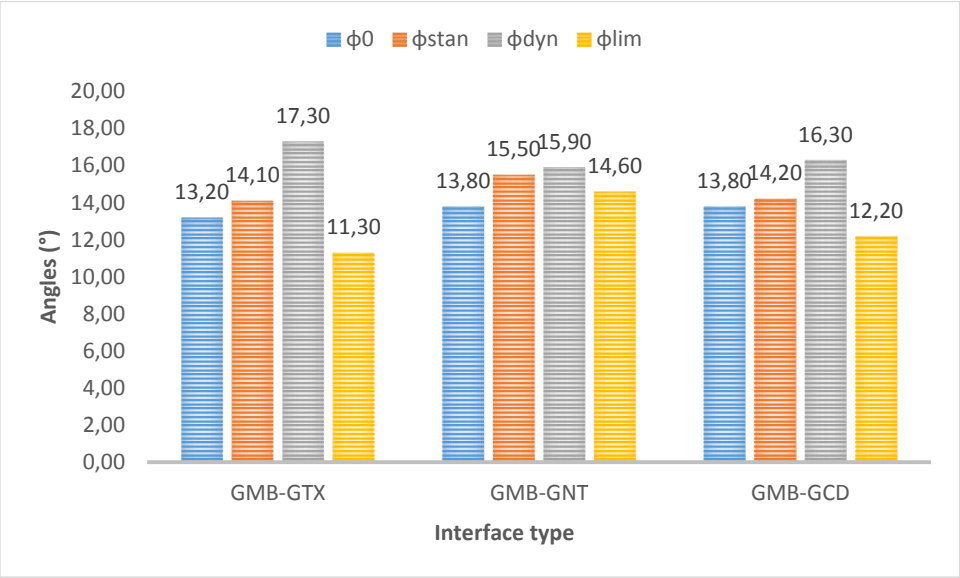

Figure 6.16. Average friction interface angles of different procedures at 20°.

In Figure 6.16. The angles, obtained carrying out the different procedures for the different interfaces tested, are plotted. The blue column represents the angle of first displacement $\phi_{0,}$ the orange one $\phi_{stand,}$ while the grey column is the ϕ_{dyn} value and the last one, the yellow one, the angle of the Force Procedure $\phi_{lim.}$ The third column, the grey one, represents the higher value for each interface; therefore, the Displacement Procedures provides the less cautionary friction value. While the cautionary angle is, for the GMB-GTX and GMB-GCD, the one obtained with the Force Procedure. It is clearly that the GTX and the GCD have a similar behaviour. Although for the GNT the lower value is the angle of first displacement. Because, as herein explained, this interface is characterised by an abrupt initial displacement, about 5 mm, and after a gradual sliding movement, therefore the first angle has a low value. For each interface, the Standard angle is intermediate between the others angles.

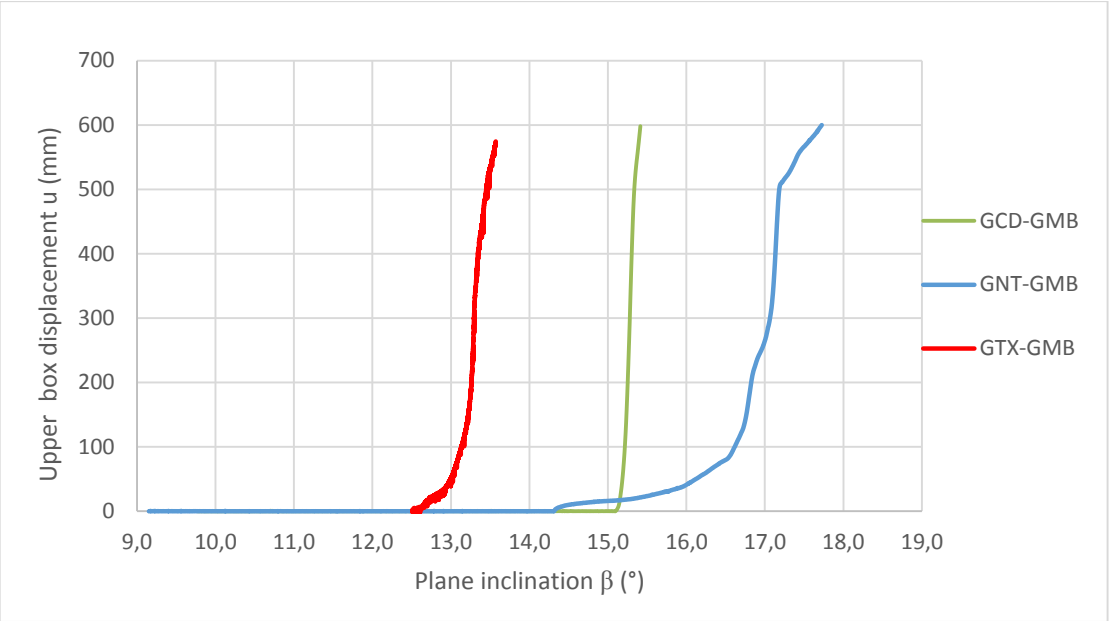

Figure 6.17. IP test on different geosynthetic interfaces at 20°, upper box displacement versus plane inclination.

In Figure 6.17. Are reported three test ruled out in the same way, one for each kind of interface. From the Figure it could be notice that the GNT-GMB interface has an abrupt initial displacement. In the global displacement, this interface has an extreme behaviour, compared with the other two. Meanwhile the GCD-GMB interface has a medium behaviour between the other two interfaces. This could be referred to the geonet core and to the proper composition of the geocomposite, which is on one hand a geotextile on the other a geonet. The same conclusion is reported in Carbone 2013.

This medium behaviour of the GCD could be founded also comparing the parameter $\lambda_{lim} = \phi_{lim}$ in the Force Procedure.

$$\lambda_{GTX} < \lambda_{GCD} < \lambda_{GNT} \qquad (11.3° < 12.2° < 14.6°)$$

6.2.2. IP TESTS ON GEOSYNTHETIC INTERFACES AT T=10°

At 10° the Standard, Displacement, Force Procedure and the "Residual Friction Procedure" are performed. The following tables reported the friction angle values for each interface tested with an applied load of 5 kPa constant in all tests
In this case are tested only two different samples and the GMB used are virgin samples.

- **GTX^U – GMB^L**

Table 6.13 Angle of fist displacement values. GTX-GMB interface

Angle of first displacement ϕ_0 (°)		
# test number	Sample 7	Sample 8
1	17.4	16.1
2	16.4	15.1
3	13.8	16.8
4		
5		
6	14.5	16.5
7	13.7	16.6
Average angle value	**ϕ_0**	**15.7°**

Table 6.13. shows the angles of first displacement. Using a virgin sample or one already tested influence the value of ϕ_0, this is visible especially in sample 7, where the angle value is 17.4° in the first test and it decreases until 13.7° in the last one. The average value is 15.7° for GTX^U – GMB^L at this temperature.
Afterward the mechanical damage of the interface geosynthetic components can influence the angle of first detachment.

Table 6.14 Displacement Procedure angle values, performed at different fixed plane inclination, average velocity values and acceleration values. GTX-GMB interface

Angle of the Standard Procedure ϕ_{stand} (°)		
# test number	Sample 7	Sample 8
1	17.5	18.0
2	17.9	16.4
3	15.7	17.6
4		
5		
6	14.8	16.6
7	14.2	15.7
Average angle value	**ϕ_{stand}**	**16.4°**

Table 6.14. reported the Standard Procedure results. As already highlighted for the angle ϕ_0, ϕ_{stand} is affected by the employ of a virgin sample or not. In this interface, this is clearly for sample 7 where it decrees from 17.5° to 14.2° and also in sample 8, from 18.0° to 15.7°. Then, the geosynthetic mechanical damage is another parameter, which influences the Displacement procedure.

For the interface, the behaviour is the same proposed for a temperature of 20°, a gradual sliding characterised by a very low velocity. In fact, in the tests performed with a plane rate of 3±0.5°/min it was quite impossible to evaluate the upper box velocity that was close to zero, and consequently also the acceleration. The problem with the Displacement procedure always is related to the definition of the kinematic parameters.

One test at β_{plane} =20° and one at β_{plane} = 25° are ruled out to evaluate appropriated dynamic values, necessaries to calculate the friction angle in the Displacement Procedure. The results of these tests are shown in Table 6.15.

Table 6.15. Displacement Procedure angle values, performed at different fixed plane inclination, average velocity values and acceleration values. GTX-GMB interface

Angle of the Displacement Procedure $\phi_{dyn,a}$ (°)

		Sample 4			Sample 5		
# test number	β_{fixed}	$\phi_{dyn,a}$	$v_{average}$ (cm/s)	γ (m/s^2)	$\phi_{dyn,a}$	$v_{average}$ (cm/s)	γ (m/s^2)
1							
2							
3							
4	**25**	**17.5**	83.95	1.06	**17.5**	91.96	1.10
5	**20**	**17.4**	32.33	0.35	**17.5**	40.38	0.25
6							
7							
8							
Average angle value		**$\phi_{dyn,a}$**	**17.5 °**				

The average value $\phi_{dyn,a}$ is 17.5°, close to the value founded in the tests performed at 20° (temperature). It is the higher values founded even this time. The different plane inclinations chosen are not affecting the friction values, as in the previous case.

At the end, for what concerns the implementation of the data given by the force captor, it is carried out not only the Force Procedure proposed by Briançon (2011) but also the Residual Friction Procedure proposed by Stoltz., performed using a " spring system" to connect the Force sensor and the upper box.

This part of research wants to investigate the Force Procedure in a semi-static condition, following a slow displacement of the upper box, permitted by the spring deformation.

Table 6.16 Force Procedure and Residual Friction Procedure angle values. GTX-GMB interface

Angle ϕ_{lim} (°)

# test number	Sample 7	Sample 8
1 Stoltz	16.8	17.3
2 Briançon	**15.3**	**14.6**
3 Stoltz **Briançon**	15.9 **17.7**	17.8 **17.0**
4		
5		
6 Briançon	**14.2**	**14.6**
7 Stoltz **Briançon**	14.3 **13.8**	14.4 **14.6**
Average angle value Briançon	ϕ_{lim}	**14.6°**
Average angle value Stoltz	ϕ_{lim}	**16.1**

In Table 6.16. are reported the values obtained performing both the procedures. It is not possible to define a univocal interpretation to compare Briançon and Stoltz procedure. In fact, regarding the average value ϕ_{lim} is 14.6° for the Force Procedure and 16.1° for the Residual Friction Procedure. Then it could seems that the second one overestimate the friction angle compared to the Briançon Procedure. While looking on singular test, sometimes, the opposite situation is presented. (sample 7; test 3). The range between the two procedures is more wide employing virgin samples and it becomes smaller using tested samples.

Even this time, in this interface the values of the Force Procedure represent the lower friction value. The other procedures overestimate the friction angle.

Figure 6.18. shows the comparison between the Force and the Residual Friction Procedure, on the same sample, parameter $\lambda_{lim} = \phi_{lim}$ is plotted against the plane inclination.

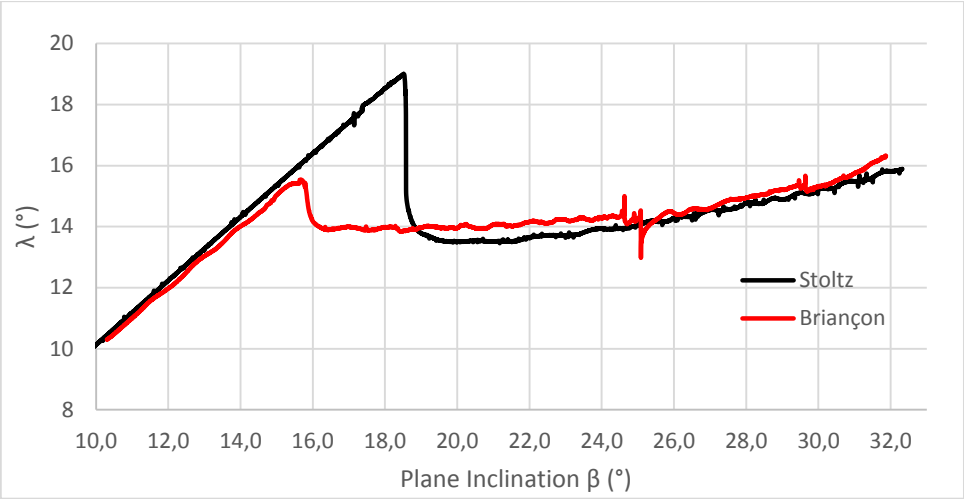

Figure 6.18. IP test according to the Force Procedure and the Residual Friction procedure, parameter $\lambda_{lim} = \phi_{lim}$ against plane inclination, interface GTX-GMB.

Some tests are carried out to put all the procedure together as shown in Figure 6.19.

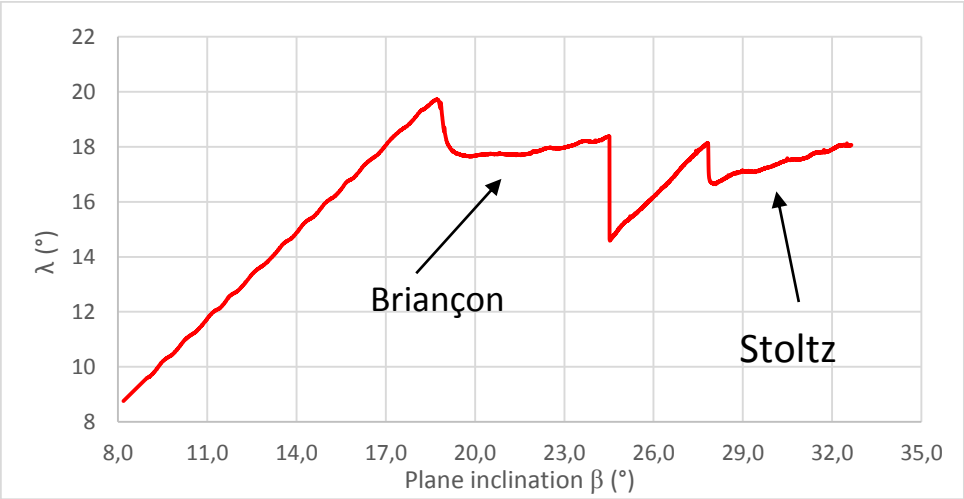

Figure 6.19. IP test, parameter $\lambda_{lim} = \phi_{lim}$ against plane inclination, interface GTX-GMB.

The liner phase contains the Displacement Procedure and the Standard, the upper box is free to slide until it reaches the end of the plane, when the Force Procedure starts, as already explained in Chapter 5, but using a spring locked to connect the upper box to the force sensor. After a reasonable time, while the plane inclination continues to increase the “spring system” used to implementing the Stolz procedure is unlocked and the Procedure is ruled out.

It is evident from Figure 6.18. How the Force Procedure had the necessary time to asset and the Residual Friction not. In fact, in the first case the parameter λ reaches the asymptote.

- **GNT^U – GMB^L**

Table 6.17 Angle of fist displacement values. GNT-GMB interface

Angle of first displacement ϕ_0 (°)		
# test number	Sample 7	Sample 8
1	16.4	16.3
2	14.9	18.0
3		
4		
5		
6	17.1	
7		
8		15.2
Average angle value	**ϕ_0**	**16.3°**

In Table 6.17 are reported the angle of first displacement results for a GNT^U – GMB^L interface in tests with virgin samples. The average value is 16.3°, which is higher than 13.3° obtain at 20° with tested samples. As already saw in the GXT-GMB the mechanical damage affect the angle of first displacement in a relevant way.

Due to a mechanical problem, the cable to connect the upper box and the force sensor was changed starting with these test, and the u_{lim} is limited at 550 mm.

Table 6.18. Standard Procedure angle values. GNT-GMB interface

Angle of the Standard Procedure ϕ_{stand} (°)		
# test number	Sample 7	Sample 8
1	17.9	16.4
2	16.2	18.1
6	18.7	
7		
8		16.8
Average angle value	**ϕ_{stand}**	**17.3°**

Table 6.18 reported the Standard Procedure results. The average value is 17.3°.

The interface behavior, in the previous test at 20°, is characterized by an abrupt initial displacement followed by a gradual sliding. In this case, this is true for sample 7 and not for sample 8 where the upper box undergoes until the plane end from the beginning with a gradual sliding. In Figure 6.20. is shown the first case and in 6.21. the second.

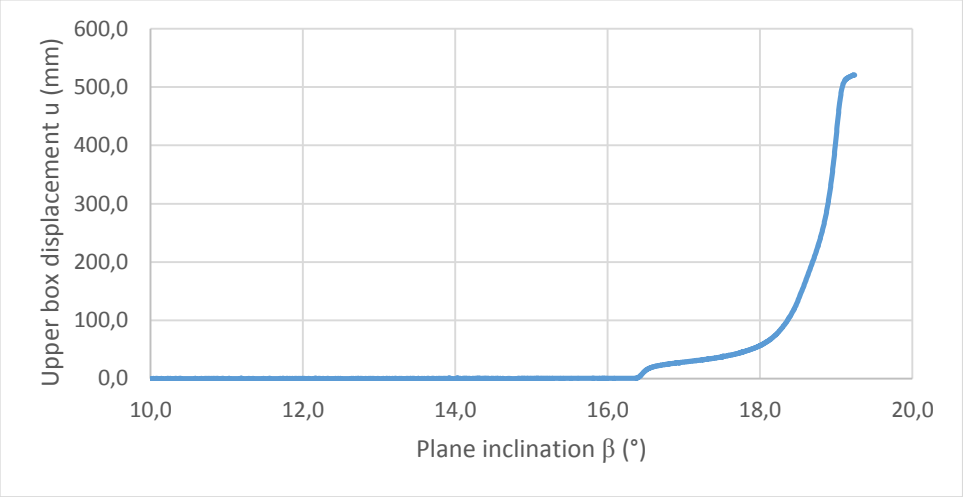

Figure 6.20. IP test according to the Displacement Procedure; Displacement of the upper box against the plane inclination, interface GNT-GMB sample 7

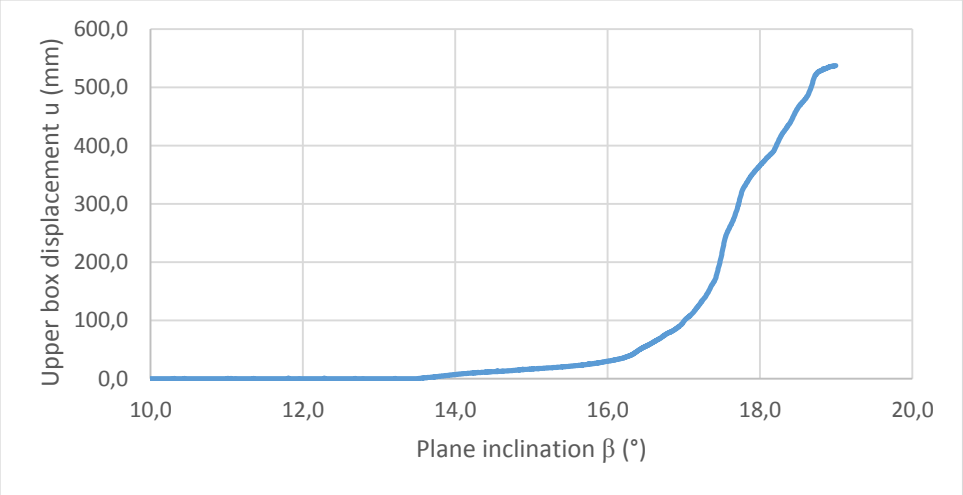

Figure 6.21.IP test according to the Displacement Procedure; Displacement of the upper box against the plane inclination, interface GNT-GMB, sample 8

Two tests at fixed plane inclination are performed to provide more appropriated kinematic values. (Table 6.19)

Table 6.19. Displacement Procedure angle values, performed at different fixed plane inclination, average velocity values and acceleration values. GNT-GMB interface

Angle of the Displacement Procedure $\phi_{dyn,a}$ (°)

		Sample 4			Sample 5		
# test number	β_{fixed}	$\phi_{dyn,a}$	$v_{average}$ (cm/s)	γ (m/s^2)	$\phi_{dyn,a}$	$v_{average}$ (cm/s)	γ (m/s^2)
1							
2							
3							
4	**20**	**17.6**	24.40	0.162	**17.7**	17.64	0.087
5	**25**	**18.9**	57.59	0.845	**17.3**	48.87	0.758
6							
7							
8							

Average angle value $\phi_{dyn,a}$ **17.7 °**

The average value $\phi_{dyn,a}$ is 17.7° is, always, the higher values obtained by testing the different procedures and the different interfaces.

At the end Force Procedure and Residual Friction Procedure are tested and compared.

Table 6.20 Force Procedure and Residual Friction Procedure angle values. GNT-GMB interface

Angle ϕ_{lim} (°)

# test number	Sample 7	Sample 8
1 Briançon	**15.6**	**16.9**
2 Stoltz	18.6	18.5
3 Briançon	**17.1**	**16.3**
4		
5		
6 Stoltz **Briançon**	18.5 **17.6**	
7 Stoltz **Briançon**		17.1 **17.6**
Average angle value Briançon	ϕ_{lim}	**17.0**
Average angle value Stoltz	ϕ_{lim}	**18.3**

In Table 6.20 reported the values obtained performing both the procedures. It is not possible to define a univocal interpretation to compare Briançon and Stoltz procedure. In fact, regarding the average value ϕ_{lim} is 16.9° for the Force Procedure and 18.1° for the Residual Friction Procedure. Then it could seems that the second one overestimate the friction angle compared to the Briançon Procedure.

It is important to report that starting with the GNT-GMB testes the force sensor suffers some mechanical problems.

- **GCD^U – GMB^L**

  The geomembranes utilized in these tests are not virgin samples.

Table 6.21 Angle of fist displacement values. GCD-GMB interface

Angle of first displacement ϕ_0 (°)		
# test number	Sample 7	Sample 8
1	16.2	16.4
2	17.2	16.4
Average angle value	**ϕ_0**	**16.5°**

The average value of the angle of first displacement for GCD-GMB interface is 16.5°, instead of 13.8° for tests at 20°. All tests values are reported in Table 6.21. It could be notice how the angles founded with sample 8 are the same in both tests, even in the Displacement Procedure as reported in Table 6.22.

Table 6.22 Standard Procedure angle values. GCD-GMB interface

Angle of the Standard Procedure ϕ_{stand} (°)		
# test number	Sample 7	Sample 8
1	**16.3**	**16.5**
2	**17.6**	**16.5**
Average angle value	**ϕ_{stand}**	**16.5 °**

The average value is 16.5°, which is in the middle between the geotextile and geonet value as founded in tests at 20°.

For this interface, as for the GTX-GMB, the movement is gradual sliding characterised by a very low velocity. For this reason, some over test are performed in dynamic conditions. The plane inclination β fixed at two different angles 20° and 25° and the upper box free to slide to until the end of the plane. In this way it is easier to evaluate the kinematic characteristics of the sliding process; upper box velocity and acceleration. Into the sliding phase the uniform accelerated motion take place. The results of these tests are shown in Table 6.23.

Table 6.23. Displacement Procedure angle values, performed at different fixed plane inclination, average velocity values and acceleration values. GCD-GMB interface

Angle of the Displacement Procedure $\phi_{dyn,a}$ (°)

		Sample 4			Sample 5		
# test number	β_{fixed}	$\phi_{dyn,a}$	$v_{average}$ (cm/s)	γ (m/s^2)	$\phi_{dyn,a}$	$v_{average}$ (cm/s)	γ (m/s^2)
1							
2							
3							
4	**20**	**14.1**	21.27	0.688	**15.1**	34.16	0.570
5	**25**	**15.6**	118.49	1.313	**15.0**	80.10	1.429
6							
7							
8							
Average angle value		**$\phi_{dyn,a}$**	**15.0°**				

The average value $\phi_{dyn,a}$ is 15.0°. Sample 8 gives every time really close results.

At last, results to compare Briançon and Stoltz procedure for this interface are reported in Table 6.24 and Figure 6.22.

Table 6.24 Force Procedure angle values. GCD-GMB interface

# test number	Angle ϕ_{lim} (°) Sample 7	Sample 8
1 Briançon	**13.0**	**12.0**
2		
3 Stoltz	16.5	13.9
4		
5		
6 Stoltz **Briançon**	16.4 **/**	16.4 **17.0**
Average angle value Briançon	ϕ_{lim}	**14.0**
Average angle value Stoltz	ϕ_{lim}	**16.4°**

The friction angle obtained with the Force Procedure is always the lower ones.

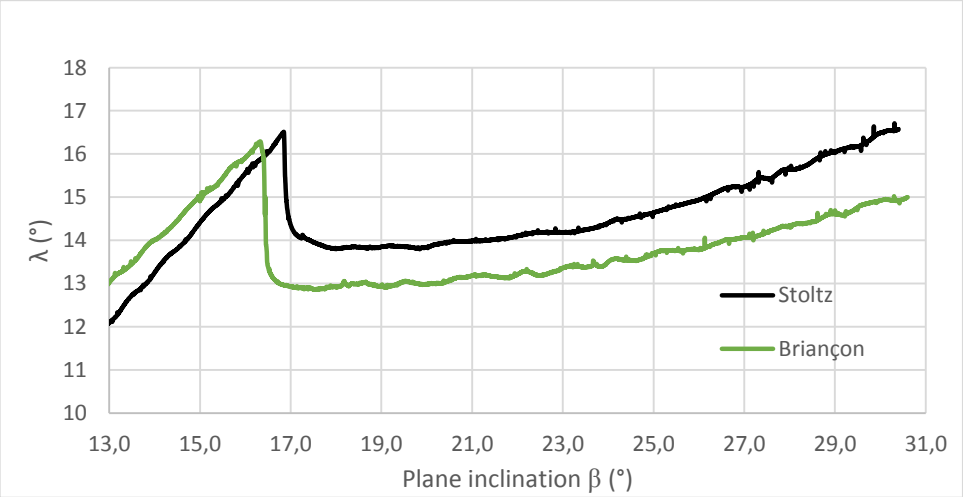

Figure 6.22. IP test according to the Force Procedure and the Residual Friction procedure, parameter $\lambda_{lim} = \phi_{lim}$ against plane inclination, interface GCD-GMB.

Summarising, the friction angles from the different procedures for each interface are:

Table 6.25 Summary of friction interface tests at 10°

Interface	ϕ_0 (°)	ϕ_{stand} (°)	$\phi_{dyn,a}$ (°)	ϕ_{lim} (°) Briançon	ϕ_{lim} (°) Stoltz
GTX-GMB	15.7	16.4	17.5	14.6	16.1
GNT-GMB	16.3	17.3	17.7	17.0	18.3
GCD-GMB	16.5	16.5	15.5	14.0	16.4

In Table 6.25 reported the average values for each procedure and for each interface tested at 10°.

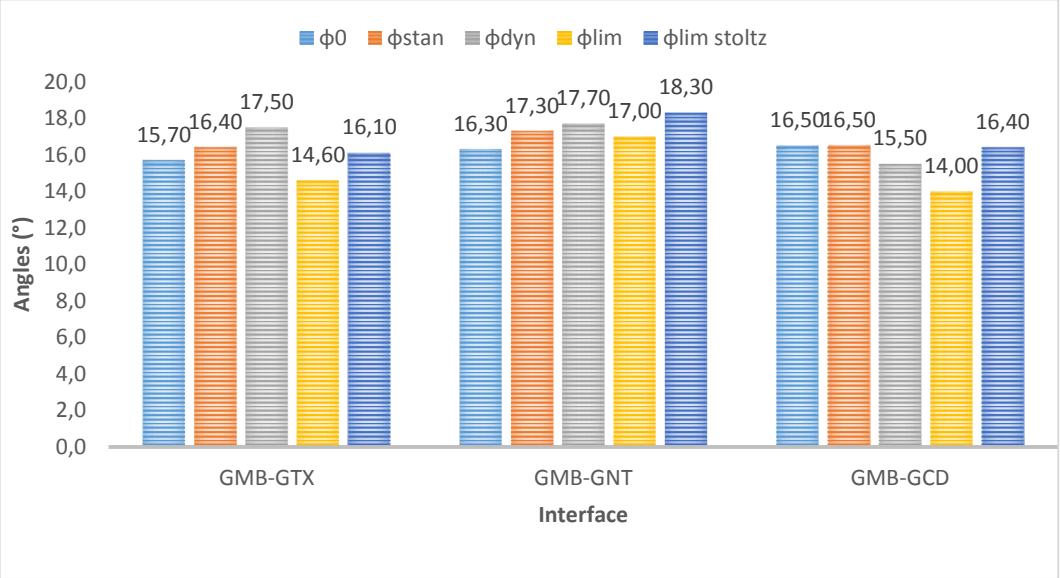

Figure 6.23. Average friction interface angles of different procedures at 10°.

Figure 6.23. shows the summary results of the friction angles obtained at 10° implementing the different procedures herein exposed. The interface behaviours are quite the same already founded in test at 20°. In fact, the lower friction angle is the one founded with the Force Procedure for GMB-GTX and GMB-GCD and not for the GMB-GNT. The Displacement Procedure overestimates the friction as before, but this time, not for the GMB-GCD, where the higher values are ϕ_{stan} and ϕ_0. The angles provided from the Residual Friction Procedure are not uniform. For

the first and last interface, it represents a middle value between the other procedures, au contrary in the GMB-GTX interface the higher angle.

At last, conclusions could be the same exposed for tests at 20°. GTX and the GCD have a similar behaviour. In fact, for these interfaces the lower value of friction angle corresponds to the Force Procedure angle, and the higher to the Displacement. Although for the GNT the lower is the angle of first displacement.

Using virgin samples the values are higher than using tested ones, then mechanical material damage influence the friction interface behaviour of the different interface tested.

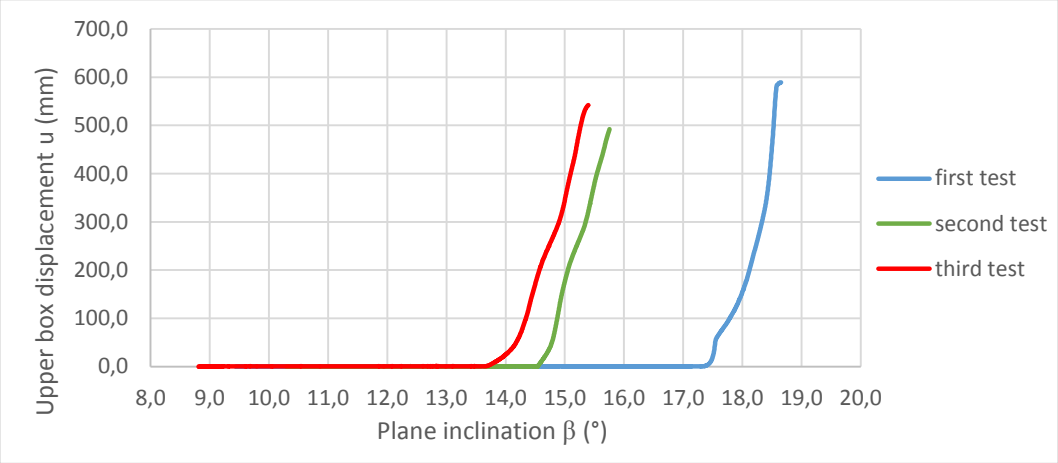

Figure 6.25. IP tests, mechanical damage of consecutive tests, GTX-GMB interface

Figure 6.25. is an example of the mechanical interface damage due to consecutive tests on a GTX-GMB interface. The mechanical damage could be easily deduced analysing the angle of first displacement for each tests. The test on the right is the first one and it has the higher angle values, ϕ_0 is more than 17°. Instead, in the second test, the one in the middle, ϕ_0 is about 14.5° and in the third one less than 14°. From the first test the angle ϕ_0 decreases about of 3°. At the end, the mechanical damage of geosynthetic materials has a great influence on the determination of the interface friction angle. The same situation could be founded checking the angles of the other procedures.

Comparing Briançon and Stoltz Procedures, the second one overestimate the friction angle respect to the first one. In fact, the values of the Residual Friction Procedure are every time higher than the Force Procedure results

Moreover, tests performed with lower ambient temperatures seems to be higher for these types of interfaces, even if from the theory the friction has to decreases at low temperatures.

6.2.3. IP TESTS ON GEOSYNTHETIC INTERFACES AT T=30°

The researcher Laura Carbone performs these tests, and for this reason are reported herein, only the average values in Table 6.26. The data are usefull compared to the others tests and to investigate the influence of temperature on the geosynthetic interfaces tested.

Table 6.26. Summary of friction interface tests at 30°

Interface	ϕ_0 (°)	ϕ_{stand} (°)	$\phi_{dyn,a}$ (°)	ϕ_{lim} (°)
GTX-GMB	15.8	16.3	16.3	13.5
GNT-GMB	15.2	16.3	18.3	15.4
GCD-GMB	15.7	16.8	18.0	15.1

As though observed in test performed at 20°already the GCD-GMB interface shows a medium behaviour between the GTX-GMB and the GNT-GMB. This situation could be referred to many parameters, as the influence of the GNT core and the affinity to GTX behaviour. (Figure 6.25.). Furthermore, in the comparison of all tests, another consideration, previously reported, finds validation. The angle obtained with the Displacement Procedure is the higher, while the lower represents the Force Procedure. Therefore, even this time the Standard and Displacement Procedure overestimate the friction angles.

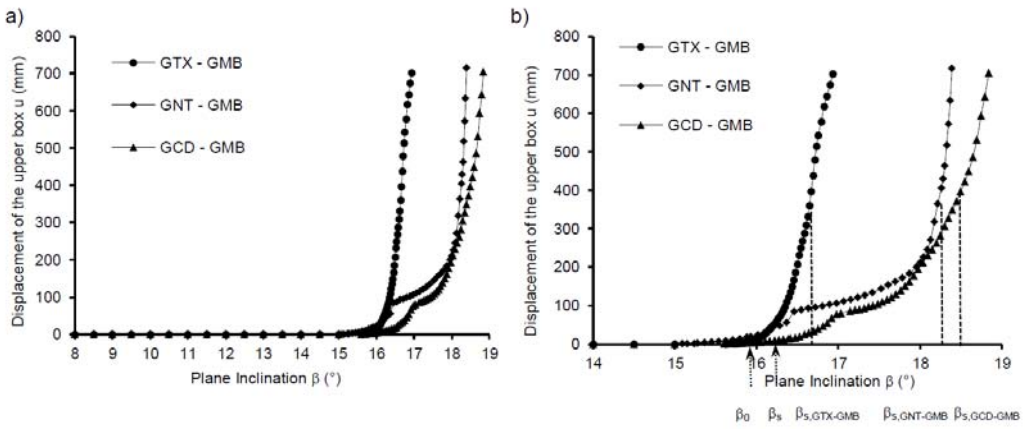

Figure 6.25. Inclined plane test according to the Dsiplacemetn Procedure, upper box displacement against plane inclination (Carbone (2013))

The same observations could be easily founded with in Figure 6.26.

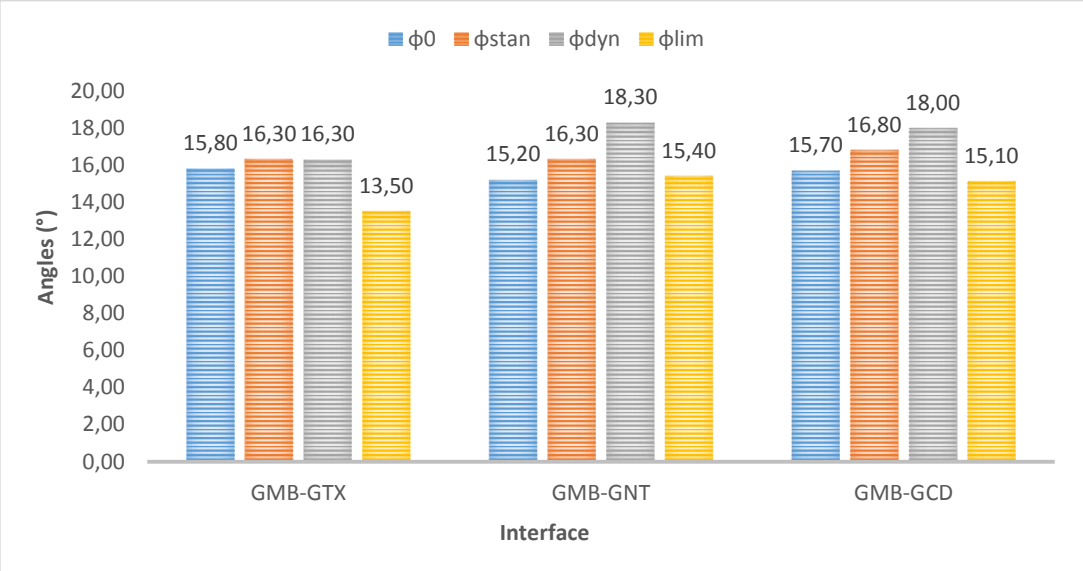

Figure 6.26. Average friction interface angles of different procedures at 30°.

At the end, a summary of the tests performed is illustrate in the following figures. The different angles, divided by the type of interface and the ambient temperature tested are plotted.

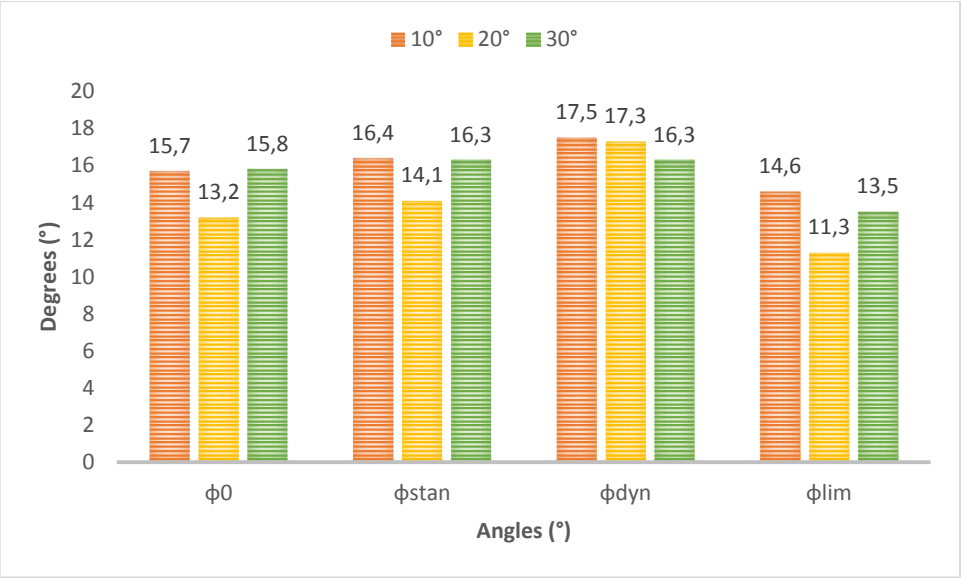

Figure 6.27 IP tests at different temperatures, GTX-GMB interface.

In Figure 6.27. reported the values for the GTX-GMB interface.

At first, it must be remembered that in all tests executed at 20°, tested samples of geomembrane are utilised, meanwhile in the others the lower layer, the geomembrane, is a virgin sample. This could have affect the correct definition of the friction angels. As though observed mechanical materials damage follows a uniform tendency. Now we want to know if it is the same for the ambient temperature.

The orange column represents tests performed at 20° and on average, the lower value obtained with each procedure for each interface. From the others two series of tests it impossible to find a good correspondence between the different angles and temperatures. In fact, sometimes the higher value is obtain at 10° and others at 30°. Generally, for this interface, exception of ϕ_0, tests at lower temperature have higher friction angles.

This trend is funded again in the GNT-GMB where, exception of $\phi_{dyn,}$ friction angles calculated at 10° seem to be the higher (Figure 6.27.). Meanwhile the GCD-GMB is not following this tendency. Effectively this time, three of the four angles considered are higher at 30° of temperature (Figure 6.28.).

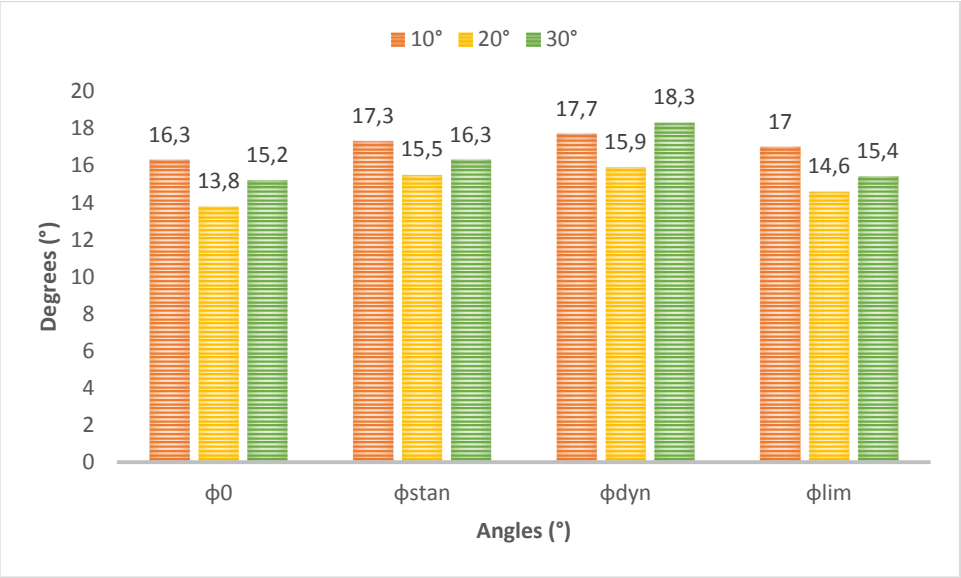

Figure 6.28. IP tests at different temperatures, GNT-GMB interface.

Both interfaces considered, GNT-GMB and GCD-GMB (Figure 6.29.), shows the same behaviour of the GTX-GMB for what concerns the lower value, represented by angles at 20°, moreover Displacement and Standard Procedure continues to overestimate the friction angle if compared to the Force Procedure.

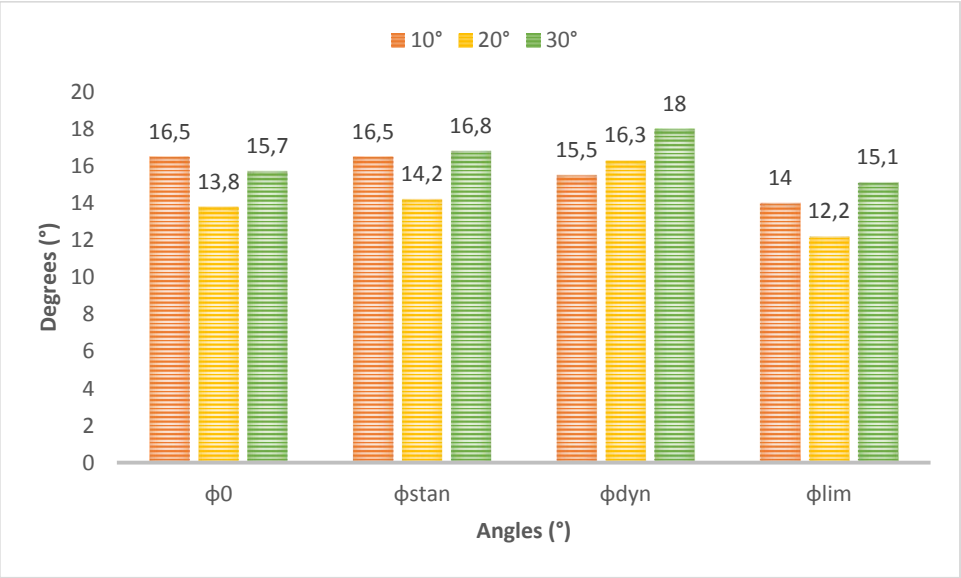

Figure 6.29 IP tests at different temperatures, GCD-GMB interface.

At the end, defining a correct tendency for temperature influence on geosynthetic interfaces is a hard point. There is not a unique trend followed by the different materials employed, too many parameters are involved.

6.2.4. IP TESTS ON TEXTURED GEOMEBRANE

The textured geombrane is tested with the geocomposite components, herein described. The two interfaces obtained are:

- Geotextile (GTX^{U}) - textured geomembrane (GMB_{T}^{L});
- Geonet (GNT^{U}) - textured geomembrane (GMB_{T}^{L}).

Testing these interfaces was hard. It was impossible to evaluate the results. This is referred to the no sliding of the first interface. The behaviour of the first interface is essentially based on pulling out and tearing of geotextile fibers in contact with the geomembrane asperities. The same consideration is reported in Frost (2001) and Hebeler (2005) researches.

7. CONCLUSIONS

In modern landfills, the use of geosynthetics, in top cover lining systems, is becoming a common practice. Design landfills with steeper slopes is nowadays required to face the need of more areas for the waste storage. For these reasons, to prevent instability problems on slopes, it is necessary to provide a correct interpretation of the mechanical properties of the geosynthetic interfaces involved.

In this research, three different interfaces have been tested: Geotextile (GTX^{U}) – smooth geomembrane (GMB^{L}); Geonet (GNT^{U}) – smooth geomembrane (GMB^{L}); Geocomposite (GCD^{U}) – smooth geomembrane (GMB^{L}). The three interfaces are representative of lining system pack composed by a smooth geomembrane and a drainage geocomposite. The pack parts have been studied separately to better understand their behaviour and to assess the GCD performance.

Furthermore the interfaces have been tested with four different procedures “Standard”, “Displacement”, “Force” and “Residual Friction”, in order to compare the results.

With the intention of giving a more appropriate characterization of the interfacial properties, some parameters involved in the frictional behaviour have been analyzed. The parameters investigated are: temperature, three different temperature have been tested; different plane inclinations and materials damage.

In generally GTX-GMB and GCD-GMB has a similar behaviour and way of slide, corresponding to a gradual slide with low velocity. While the GNT-GMB interface is characterized by an abrupt initial displacement (Figure 6.6.).

Globally the interface comportment is plotted in Figure 6.17. Where it is clearly visible how the GCD-GMB has got an intermediate behaviour between the GTX and GNT. The geotextile shows a different attitude when it is in direct contact with the geomembrane (GTX-GMB) or when there is the geonet support (GCD-GMB). The same conclusion and also part of the followings could be founded in Carbone et al (2013) research, where the interfaces tested are the same.

Table 6.12, 6.25, 6.26 report the summary tests results at respectively, 10°, 20° and 30° degrees. These tables and the corresponding Figures: Figure 6.16, 6.23 and 6.26 are helpful to understand the differences between the procedures utilised. It could be notice that the “Force” Procedure gives the more cautionary friction values. The angles evaluated with this procedure are not affected from the limit displacement and the plane rate inclination. Also in comparison with the “Residual Friction” Procedure, other procedure that utilises the force data to obtain the friction angle, the Force one gives always lover values, cautionary.

Anyway, the two procedure in force and the “Displacement” procedure allow to study the interface behavior during all the sliding phases, even if the three different angles of the different procedures are calculated in dissimilar situation. In fact, only the “Displacement” allows to evaluate a friction angle during a dynamic phase, but it overestimates, compared to the “Force Procedure”, the final values.

As herein already expressed sometimes it could be difficult define the upper box acceleration. For these reasons tests with a fixed inclination have been performed. For example Table 6.3 and 6.11 show how the plane inclination chosen do not influence the friction angle, but only the upper box velocity and acceleration, which are balanced by the plane inclination in the same way. Finally, performing this kind of test helps to evaluate easily the dynamic parameters as introduced by the studies performed at the ICEA department of the Padua University.

At the end, the “Standard” procedure is not a rigorous method, because it considers a static approach in dynamic conditions. Furthermore, the angles compared to the other procedures seem to be overestimated. The same conclusion could be notice for the angle of first displacement, which is influenced by to many parameters and

is not a representative value of the real interface behaviour. A Standard review is suggest, as confirmation of Carbone et al. study (2013).

The two last parameters investigated are mechanical damage and temperature. The first one, it is clearly visible in Figure 6.24, where three different consecutive tests performed on the sample are plotted. The mechanical damage has a first order importance not only on the angle of first displacement, the more sensible, but also on the other friction angles. Moreover, tests performed at 10° have been done with virgin samples of geomembranes and geosynthetics and the values are higher, au contrary the geomembranes utilised in tests at 20° are tested samples.

As though observed mechanical materials damage follows a uniform tendency. Now we want to know if it is the same for the ambient temperature.

The temperature influence is a delicate issue to discuss. Temperature is a variable parameter and it could be also affected by the relative humidity, which, during the campaign program was not possible to recorded. Firstly, it necessary to notice that not all the experiments have been performed with virgin samples, so that could have influenced the temperature results. From the temperature, analysis is not possible to define a uniform tendency, as for the mechanical damage; in fact, sometimes the higher values in tests performed at 10° degrees and sometimes at 30°. However the temperature influence trend is plotted in Figure 6.27, 6.28, 6.29, respectively for GTX-GMB, GNT-GMB; GCD-GMB. At the end, defining a correct tendency for temperature influence on geosynthetic interfaces is a hard point. There is not a uniform trend followed by the different materials employed, because too many parameters are involved.

For what concerns the textured geomebrane tested, it must be notice that, it was impossible to elaborate the results. There was no visible sliding of one geosynhtetic to another. In the case of GTX-GMBtextured, the interface behaviour is essentially based on pulling out and tearing of geotextile fibers in contact with the geomembrane asperities.

REFERENCES

- EN ISO 10318: "Geosynthetics— Terms and definitions" (2000);
- IGS, International Geosynthetic Society website;
- R. Bathurst, "Geosynthetic Classification and functions", IGS (2007);
- D. Kay, E. Blond, J. Mlynarek, "Geosynthetics durability", (2004);
- Koerner, R.M., "Designing with geosynthetics" Prentice Hall, Upper Seddle River, New Jersey, USA, Fourth Edition (1998)
- J. Vashi, M. Desai, A. Desai, "Geosynthetic material and its properties for reinforced earth structures";
- S. Cola, corso di "Miglioramento dei terreni ed opera in terra" UNIPD;
- P. Simonini, corso di "Geotecnica nella difesa del suolo", UNIPD;
- Greengroupholding website;
- Feodorove, V, Manea, S; Batail, I, Sofrone, D; "Use of geosynthetics in landfills", IGS;
- D. Kay, E. Blond, J. Mlynarek, "Geosynthetics durability: A polymer chemistry issue", (2004), 57th Canadian Geotechnical Conference;
- EPA, United States Environmental Protection Agency; "Geosynthetic Clay Liners Solid Waste Landfills" (2001);
- M. Sadlier, "Geosynthetics in Wastewater Treatment", IGS;

- GLR, "Geotechnics of landfill design and remedial work", Technical recommendations. Ed: Ger- man Geotechnical Society. Ernst und Sohn, Berlin, (1993);

- Floss, R.; Fillibeck, J.: The experimental shear strength evaluation of geomembrane – clay liner and geomembrane – geotextile interfaces. Proc. 6th International Conference on Geosynthetics Volume I, Atlanta, Georgia, USA, Industrial Fabrics Association International, (1998);

- J.P. Giroud, R.C. Bachus and R. Bonaparte (1995) "Influence of water flow on the stability of geosynthetic soil layered system on slopes". Geosynthetic International 2;

- Stark, T.D. & Newman, E,J., " Design of a landfill final cover system", Geosynthetics International 10, (2010);

- EPA, United States Environmental Protection Agency; "Geosynthetic Clay Liners Solid Waste Landfills" (2001);

- Hillman, R. P & Stark, T. D. "Shear behavior of PVC geomembrane/geosynthetic interfaces". Geosynthetics International 8;

- Eid, Hisham T. "Shear strength of geosynthetic composite systems for design of landfill liner and cover slopes", Geotextiles and Geomembranes 29, (2011);

- O'Sullivan & Quigley "Geotechnical Engineering & Environmental Aspects of Clay Liners for Landfill Projects");

- Bouazza, A Zornberg, JG Adam, D. "Geosynthetics in waste containment facilities: recent advances" 7th Intl. Conf. on Geosynthetics (2002);

- Skempton, A.W., "The Bearing Capacity of Clays," Building Research Congress, London.(1951);

- Giroud J.P., Beech J.F.,"Stability of soil layers on geosynthetic lining system", Proceedings of Geosynthetic'89 Conference , San Diego, USA, (1989);

- Koerner R., Hwu B.L “Stability and tension considerations regarding cover soils on geomembrane lined slopes” Geotextiles and Geomembranes , 10, . (1991);

- Briançon, L Girard, H Poulain, D “ Slope stability of lining systems—experimental modeling of friction at geosynthetic interfaces”, Geotextiles and Geomembranes 20, (2002);

- Girard, H Haddane, K Poulain, D “Stability and anchorage of geosynthetic systems on slopes: development of a new designing tool” International Workshop Hydro-Physico-Mechanics of Landfills” LIRIGM, Grenoble 1 University,France , (2005);

- Floss, R, Brau, G. “Design fununda mentals for geosynthetic soil technique”; Asian Regional Conference on Geosynthetics, (2005);

- Sowers, G. F., “Settlement of Waste Disposal Fills.” Proceedings of the 8th International Conference on Soil Mechanics and Foundation Engineering, Moscow,(1973)

- Wall, D. K. and Zeiss, C., "Municipal Landfill Biodegradation and Settlement." Journal of Environmental Engineering, ASCE, Vol. 121, No. 3, (1995);

- Rajesh, S; Viswanadhanìm, B.V.S, “Hydro-mechanical behavior of geogrid reinforced soil barriers of landfillcover systems”, (2010);

- Jessberger, H.L., Stone, K.J.L. “Subsidence effect on clay barriers.” Geotechnique 41, (1991);

- Fox, P.J., DeBattista, D.J., Mast, D.G. “Hydraulic performance of geosynthetic clay liners under gravel cover soils”. Geotextiles and Geomembranes 18,(2000);

- Keck, K.N., Seitz, R.R.. “Potential for Subsidence at the Low-level Radioactive Waste Disposal Area”. INEEL/EXT-02e01154. Idaho National Engineering and Environmental Laboratory, U.S. Department of Energy. (2002)

- Sharma, H.D., De, A.. “Settlement of municipal solid waste landfills.” Journal of Geotechnical and Geoenvironmental Engineering (2007);

- Landreth, R.E., Carson, D.A.. RCRA "Cover systems for waste management facilities." Geotextiles and Geomembranes 10, (2001);

- Rowe, R.K., Quigley, R.M., Brachman, R.W.I., Booker, J.R., "Barrier Systems for Waste Disposal Facilities", E & FN Spon. Taylor & Francis Books Ltd, London, (2004)

- MacLaughlin, M. Sitar, N. Doolin, D. Abbot, T., "Investigation of slope-stability kinematics using discontinuous deformation analysis", International Journal of Rock Mechanics and Mining Sciences, (2001);

- E. Deladi. "Static friction in rubber-metal conctacts with application to rubber pad forming processes". (2006);

- Broniec, Z., Lenkiewicz, W., "Static friction processes under dynamic loads and vibration", Wear, Vol. 80. (1982):

- Roberts, A.D., Thomas, A.G., "Static friction of smooth clean vulcanizedrubber", NR Technology;

- Johnson, K.L., "Surface interaction between elastically loaded bodies under tangential forces", Proceedings of the Royal Society of London, Series A, Mathematical and Physical Sciences.

- Calligan, J.M., McCullough, P.,"On the nature of static friction";

- Nolle, H., Richardson, R.S.H., "Static friction coefficients for mechanical and structural joints";

- Bowden. F, P, and Tabor, D. "The Friction and Lubrification of Solid". Part II, (1964);

- JF. Ganghoffer, J Schultz, "Interaction between adhesion and friction"; (1997);

- R. Thield, "Cohesion (or adhesion) and friction angle in direct shear tests". Geosynthetics (2009);

- G. L. Hebeler, J. D. Frost, A.T. Myers, "Quantifying hook and loop interaction in textured geomembrane-geotextile systems". (2005);

- J. D. Frost, S. W. Lee, "Microscale study of geomembrane-geotextile interactions". (2001);

- De A., Zimmie T.F., "Estimation of dynamic interfacial properties of geosynthetics". Geosynthetics International (1998);
- N. Ivy, "Asperity height variability and effects";
- L. Briançon, H. Girard, JP. Gourc, "A new procedure for measuring geosynthetic friction with an inclined plane", Geotextile and Geomembrane, 29 (2011);
- L. Briançon, H. Girard, D. Poulain, "Slope stability of lining systems.- Experimental modelling of friction at geosynthetic interfaces", Geotextile and Geomembrane, 20 (2002);
- EN ISO 12957-2, 2005. Geosynthetic-determination of friction charactheristics, Part 2: Inclined Plane Test. Brussels: European Committee for Standardisation;
- H. Girard, H. Fisher, E. Alonso, "Problems of friction posed by the use of geomembranes on dam slopes – examples and measurements", Geotextile and Geomembrane, 9 (1990);
- JP. Gourc & R. Reyes Ramirez, "Dynamics-based interpretation of the interface friction test at the inclined plane" Geosynthetic International, 11 (2004);
- JP. Gourc & R. Reyes Ramirez, "Use of the inclined plane test in measuring geosynthetic interface friction relationship" Geosynthetic International, 10 (2003);
- EM. Palmeira, Jr. NR. Lima, LGR. Mello, "Interaction between soil and geosynthetic layers in large scale ramp test" Geosynthetic International, 9 (2002);
- M. Izgin, Y. Wasti, "Geomembrane sand interface frictional properties as determined by inclined board and shear box tests" Geotextile and Geomembrane, 16 (1998);
- EM. Palmeira, "Soil- geosynthetic interaction: modelling and analysis" Geotextile and Geomembrane, 27 (2009);

- HN. Pitanga, JP. Gourc, OM. Vilard, "Interfaces shear strength of geosynthetics: evaluation and analysis of inclined plane test" Geotextile and Geomembrane, 27 (2009);

- HN. Pitanga, JP. Gourc, OM. Vilard, "Enhanced measurement of Geosynthetic Interface Shear strength using a modified Inclined Plane Device" Geotechnical Testing Journal (2011);

- S. Lalarakotodon, JP. Gourc, P. Vilard, "Shear strength characterisation of geosynthetic interfaces on inclined planes" Geotechnical Testing Journal 22 (1999);

- Y. Wasti, ZB. Ozduzgun, "Geomembrane—Geotextile interface shear properties as determined by the inclined board and shear box tests" Geotextile and Geomembrane, 19 (2001);

- WXT. Wu Wang, F. Aschauer, "Investigation on failure of a geosynthetic lined reservoir", Geotextile and Geomembrane 26 (2008);

- L. Carbone, JP. Gourc, L. Briançon, N. Moraci, P. Carrubba "Geosynthetic interface friction using Force Procedure at the Tilting Plane" (2012);

- L. Carbone, JP. Gourc, L. Briançon, N. Moraci, P. Carrubba "What value of interface friction to select for geosynthetic liner on landfill slopes?" Geosynthetic International (2013);

- G. Stoltz, R. Gallo, D. Poilain; N. Touze-Foltz, "Testing procedure with an inclined plane device to assess the residual friction characteristics at geosynthetics interfaces", (2012).

AKNOWLEDGEMENTS

Now at the end of the best years of my life I have to thank many persons.
First of all my families to support me because without you I will be never be there. Mum and dad thanks to make me such a strong and determinate person. Matilde thanks to be my little sister, with love always.
Hereafter the University of Padova, my supervisor Professor P. Carrubba for giving me the possibility of being part of the Erasmus Program. All the staff of the LTHE laboratory of the University Joseph Fourier in Grenoble, Professor JP. Gourc for his helpfulness during my internship, the technicians Henry and Helene for their help with my experiments and Laura Carbone for her help and assistance during the redaction of this work.
I have to thank Padova to let me know people like my university mates. Alessio because you are my best friend, through everything and I could say only thank you now. Nicola thanks to be always by my side after all. All the others that made these years amazing: Chiara, a girl in a man word’s, Francesco, Matteo my tutor during the last exam, Gobby and your happiness, Eleonora the best discovery of these last months, Fox, Zoff, Francesca; Laura; Casta, Giulio; Pier, Paolo. I know I am forgetting someone but I will never forget the time spent with you. Elisa for these eleven years together, Ylenia in good and bad times, Alberto for the parties and the confidence time, all my innumerable flat mates: Chicca, Carla; Igina and Giorgia. Thank you all to be my world during the university years.
My friends at home: Baga and Valentino, because you were there in bad moments, Bafo, Alice, Beppe, Martina, for the evening spent together.
Now I need to thank the people how have been my family for six unique and unrepeatable months, the Erasmus Family. First of all Teresa, Giulia and Eric for the great time, the parties and the incredible situations we have spent together, I miss our dinners, our laughs I miss you. Jessica, the other piece of the family, for the support and the constant help at the lab. Armel for the wonderful sky days and all the others Pier, Giulia M, Claudia and our dancing evening; Celine, Carlos for loving my cakes; Ilaria, Cecile, François, Giovanni, Clements, Andreas, Charliee, Marta; Edita, Basilio and Andrea for the time spent to cook together.
At last Luca because you have spent your free day with me during this summer and you are still here now.
Thanks to everyone.

Melissa